ON A TYPE

OF

FREQUENCY INDEPENDENT ANTENNA

A THESIS

BY

SUDHANGSHU BHUSHAN KARMAKAR

SUBMITTED TO THE DEPARTMENT OF ELECTRICAL ENGINEERING, EAST PAKISTAN UNIVERSITY OF ENGINEERING AND TECHNOLOGY, DACCA IN PARTIAL FULFILMENT OF THE REQUIREMENTS FOR THE DEGREE OF MASTER OF SCIENCE IN ELECTRICAL ENGINEERING.

JUNE , 1965.

C E R T I F I C A T E

THIS IS TO CERTIFY THAT THIS WORK WAS DONE BY ME AND IT HAS NOT BEEN SUBMITTED ELSEWHERE FOR THE AWARD OF ANY OTHER DEGREE OR DIPLOMA.

S. B. Karmakar

(SIGNATURE OF THE CANDIDATE)

Exam Committee :-

1. Abdul Matin Patwari
(SUPERVISOR) Chairman

2. [signature]

3. Mohammed Azizul Islam

A C K N O W L E D G E M E N T

IT IS A MATTER OF GREAT PLEASURE ON THE PART OF THE AUTHOR TO EXPRESS HIS EVER LASTING INDEBTEDNESS TO THOSE WHO HAVE ASSISTED IN THIS STUDY AND WITHOUT WHOSE AID AND ENCOURAGEMENT THIS WORK WOULD HAVE NOT BEEN COMPLETED.

IN PARTICULAR, THANKS ARE CONVEYED TO PROF. ABDUL MATIN PATWARI WHO HAS PROVIDED THE INSPIRATION FOR THE WORK AND WHOSE COUNSEL HAS BEEN FOLLOWED IN EACH STEP IN THE PROCEDURE. IT MAY TRULY BE SAID THAT WHATEVER SUCCESS HAS BEEN ACHIEVED IS IN A LARGE MEASURE ATTRIBUTABLE TO HIS FORESIGHT AND GUIDANCE.

THE KIND ENCOURAGEMENT AND VALUABLE ADVICE RECEIVED FROM OTHER MEMBERS OF THE STAFF OF THE DEPARTMENT OF ELECTRICAL ENGINEERING,E.P. UNIVERSITY OF ENGINEERING AND TECHNOLOGY ARE HIGHLY APPRECIATED AND ALSO GRATEFULLY ACKNOWLEDGED.

C O N T E N T S

LIST OF FIGURES

C H A P T E R - I

I N T R O D U C T I O N

I N T R O D U C T I O N

In radiated wave propagation a most essential part of the communication channel is the antenna which " launches" the electromagnetic energy at the transmitting end and " captures" part of this energy at the receiving end. It is observed[5] that a circuit large compared with wave length has the possibility of loosing energy because induced electric fields from time varying currents and charges of the circuit may shift in phase as a result of retardation over circuit and may have components in phase with current.

Hence the obvious conclusion, the antenna which is to perform duel functions of an impedance matching device and a radiator is simply a circuit made purposely large compared with wave length to increase the importance of radiation. The physical form of the antenna is dictated by practical consideration[6], and in general dependent upon the frequency of operation. In general, also, the directive gain and impedance of an antenna are functions of its size in wave lengths. The characteristics of major importance of an antenna are its impedance and its directional properties. Depending upon the application, one or the other (or both) of these characteristics may limit the useful band width, the required or desired bandwidth also varies markedly with application. Because of the wide varieties of operational requirements that exist, there is no unique definition of antenna bandwidth. Hence it may be pointed out here that the term broadband antenna does not convey anything unless we specify the minimum bandwidth an equipment must cover before we can call it a broadband one. In the past, this term has been applied to describe antennas whose radiation pattern and input impedance were acceptable

over a frequency range of 2 or 3 to 1.

The development of broadband antenna led to the concept of a new type of antenna termed frequency independent antenna. In this type of antenna, the pattern as well as the impedance is practically independent of frequency for all frequencies above a certain value.

The concept of frequency independent antenna came from the common experience[1] that if all the dimensions of a lossless antenna are increased by a factor K, the pattern and impedance remain fixed if the operating wavelength is also increased by the factor K. In other words, the performance of a lossless antenna is independent of frequency if its dimensions measured in wavelength are held constant.

It follows that if the shape of the antenna were such that it could be specified entirely by angles, its performance would be independent of frequency. Of course, all such angle structures must extend to infinity,so the key problem is to find what structures, if any, will retain the frequency independent properties when truncated to a finite length. The infinitely long biconical antenna has a geometry that can be expressed entirely in terms of angles (the cone angles). It is also an example of structure that does not retain frequency independent characteristics when truncated[6], for both the pattern and inpedance of finite length biconical antenna vary greatly with frequency. In contrast, the equiangular spiral antenna does retain its frequency independent properties when truncated as long as the arm lengths are longer than about one wavelength at the lowest frequency at which it is desired to operate. V.H. Rumsey[1] has given a general equation of antenna structures whose performance will be independent of frequency.

The concept of frequency independent antenna introduced by Rumsey has found practical realization in two separate developments,equiangular structures and log-periodic structures.

C H A P T E R - II

GENERAL SURVEY

GENERAL SURVEY

The present development of broadband antenna and frequency independent antenna is the result of earlier investigation upon the problem by an intuitive or cut and try approach.

Some of the earliest broadband antennas were long wire types designed to operate in the high frequency band or in the low frequency band[4]. For the most part, they were broadband only in the sense that impedance remained relatively constant over useful range, in general no attempt was made to achieve a constant pattern. Among these antennas the well known rhombic antenna has held a dominant place since the early days of radio. The antenna shown in Fig. 1. is essentially a resistance terminated transmission line that has been opened out to form the four sides of a rhombus.

Because of the travelling wave current distribution along the terminated line, the main beam is in the forward direction(towards the termination) at an angle that depends, in a complicated fashion, on the included angle of the rhombus and the length of the sides in wavelengths. The beam is quite broad in the vertical plane and the angle above ground of the maximum increases as the frequency decreases. This change of angle with frequency is in the correct direction for transmission or reception of ionispherically reflected wave, so a rhombic antenna of fixed dimensions is usable over a wide frequency range (of the order of four to one) in the short wave band.

The wave antenna, consisting of a long elivated wire parallel to the ground and resistance terminated in both ends is another travelling wave

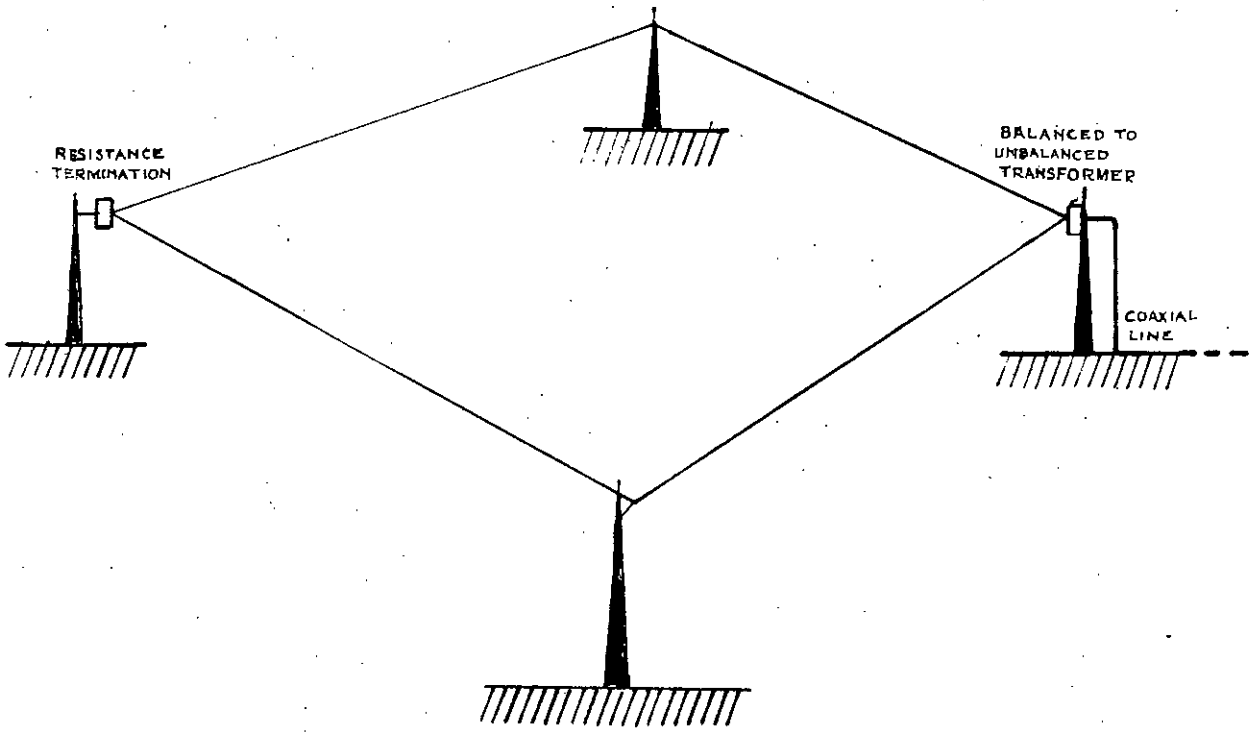

FIG. 1. RHOMBIC ANTENNA

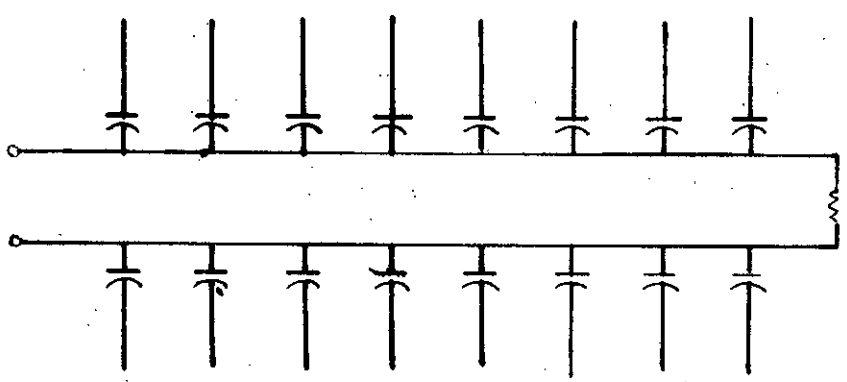

FIG. 2. FISHBONE ANTENNA

type antenna[4]. In contrast with most antennas which operate best over a highly conducting ground the wave antenna depends for its operation upon the finite conductivity of the earth beneath it. This antenna has an impedance that is nearly independent of the length of the wire in wavelength and hence with frequency.

The fish bone antenna[4] shown in Fig. 2. is a better development for broadband antenna. The antenna consists of a long resistance terminated transmission line loosely coupled by capacitors to an array of closely spaced (less than $\lambda/4$) untuned, horizontal dipoles. Because of the capacitive coupling of the elements to the transmission line is lighter at higher frequencies, fewer of the elements are strongly excited. Hence the effective length of the array varies inversely with frequency in such a manner as to maintain a fairly constant pattern, gain and impedance, over the useful bandwidth of more than two to one.

In contrast to the above antennas, there is a class of antennas which owes its broadband properties to broad and specially shaped surfaces[4]. It has been recognised that fat antennas had smaller impedance variations than thin one.

A discone shown in Fig.3. maintains a good impedance and pattern characteristics over a four to one bandwidth.

Another group of antennas, some of which display fairly wide bandwidths, consist of various helical and spiral shapes. When the circumference of a helical antenna is of the order of free space wavelength, the antenna radiates in the axial mode -- that is, with the maximum radiation along the axis of the helix. In this mode, the helical antenna has desirable impedance, pattern and circular polarization properties over nearly an octave.

The bandwidth can be increased by expanding the diameter of the helix along its length to form a conical mono filar helix fed from the base end.

FREQUENCY INDEPENDENT AND LOG-PERIODIC ANTENNAS

As stated earlier, Rumsey put forth the idea that a structure entirely definable by angles, without any characteristic length dimension, should have properties that are independent of the frequency of operation[1]. He proposed that an equiangular spiral structure which satisfies the angle requirement, might have the desired properties and Dyson[3] undertook a comprehensive experimental study of an antenna based upon the equiangular spiral geometry shown in Fig. 4. Experimental investigation established that this particular geometry did indeed retain its frequency independent properties after truncation and this design was the basis for a large class of successful frequency independent antennas.

When this angular structure is excited in a balanced manner at the origin, the current flows outward with small attenuation along the spiral arms until a region of given size in wavelengths is reached[4]. In this region (the active or radiating region) essentially all of the incident energy transmitted along the spiral arms is radiated, and somewhat beyond this region the presence or absence of the arms is of no consequence. Because the radiating region is of constant size in wavelengths, it moves toward the origin as the wavelength of operation decreases.

The size of effective radiating aperture thus automatically adjusts or scales with frequency of operation in such a manner that the antenna behaves the same at all frequencies. Because of the spiraling of the arms,

this scaling in accomplished by a rotation of the radiated field about the axis of the antenna.

It is now known that this automatic scaling of the radiating aperture is a condition for operation in a frequency independent manner.[4] It is interesting to note that Springer observed this phenomenon on the expanding helix, but unfortunately the methods of construction and excitation limited the bandwidth obtainable to somewhat over an octave, so the importance of scaling of effective aperture with frequency was not fully recognized.

The equiangular spiral antenna is bidirectional, radiates a very broad, circularly polarized beam on both sides of its surface. A more practical version of this antenna is the conical equiangular spiral shown in Fig.5. Whereas the planar structure is bidirectional, with the same pattern on each side, the effect of forming the equiangular structure on the surface of a cone, of small cone angle, is to make the antenna unidirectional.

The radiation which is approximately circularly polarized, is now confined to one hemisphere, with the maximum radiation off the apex of the cone the antenna is a balanced structure with the feed voltage applied between the two arms at the apex. For convenience, and to avoid disturbing the field about the antenna the feed line is a co-axial cable which is run up along, and soldered in contact with , one of the arms. Because the amplitude of antenna current on the arms (and also on the outside of the co-axial cable) fall off quite rapidly with distance from the apex the region near the ends of the arms where the cable enters is essentially a field free region. Hence this type of feed automatically provides a frequency independent balun[6] , permitting the feeding of the balanced antenna

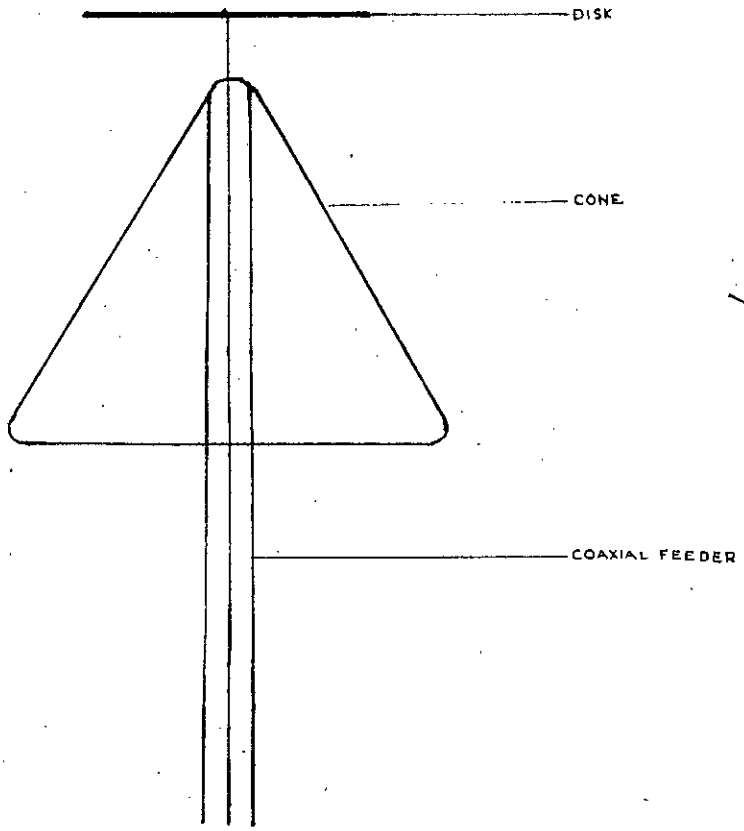

FIG. 3. DISCONE ANTENNA

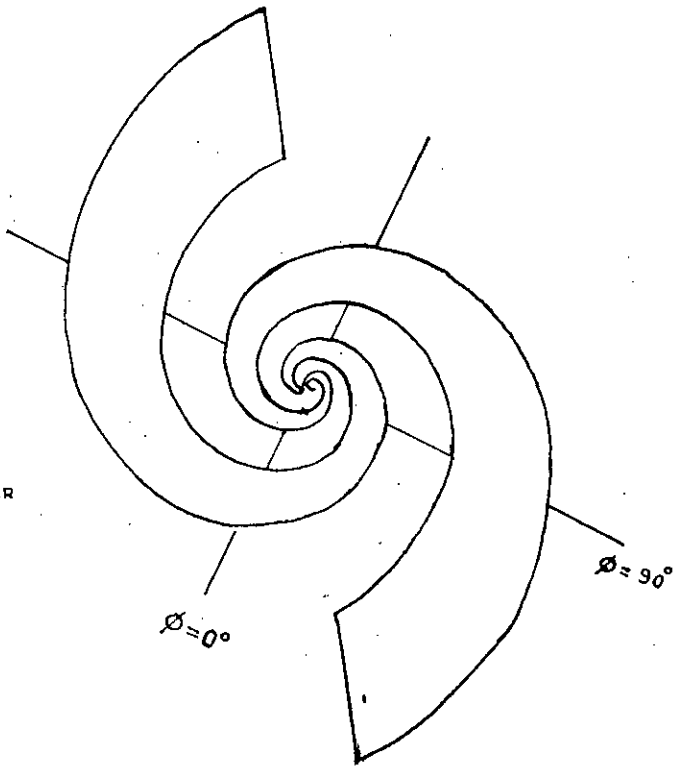

FIG. 4. EQUIANGULAR SPIRAL ANTENNA

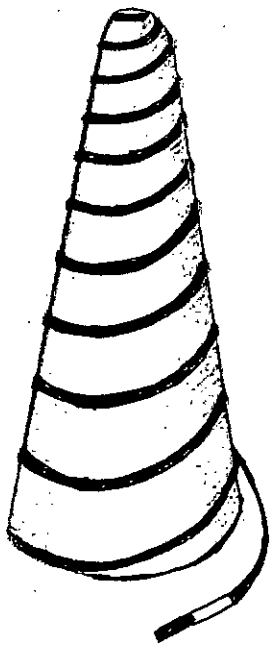

FIG. 5. CONICAL EQUIANGULAR SPIRAL ANTENNA

by means of an unbalanced co-axial line. To maintain physical symmetry, a dummy cable is soldered to the other arm. Antennas of this type have been successfully constructed to operate over bandwidths of better than 20 to 1 and there seems to be no fundamental limitation on the maximum bandwidth attainable. The low frequency limit of operation is set by the dimensions at the large end (the base radius should be greater than a quarter of a wavelength at the lowest frequency of operation) whereas the upper frequency limit is set by how finely the equiangular structure can be molded at the apex and hence on the minimum diameter of feed cable that can be used. A somewhat different practical realization of the frequency independent concept is the class of antennas known as log-periodic[6,2] . In this class of structures the broadband properties are obtained by making the pattern and impedance characteristics periodic with the logarithm of frequency. If then it can also be arranged that the radiation characteristics do not change appreciably over a period, a nearly frequency independent antenna results.

DuHamel proposed that it should be possible to force radiation from otherwise ' angle structures' by the use of appropriately located discontinuities[2,4] . One of the first geometries chosen to investigate the validity of this concept was that shown in Fig. 6. Here two wedge shaped metallic angle structures have teeth cut into them along circular arcs. The radii of the arcs which define the location of successive teeth are chosen to have a constant ratio $\tau = R_{n+1} / R_n$. This same ratio τ defines the lengths and the widths of successive teeth.

From the principle of modeling it is evident for this structure, expending from zero to infinity and energized at the vertex, that whatever properties it may have at a frequency f will be repeated at all frequencies given by $\tau^n f$ where n is an integer. When plotted on a logarithmic scale,

these frequencies are equally spaced with a period equal to the logarithm of τ ; hence the name ' log-periodic' structure. Log-periodicity guarantees only periodically repeating radiation pattern and impedance.

The above antenna was designed to have one other rather special property ; namely, that the metal cut away from the plane sheet to form the antenna arms has identical shape with the metal that remains. In other words, the complementary slot antenna has the same size and shape as the metallic dipole antenna.

In this connection a very interesting point was noted by Mushiake in one of the Tohoku University Reports[1]. It is that the impedance of any plane sheet antenna whose shape is the same as the shape of its complement (except for a trivial change of co-ordinates) is independent of frequency and equal to 60π = 189 Ohms. When the antenna and its complement are fitted togather they completely cover the whole plane without overlapping. The constant impedance of self complementary antenna[1] follows from the relation $Z_1 Z_2 = (60\pi)^2$. Z_1 is the impedance of the antenna and Z_2 that of its complement.

Another form of log-periodic structure is the log-periodic dipole array[4,6] shown in Fig. 7. In this array the length of each element bears a fixed ratio τ to the length of the preceding element. Moreover, adjacent element spacings bear the same ratio one to another. It is evident from the principle of scaling that whatever pattern and impedance characteristics the array may have at a frequency f_n which makes n th element resonant, it will have the same characteristics at a higher frequency f_{n+1} which makes (n+1)th element resonant[6]. That is the characteristics will repeat periodically at all frequencies given by $\tau^n f$. If τ is kept sufficiently close to unity, the characteristics will not change appreciably within a period

and the result in an array which is approximately frequency independent.

A further development of the log-periodic principle is the log-periodic resonant V array[6] shown in Fig. 8. This array is designed to operate in several different modes. In the lowest order $\lambda/2$ mode, the performance is approximately the same as that of the log-periodic dipole array described above. The active portion centres around those elements whose lengths are near half wavelength at the operating frequency, and in this mode the forward tilting of the elements has small effect. As the operating frequency is increased or decreased the resonant length moves forward or backward. This scheme ensures a unidirectional beam and provides increased directivity. Tremendous bandwidths (better than 20 : 1) have been obtaind with a relatively compact array.

In contrast to the angular antenna, the logarithmically periodic antenna can be called a pseudo frequency independent antenna, as its electrical properties vary periodically with the logarithm of the frequency.

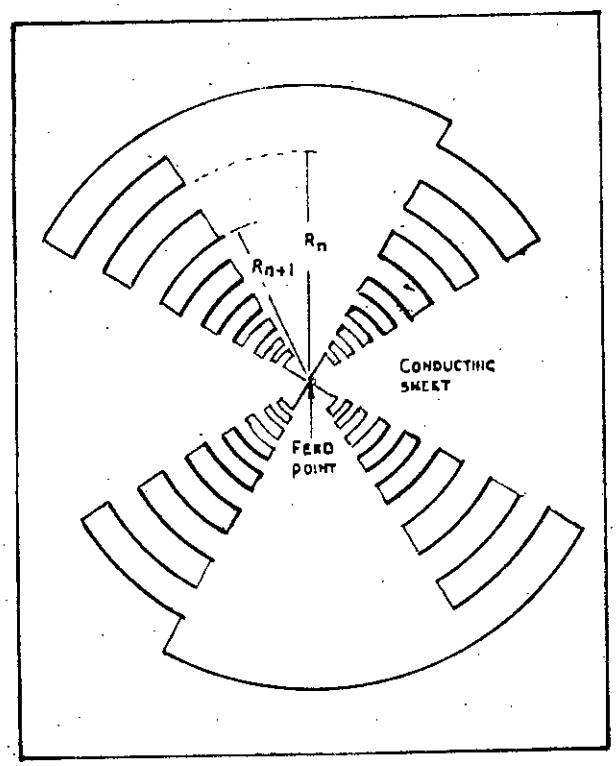

FIG. 6. SHEET METAL LOG PERIODIC ANTENNA

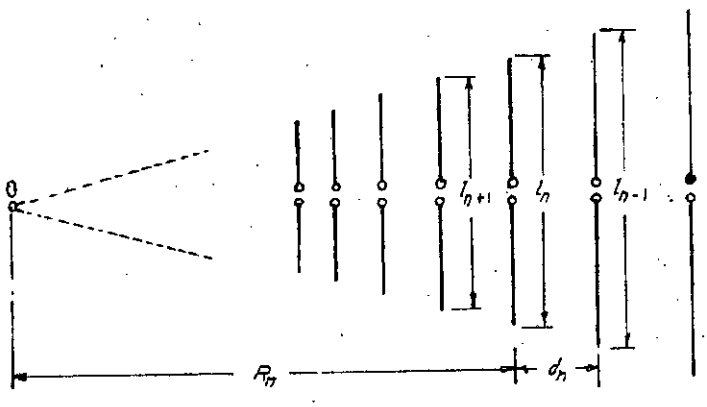

FIG. 7. LOG PERIODIC DIPOLE ARRAY

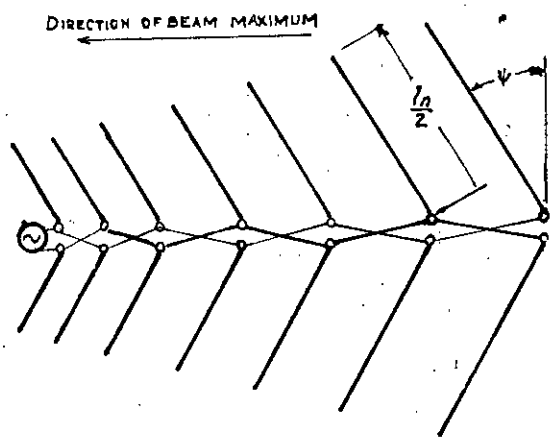

FIG. 8. LOG PERIODIC RESONANT-V ARRAY

C H A P T E R - III

THE PROBLEM AND THE PRESENT POSITION

THE PROBLEM AND THE PRESENT POSITION

The purpose of the present experiment is to study the electrical characteristics of a type of antenna similarly constructed as shown in the Figs. 14 and 30. First a single antenna similar to one shown in Fig. 14 will be studied and its electrical characteristics will be measured at different frequencies. Next two identical antennas of above kind will be placed at the opposite sides of a square base pyramid and the electrical characteristics of the combined antennas will be measured. Finally four identical antennas will be placed at the four sides of a square base pyramid and the combined electrical characteristics will be studied.

In the same way four identical antennas each constructed similar to Fig. 30 will be placed at the four sides of a square base pyramid and the antennas at the opposite sides will be shorted at the smaller ends and they will be fed by a co-axial cable and the combined electrical characteristics will be calculated and studied. The dependance of the electrical characteristics with frequency will also be noted.

This particular problem is investigated with a view to observing whether frequency independent characteristics can be obtained. Although this particular problem has not been investigated before log-periodic dipole array has been investigated in some detail[2,4,6] because of the insight it gives into what are believed to be general requirements for successful frequency independent operation. Some of the recent developments of frequency independent and log-periodic antennas are shown in the accompaning Figs. 9,10 taken from reference 1.

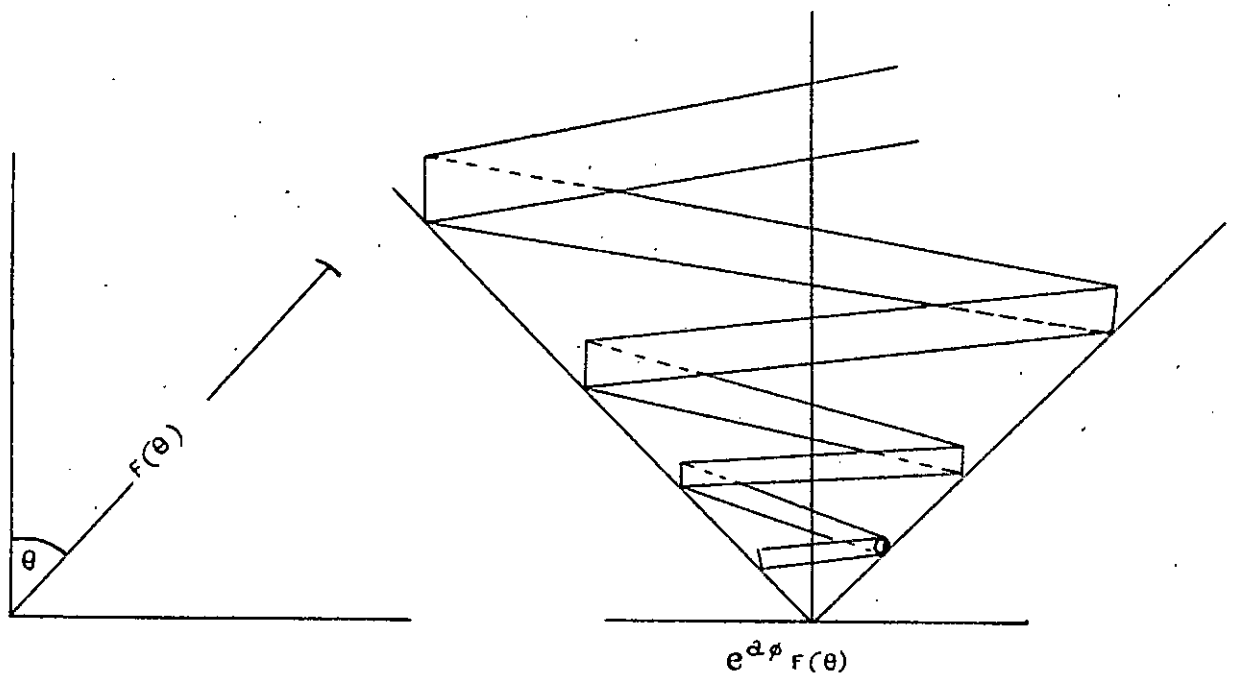

FIG. 9. FREQUENCY INDEPENDENT ANTENNA DESIGN

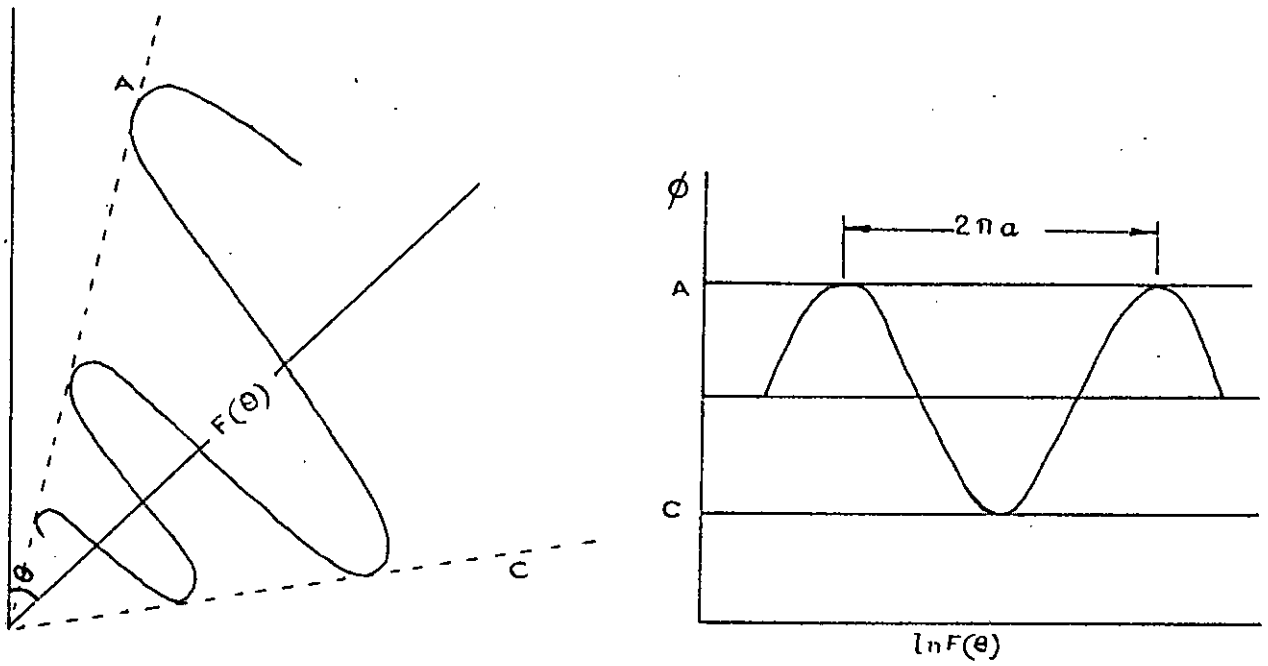

FIG. 10. LOG-PERIODIC ANTENNA DESIGN

C H A P T E R - IV

THEORETICAL INVESTIGATION

THEORETICAL INVESTIGATION

The performance of an antenna would remain constant if the ratio between the physical dimensions of an antenna and the operating wavelength was kept constant. This leads to the conclusion that antenna specified entirely by angles should exhibit the above characteristics. But the most serious draw back to the above approach is that the structure must extend to infinity since otherwise it must have at least one dimension to be specified in linear unit[1]. Now if the performance of the infinite structure can be approximated by that of a finite one above drawback can be overcome. The problem is then to determine how rapidly, if at all, the performance of the finite structure converges to that of the infinite one.

Before investigating into this problem let us find a general solution of a frequency independent antenna.

GENERAL APPROACH

To illustrate the general approach let us consider all plane curves which remain essentially the same when scaled to a different unit of length[1]. Such curves can be used to determine the shape of a plane sheet antenna by taking the input terminal at the common point of intersection of four curves as shown in Fig. 11.

It follows that the antenna is unchanged when scaled to a fixed wavelength provided we add the condition that the terminals stay fixed when the scale is changed. Now the fact that a typical curve remains essentially unchanged by a change of scale implies that the new curve can be made to

coincide with the old one by translation and rotation. Since a translation is eliminated by the requirement that the common point remains fixed, the problem is to determine all curves such that a change of scale is equivalent to rotation. This can be stated symbolically in the form

$$Kr(\phi) = r(\phi + C) \quad \ldots\ldots\ldots \quad (1)$$

where $r(\phi)$ denotes the radius r as a function of the polar angle ϕ, K is the scale change and C is the angle of rotation to which it is equivalent. Thus K depends upon C but K and C are independent of ϕ and r.

$$r(\phi)\frac{dK}{dC} = \frac{\partial r(\phi + C)}{\partial C} \quad \ldots\ldots\ldots\ldots\ldots\ldots \quad (2)$$

$$K\frac{dr(\phi)}{d\phi} = \frac{\partial r(\phi + C)}{\partial \phi} \quad \ldots \quad \ldots\ldots \quad (3)$$

But, $$\frac{\partial r(\phi + C)}{\partial C} = \frac{dr(\phi + C)}{d(\phi + C)} = \frac{\partial r(\phi + C)}{\partial \phi} \quad \ldots \quad (4)$$

So, $$r\phi\frac{dK}{dC} = K\frac{dr(\phi)}{\partial \phi} \quad \ldots \quad \ldots \quad (5)$$

Or $$\frac{dr}{d\phi} = ar \quad \ldots \quad \ldots \quad \ldots \quad (6)$$

Where $a = \frac{1}{K}\frac{dK}{dC}$ and hence independent of ϕ

From (6) $r = r_o e^{a\phi} \quad \ldots \quad \ldots \quad \ldots \quad (7)$

Where r_o is a constant.

Now, let us measure r in terms of wavelength

So, $$r' = \frac{r}{\lambda} = \frac{r_o e^{a\phi}}{\lambda} = \frac{r_o e^{a\phi}}{e^{\ln\lambda}} = r_o e^{a\left(\phi - \frac{\ln\lambda}{a}\right)}$$

Or, $r' = r_o e^{a(\phi - \phi_o)} \quad \ldots \quad \ldots \quad (8)$

Where $\phi_o = \frac{\ln\lambda}{a}$

The equation (8) contains two parameters, a, which represents the rate of expansion and ϕ_o which represents the orientation. The equation(7) and (8) remain identical except in the case that in the later case there is a rotation by ϕ_o . The general problem is to find all surfaces which have the property that a change in the unit of length is equivalent to a certain rotation. The above drawback can also be eliminated if we can replace the rotation by uniform expansion.

V.H. Rumsey has shown[1] that any antenna structure that can be described by the equation,

$$r = e^{a(\phi + \phi_o)} F(\theta) \qquad \ldots \qquad \ldots \qquad (9)$$

where r, θ and ϕ are the usual spherical coordinates, a and ϕ_o are constants, $F(\theta)$ is a function of θ , then the operation of the antenna will be independent of frequency.

It has also been pointed out that the currents on the antenna described by equation (9) follow a spiral path[1] and a resonance will build up in the current distribution where the mean circumference of this spiral is about one wavelength. This resonance is highly damped by radiation so that most of the current is dissipated at the region of resonance. This results in negligible end effect so that the performance of the finite structure is almost the same as that of the infinite one.

BASIC APPROACH TO THE ANALYSIS OF ANTENNA ARRAY

Let an array of equispaced isotropic radiators be constructed as shown in the Fig. 12. The elements having equal current amplitudes and a spacing d less than one half of operating wavelength. At a distant point the electric fields from these radiators will add with a phase angle between them which is dependent upon the relative phasings of the radiator currents

and the relative phase delays produced by the difference in path lengths to the distant point[4].

For the array shown in Fig. 12 the phase difference due to path length difference between adjacent elements is $(2\pi/\lambda)\, d \cos\phi$ radians. If the elements of the array are fed with a progressive phasing of currents equal to α, where α represents the angle by which the current in a given element leads the current in the preceding element, then at the distant receiving point the phase difference of the fields produced by adjacent elements will be

$$\psi = \alpha + \frac{2\pi}{\lambda} d \cos\phi = \alpha + Kd \cos\phi \quad \ldots \quad \ldots \quad (10)$$

Where $K = 2\pi/\lambda$ is the freespace phase shift constant.

The total electric field at any distant point will be given by the phasor sum

$$E_t = E_o \left[1 + e^{j\psi} + e^{2j\psi} + \ldots\ldots e^{j(n-1)\psi} \right] \quad \ldots \quad (11)$$

Or,
$$E_t = E_o \frac{e^{jn\psi} - 1}{e^{j\psi} - 1} \quad \ldots \quad \ldots \quad (12)$$

So E_t to be maximum $\frac{dE_t}{d\psi} = 0 = jn\psi$ ...(13)

So maximum radiation angle ϕ_m is given by

$$\cos\phi_m = -\frac{\alpha}{Kd} \quad \ldots \quad \ldots \quad (13)$$

Now if the elements are fed in phase i.e. $\alpha = 0$, $\phi_m = 90^\circ$ maximum radiation is broadside. If sucessive elements are fed with a lagging phase value, $\alpha = -Kd$ then $\phi_m = 0$, so the maximum radiation is entirely in the forward direction[4]. And an endfire radiation in the forward direction will be obtained. For values of α between $-Kd$ and $+Kd$, the angle of maximum radiation is at an angle between 0° and 180° as given by equation (13).

By symmetry about the axis of the array, there is another maximum at an angle

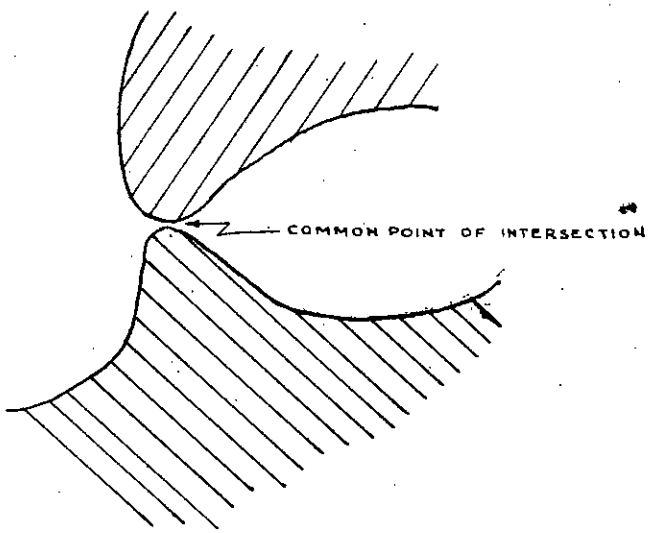

FIG. 11. INTERSECTION OF FOUR CURVES

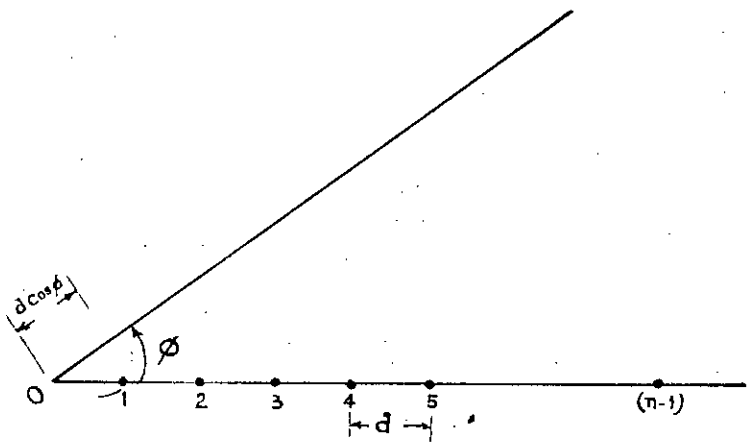

FIG. 12. ARRAY OF EQUISPACED ISOTROPIC RADIATORS

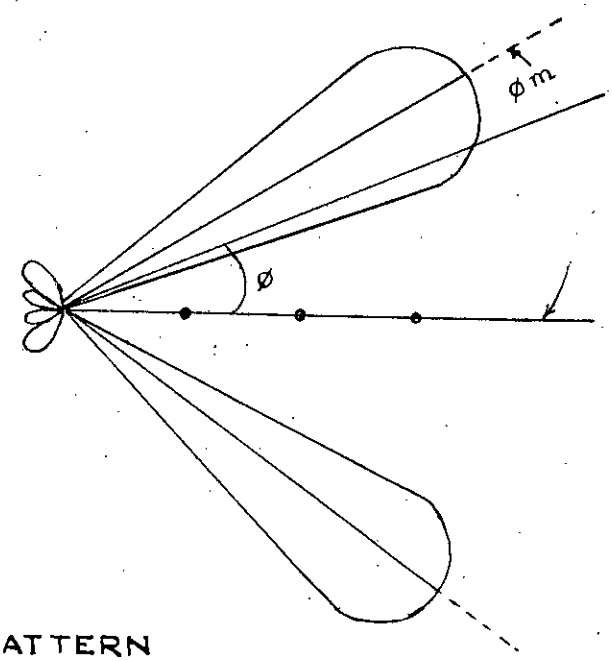

FIG. 13. RADIATION PATTERN

between 0° and -180°, which is also given by equation (13). The equation can not be satisfied for any real value of ϕ_m for $|\alpha| > Kd$.

The resultant radiation pattern E_t for the array under discussion is shown[4] in Fig. 13 for different values of ϕ for some chosen values of α, λ and d.

ANTENNA UNDER INVESTIGATION

An antenna was constructed as shown in the Fig. 14. When the resonance frequency is reached one of the elements of kk', jj', ii'... aa' will rediate and the elements kj', ji' .... cb', ba' will cause progressive phase difference. The 30° envelope was chosen so that the operating length becomes $\lambda/4$ in the range of frequencies 250 Mc/s to 950 Mc/s.

Let us picture the above structure in the Z - plane from w-plane by the following transformation[2,7].

Let $z = \ln w$ ... ... (14)

where w and z are in general complex numbers, if

$z = x + jy$ and $w = \rho e^{j\theta}$ ... ... (15)

Then, $x = \ln\rho$ and $y = \theta$ ... ... (16)

The elements are pictured in the z-plane as shown in the Fig.15. The distance is measured from the apex of the array and the elements are numbered starting with the largest element as number 1.

Let us consider a particular frequency f at which element 4 is $\lambda/4$ long. In the transmission region (element 13 to 7), the amplitude of voltage along the line is approximately constant and the phase snift between element position increases gradually. In the active region(elements 7 to 4) the amplitude drops sharply because of power absorbed by the strongly

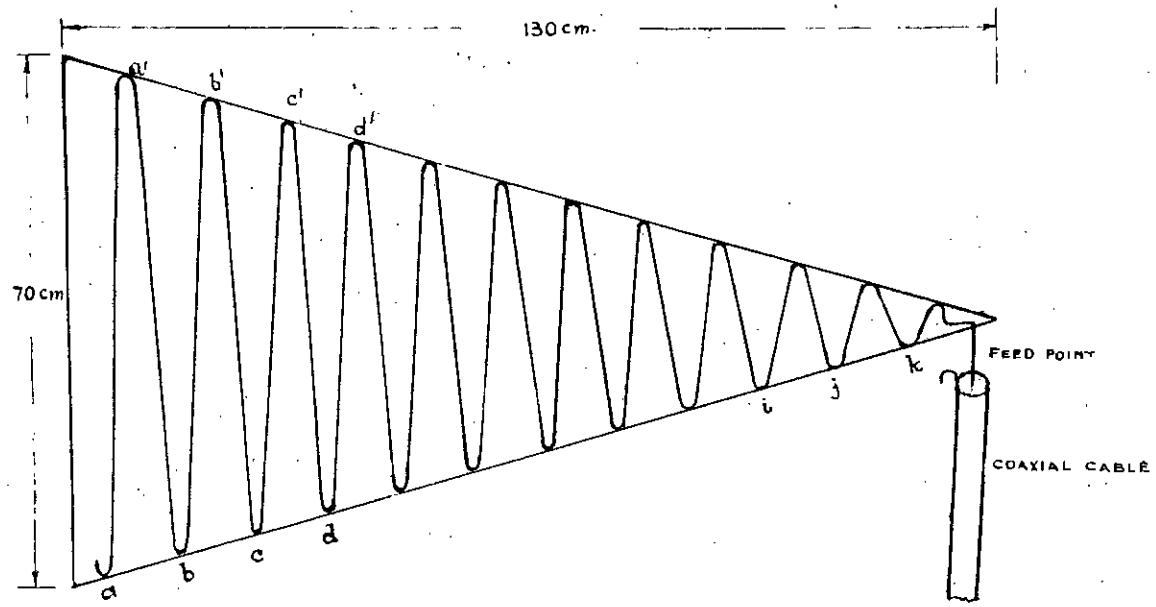

FIG. 14. SINGLE ANTENNA UNDER INVESTIGATION

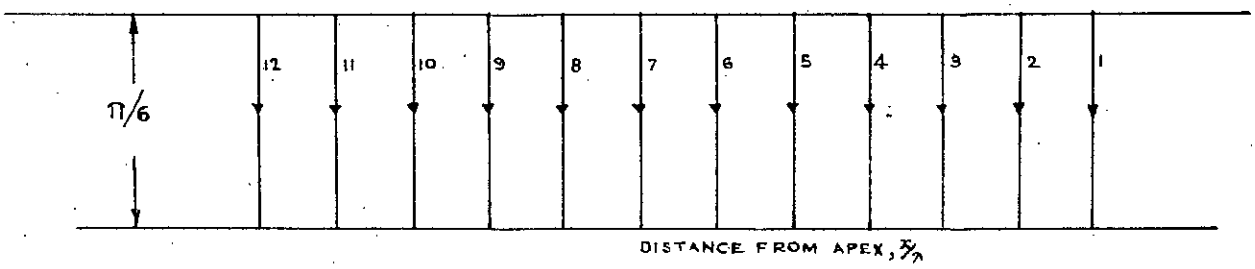

FIG. 15. Z-PLANE PICTURE OF THE ANTENNA ARRAY

radiating elements, and the phase shift averages about 90° between adjacent elements. In the unexaited or reflection region (element 3 to 1) the amplitude drops to very \$low values and the phase shift between element positions is very small[4].

From the consideration of current amplitudes it is evident that the only elements that will contribute appreciably to the radiation are elements 7,6,5 and 4. For these elements the phase difference between adjacent numbers is approximately 90° leading and so a back fire radiation will be expected.

As the operating frequency is decreased or increased the active region impedance remain almost constant. Since from the construction of the antenna the radiating elements are not perpendicular to the axis but inclined at an angle, the radiation will not be exact back endfire but at an angle ϕ_m. It may be concluded that there are three distinct regions on the antenna array[4] namely,

1. Transmission line region.

The antenna elements in the transmission region are short compared with the resonant length, so the element presents a relatively high capacitive impedance. The element current leads the preceding element current approximately by $\alpha = \pi - \beta d$ where d is the element separation and $\beta = 2\pi/\lambda$. Because of the phasing and close spacing of the elements radiation from this region will be very small and in the back fire direction.

2. Active region.

In the active region the element length approach the resonant length so the element impednace has an appreciable resistive component. The current is slightly leading just below resonance and slightly lagging just above a

resonance. This combination of condition will produce a strong radiation in the backfire direction.

3. Reflection region.

The element lengths in the reflecting region are greater than the resonant length so the element impedance becomes inductive. The small amount of radiation is still in the backfire direction.

C H A P T E R - V

EXPERIMENTAL INVESTIGATION

EXPERIMENTAL INVESTIGATION

The experimental investigation can be divided broadly into two parts (i) Measurement of Radiation Intensities (ii) Measurement of Input Impedance.

The radiation intensities were measured by heterodyne principle and the input impedance was calculated by using a slotted transmission line. The experimental set up for the measurement of radiation intensities is shown in Fig. 16. And the experimental set up for the measurement of input impedance is shown in Fig. 25. The process included the reading of the final result from a Smith Chart.

A. Single Antenna under Investigation.

A simple antenna was constructed as shown in Fig. 14. The radiators were placed at an equal distance, and the axis of the antenna was placed horizontally at a height of 1.5m from the ground. The antenna was fed from a signal generator. The input to the antennas was given by the inner conductor of a co-axial cable and the outer conductor was kept open. Now the frequency of the local oscillator was varied slowly and when the difference between the fed frequency and the frequency of the local oscillator became 30 Mc/s, IF Amplifier indicator showed deflection indicating the radiation intensity at the point where the test antenna was placed. By repeating this procedure the radiation intensities were measured at a distance of 4m from the antenna at an interval of 10 degrees between the frequency range of 250 Mc/s to 900 Mc/s. Zero degree position was counted

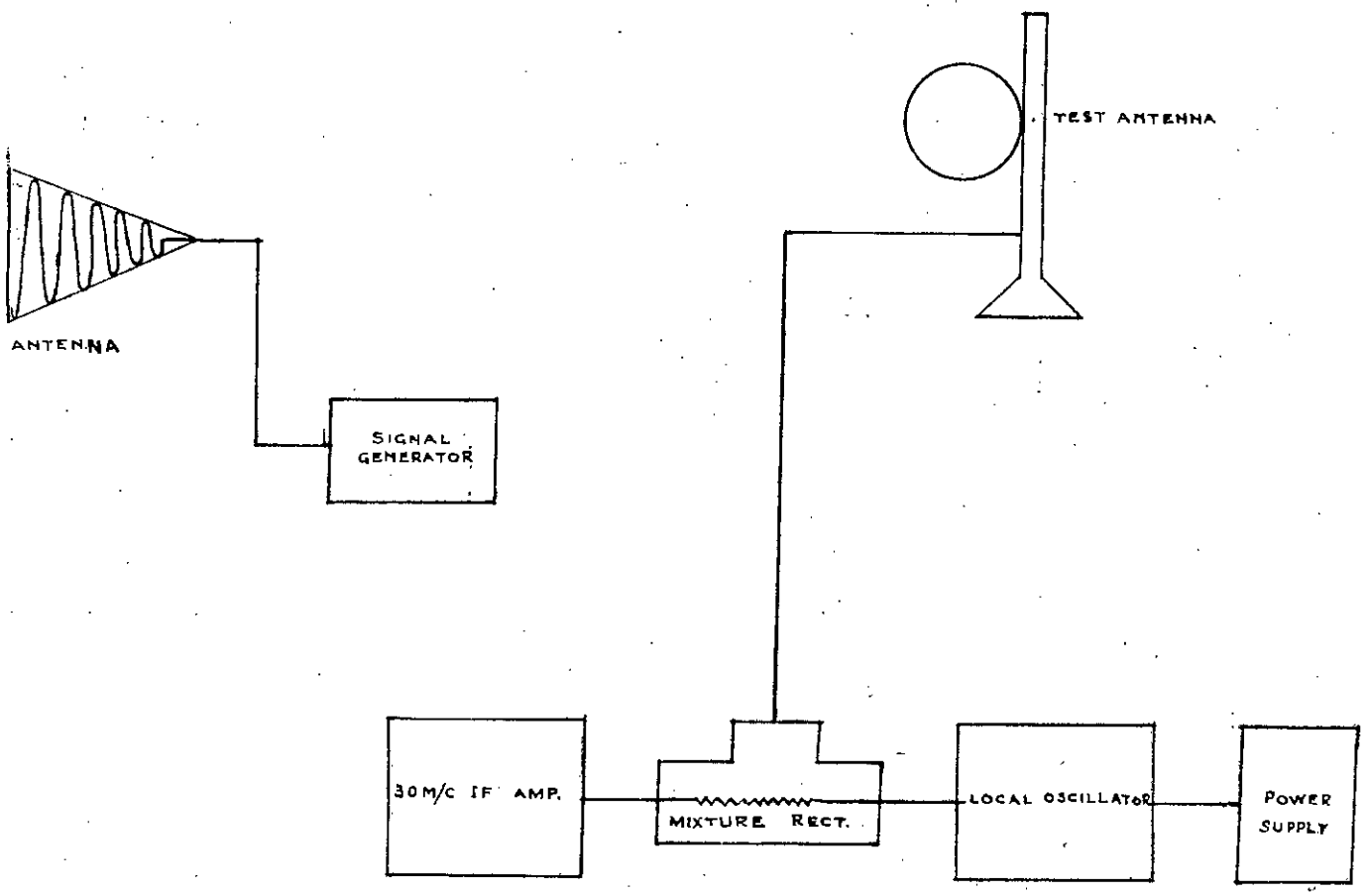

FIG. 16. EXPERIMENTAL SET UP FOR THE MEASURMENT OF RADIATION PATTERN

from the line on which the apex of the antenna would fall when the axis of the antenna was made horizontal. The measured values are shown in the table I and the radiation patterns are shown in Figs. 17a,17b,17c,17d,17e 17f,17g,17h.

Next to measure the input impedance of the antenna, one end of the transmission line was fed by the signal generator and the other end was shorted. The output from the transmission line was given to a microammeter. The microammeter did not indicate anything. Now, when the length and position of the stub were changed, the ammeter indicator showed some deflection and by proper adjustment, maximum deflection was obtained. Now a voltage standing wave pattern was on the transmission line. Next the short circuit was removed and the antenna under investigation was put in that position with the help of a co-axial cable. This time also a standing wave pattern was obtained but the position of the minimum current was shifted. The shift was measured in terms of the operating wavelength. The values of maximum and the minimum currents were measured. Now with the help of a calibration curve shown in Fig. 18 corresponding values of voltages were found. The VSWR, S was obtained by taking the ratio of $V_{max.}/ V_{min.}$ The minimum value of the impedance i.e. resistive portion was obtained from the relation $Z_{min} = 50/S$. This point was noted on a Smith Chart. The length of the co-axial cable was measured in terms of the operating wavelength. The point on the Smith Chart was moved either towards the generator end or towards the load end as the case might be according to the shift of the position of minimum current. The point was further moved towards the load end to a distance equal to the length of the co-axial cable. This final position of the point on the Smith Chart gave the value of the input impedance at that frequency as shown in Fig.19.

By repeating this procedure the values of the input impedance were calculated at different freqeuncies. The calculated values are shown in table II. Impedance vs. frequency curve is shown in Fig. 20.

TABLE - I

MEASUREMENT OF RADIATION INTENSITIES

SINGLE ANTENNA

AXIS HORIZONTAL

250 MEGA CYCLES

Pos.in deg.	Radiation in db.	Pos.in deg.	Radiation in db.	Pos.in deg.	Radiation in db.
0	29.0	120	16.0	240	22.0
10	33.0	130	16.0	250	16.0
20	24.5	140	23.0	260	20.0
30	25.0	150	23.0	270	25.0
40	30	160	19.0	280	26.0
50	23.0	170	17.0	290	25.5
60	28.0	180	17.0	300	29.0
70	26.0	190	18.5	310	23.0
80	17.5	200	21.0	320	28.0
90	25.0	210	18.5	330	25.0
100	24.0	220	22.0	340	27.0
110	17.0	230	22.5	350	28.0

300 MEGA CYCLES

0	22.0	120	23.0	240	12.0
10	25.0	130	21.5	250	18.0
20	32.0	140	19.0	260	16.0
30	35.0	150	18.0	270	19.0
40	29.0	160	16.5	280	18.0
50	30.5	170	170	290	26.5
60	15.0	180	18.0	300	28.5
70	22.0	190	19.0	310	28.0
80	19.0	200	17.5	320	24.0
90	22.0	210	18.0	330	30.0
100	18.5	220	10.0	340	33.0
110	25.0	230	13.0	350	28.0

400 MEGA CYCLES

Pos.in deg.	Radiation in db.	Pos. in deg.	Radiation in db.	Pos.in deg.	Radiation in db.
0	28.0	120	13.0	240	12.0
10	22.0	130	5.0	250	5.0
20	21.0	140	6.0	260	4.0
30	2.05	150	8.0	270	10.0
40	25.0	160	3.0	280	22.0
50	13.5	170	1.0	290	18.5
60	3.0	180	4.0	300	17.0
70	7.0	190	1.0	310	18.5
80	12.0	200	8.5	320	17.0
90	10.0	210	10.0	330	22.0
100	13.0	220	8.0	340	28.0
110	14.5	230	8.0	350	25.0

500 MEGA CYCLES

0	30.0	120	15.0	240	17.0
10	20.0	130	9.0	250	15.0
20	19.0	140	11.0	260	14.0
30	23.0	150	11.0	270	23.0
40	14.0	160	10.0	280	25.0
50	22.0	170	8.0	290	20.0
60	6.0	180	10.0	300	27.0
70	5.0	190	7.0	310	26.0
80	7.0	200	11.0	320	22.0
90	12.0	210	13.0	330	22.0
100	19.0	220	13.5	340	23.0
110	22.0	230	14.0	350	29.0

600 MEGA CYCLES

Pos.in deg.	Radiation in db.	Pos.in deg.	Radiation in db.	Pos. in deg.	Radiation in db.
0	29.0	120	17.0	240	22.0
10	31.0	130	12.0	250	26.0
20	28.0	140	15.0	260	23.0
30	30.0	150	13.5	270	27.0
40	30.0	160	16.0	280	22.0
50	27.0	170	15.5	290	26.0
60	18.0	180	16.0	300	24.0
70	19.0	190	14.5	310	24.0
80	15.0	200	15.0	320	26.5
90	19.0	210	16.0	330	29.5
100	23.0	220	17.5	340	30.0
110	20.0	230	20.0	350	31.0

700 MEGA CYCLES

0	21.0	120	16.5	240	19.0
10	20.0	130	15.0	250	14.0
20	28.5	140	16.0	260	15.0
30	27.0	150	16.5	270	12.0
40	20.0	160	14.0	280	14.0
50	19.0	170	14.0	290	19.0
60	19.0	180	12.0	300	21.5
70	21.0	190	18.0	310	26.5
80	22.0	200	17.0	320	27.5
90	20.0	210	18.0	330	21.0
100	18.5	220	13.0	340	21.0
110	20.0	230	13.5	350	26.0

800 MEGA CYCLES

Pos.in deg.	Radiation in db.	Pos.in deg.	Radiation in db.	Pos.in deg.	Radiation in db.
0	25.0	120	16.0	240	21.0
10	25.0	130	14.0	250	20.0
20	28.0	140	16.0	260	19.0
30	28.0	150	15.0	270	19.0
40	25.0	160	15.0	280	18.0
50	23.0	170	14.0	290	22.0
60	18.0	180	14.0	300	22.0
70	20.0	190	16.0	310	25.0
80	20.0	200	16.0	320	27.0
90	20.0	210	17.0	330	25.0
100	20.0	220	15.0	340	25.0
110	20.0	230	16.0	350	28.0

900 MEGA CYCLES

0	23.0	120	16.0	240	20.0
10	22.0	130	15.0	250	17.0
20	28.0	140	16.0	260	17.0
30	27.0	150	15.0	270	16.0
40	22.0	160	14.0	280	16.0
50	21.0	170	14.0	290	20.0
60	18.0	180	13.0	300	21.0
70	21.0	190	17.0	310	25.0
80	21.0	200	16.0	320	27.0
90	20.0	210	17.0	330	23.0
100	19.0	220	14.0	340	23.0
110	20.0	230	15.0	350	27.0

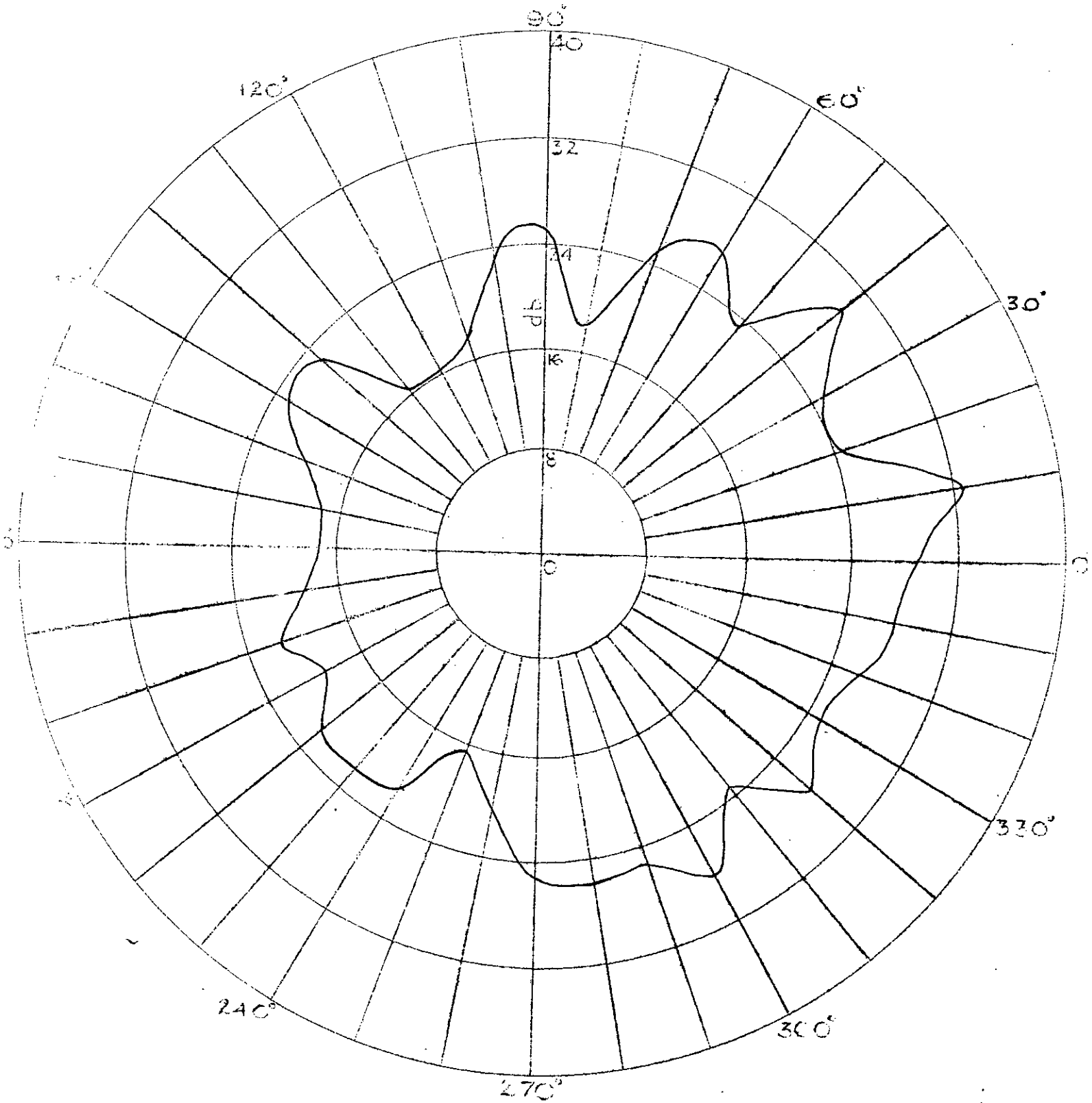

Fig. 17a Radiation Pattern at 250 Mega Cycles

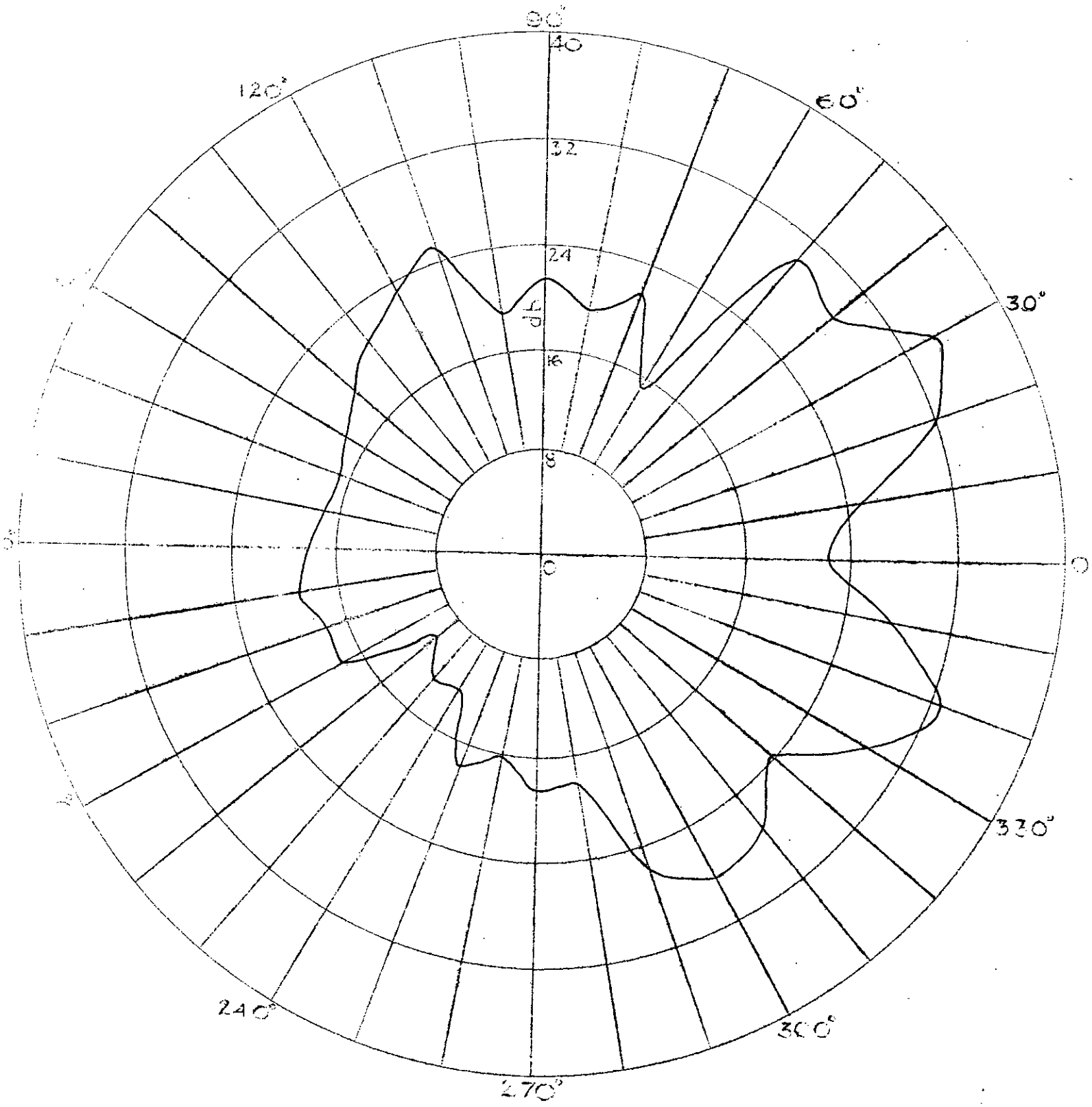

Fig. 17b Radiation Pattern at 300 Mega Cycles

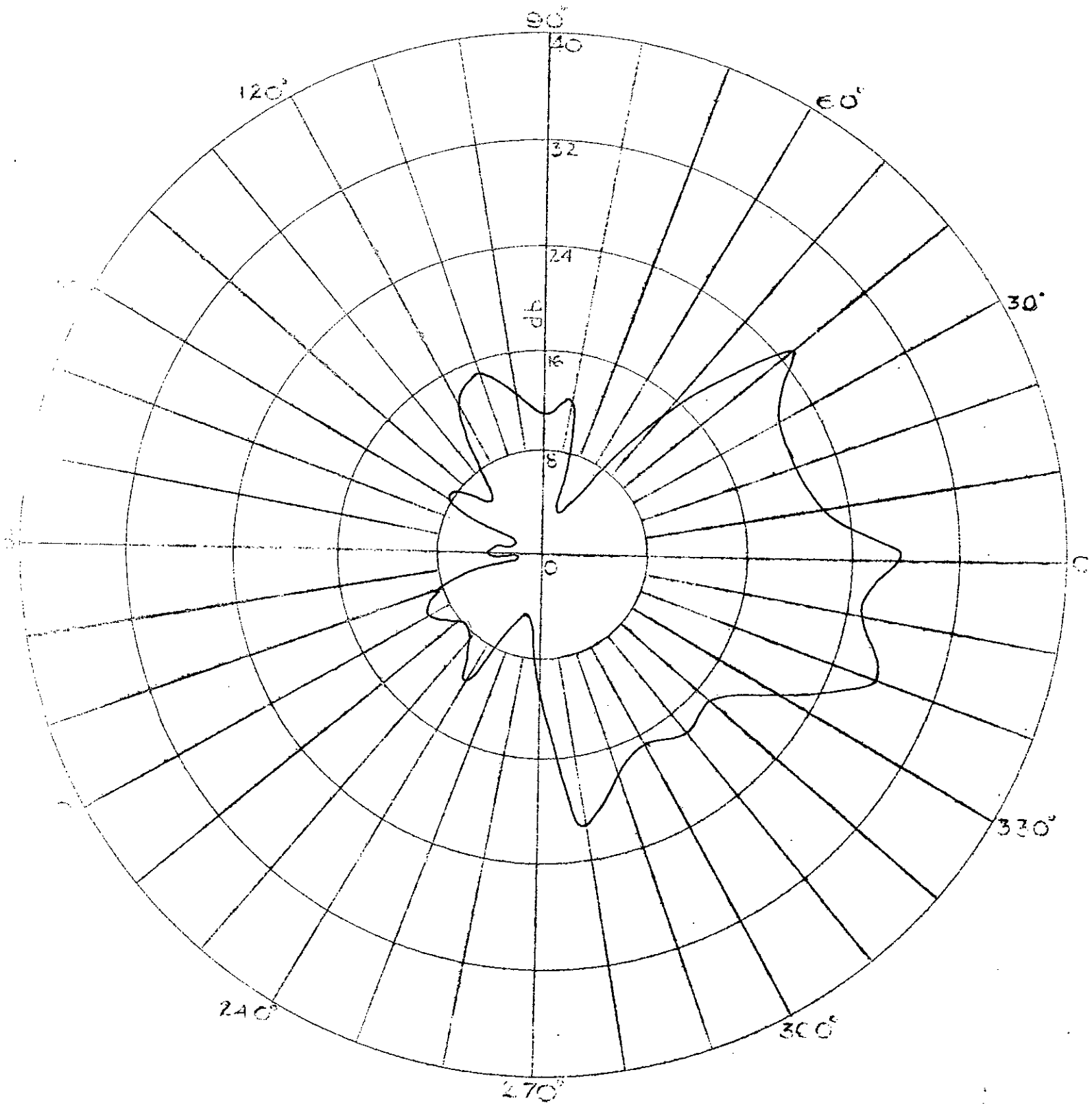

Fig. 17c Radiation Pattern at 400 Mega Cycles

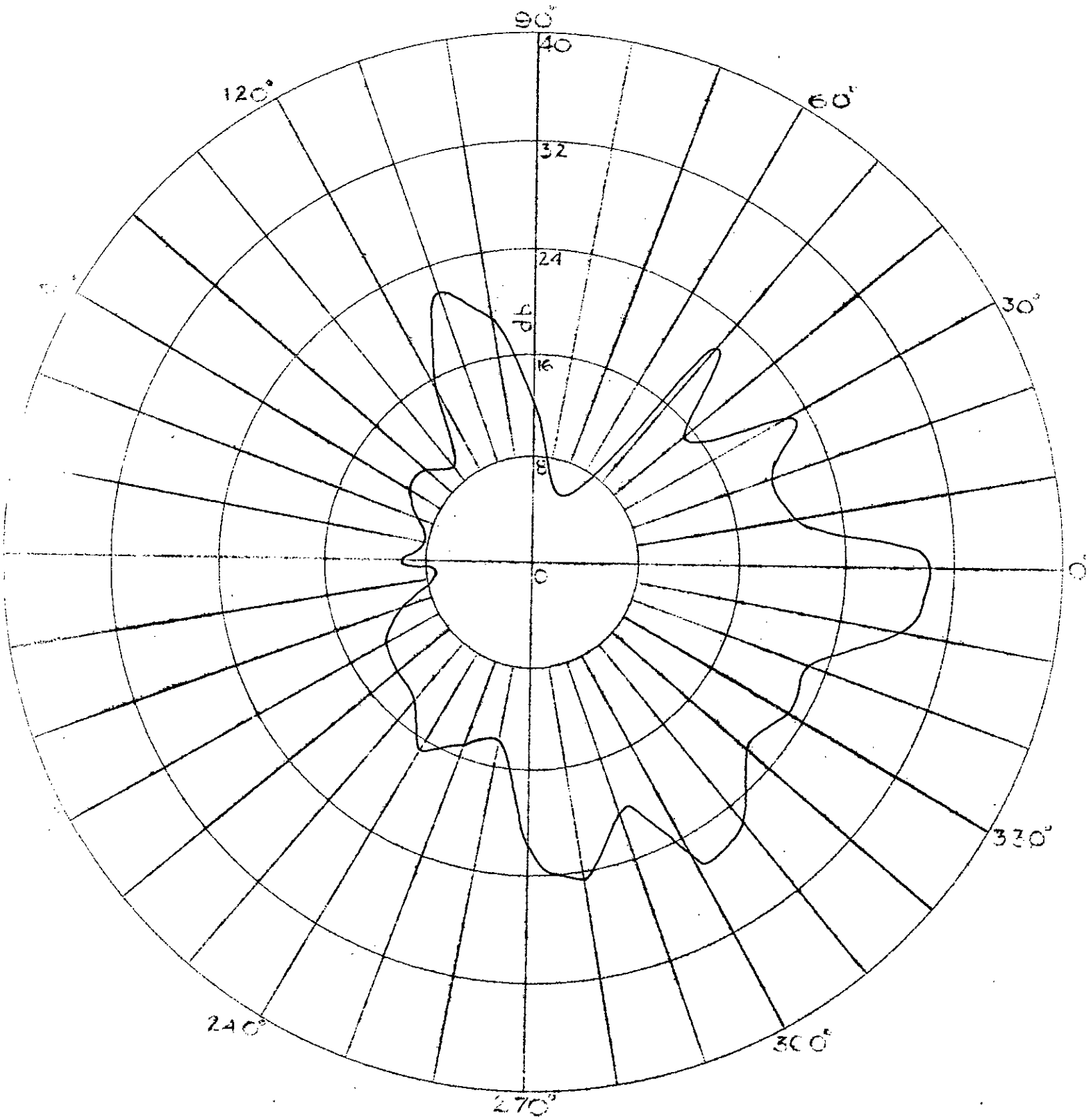

Fig. 17d Radiation Pattern at 500 Mega Cycles

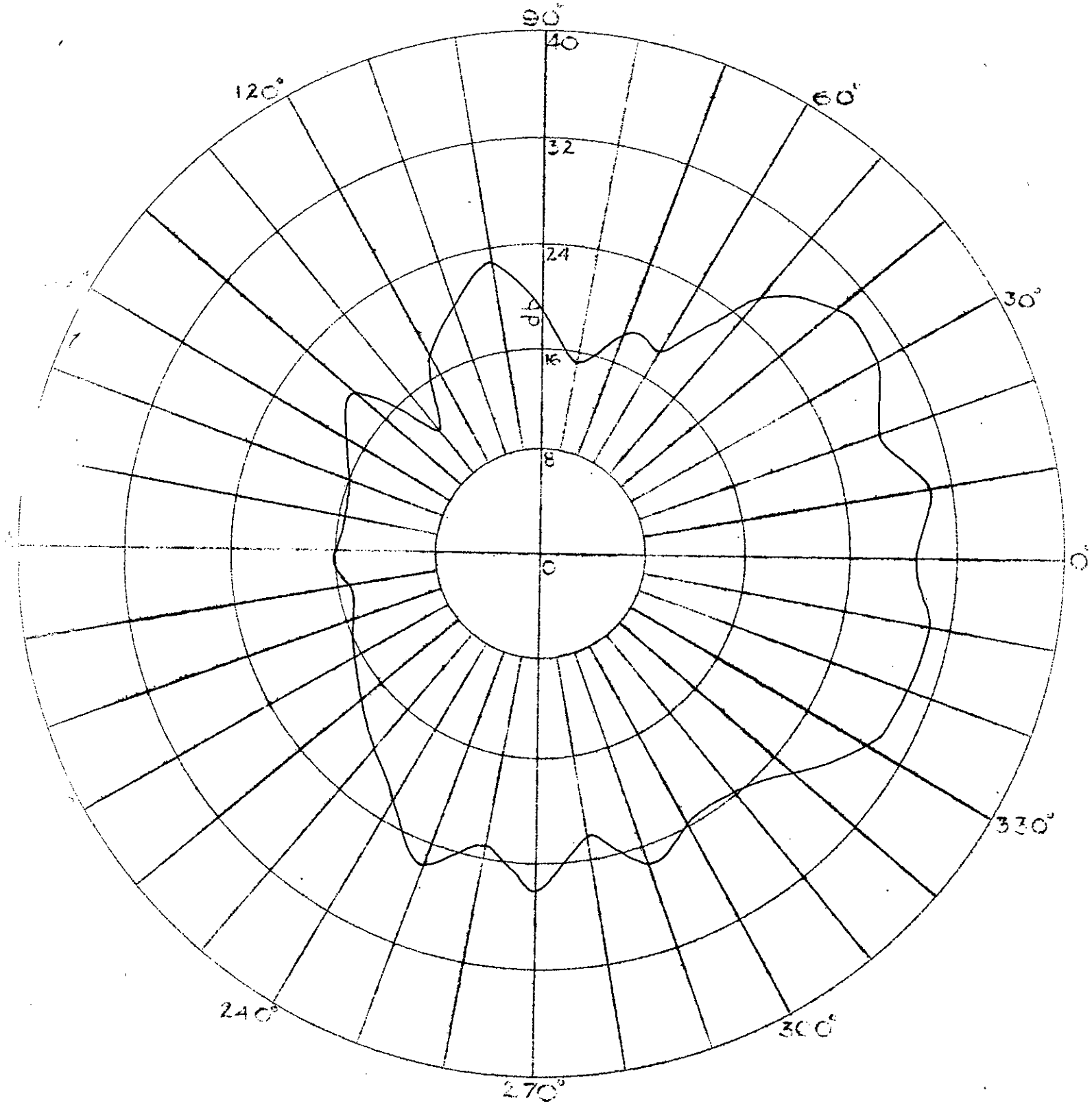

Fig. 17e Radiation Pattern at 600 Mega Cycles

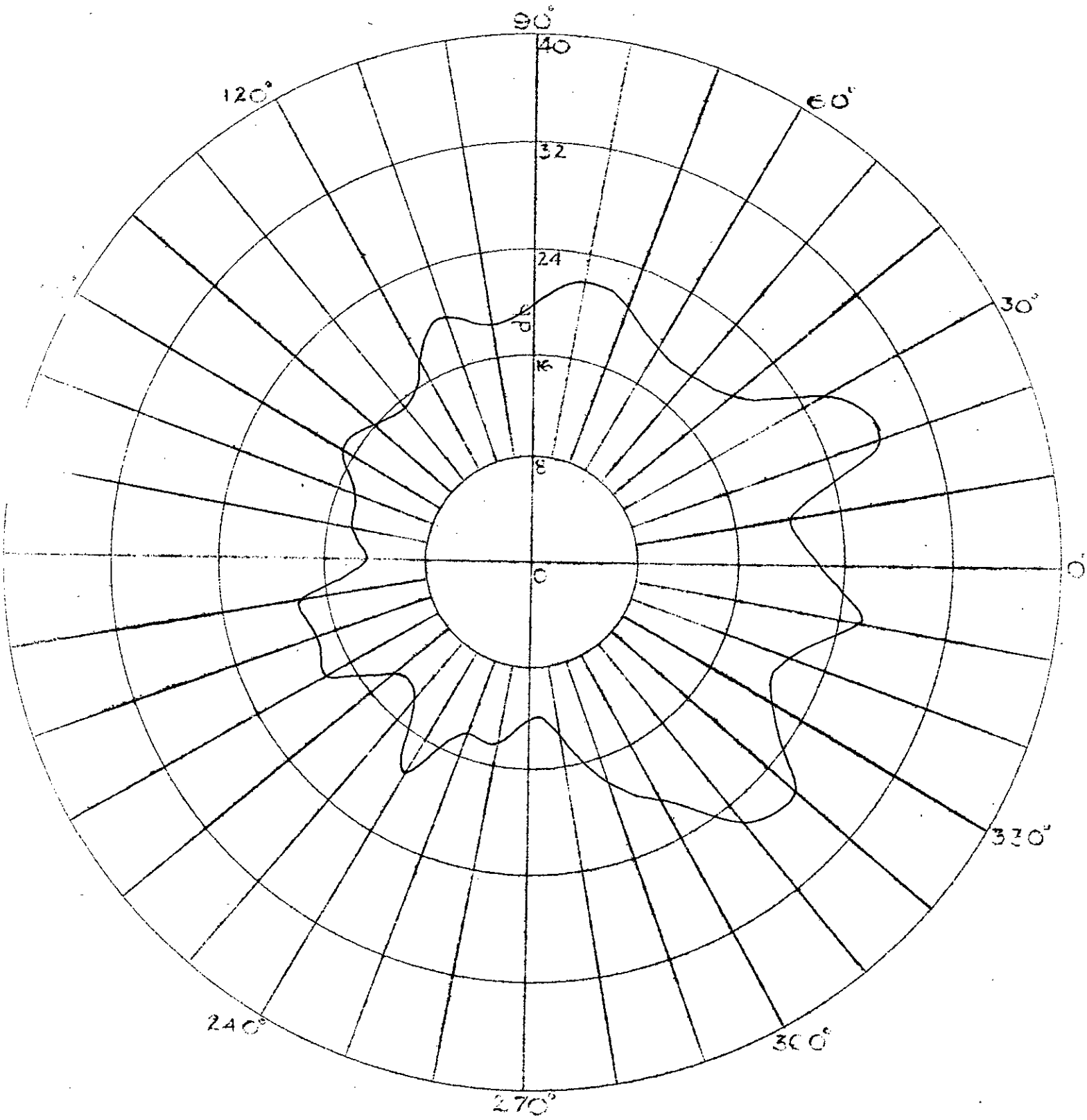

Fig. 17f Radiation Pattern at 700 Mega Cycles

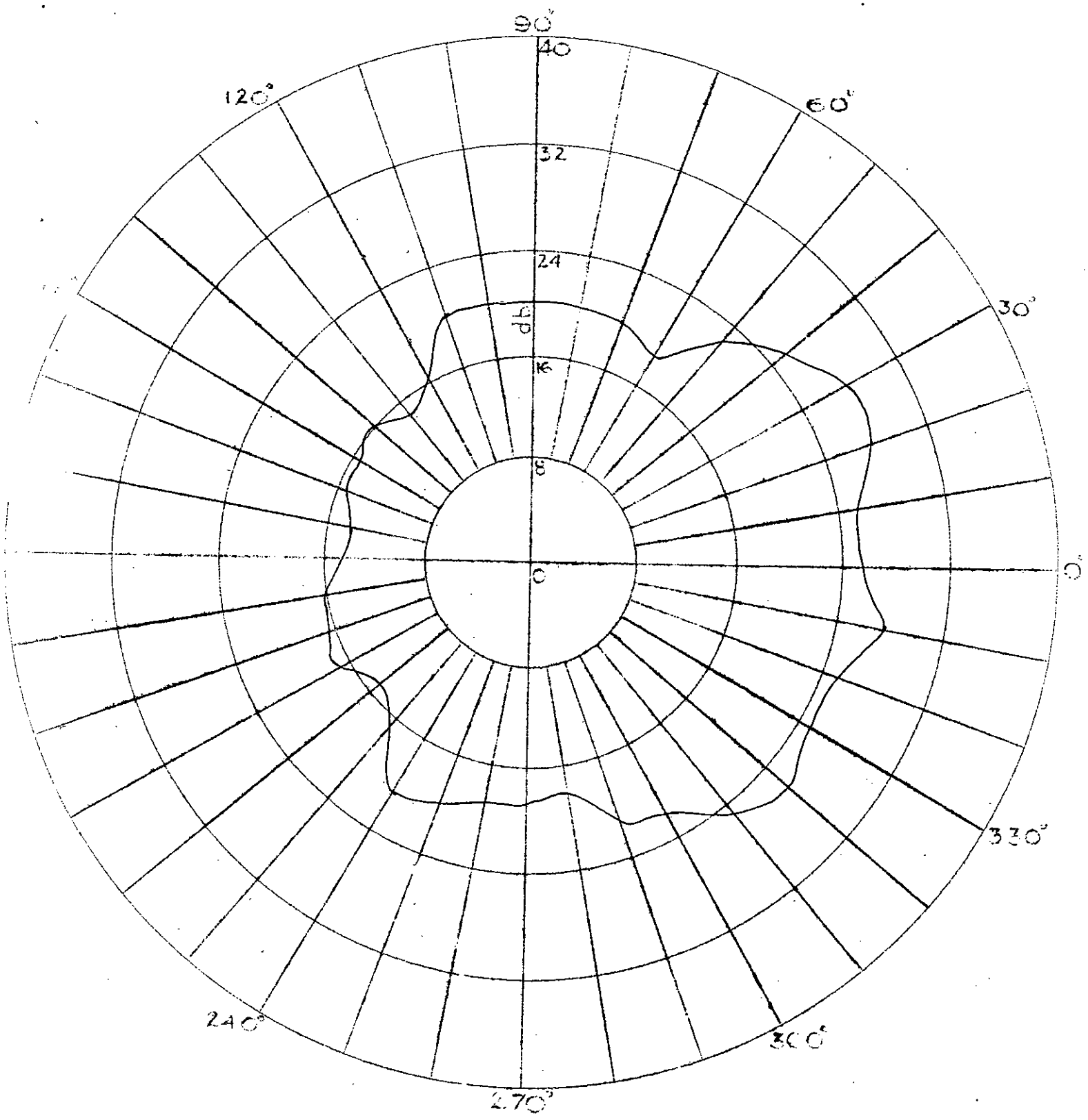

Fig. 17g Radiation Pattern at 800 Mega Cycles

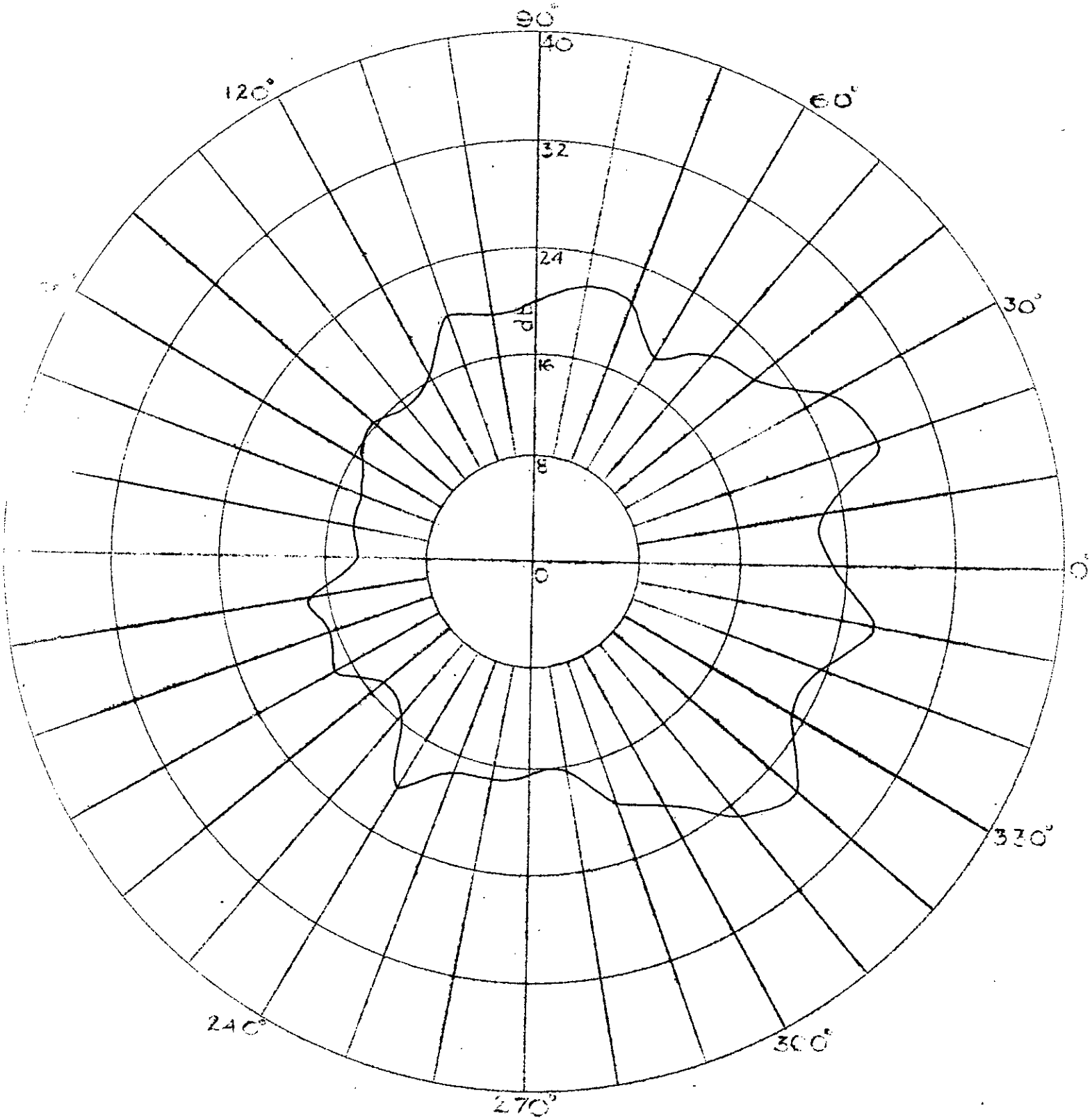

Fig. 17h Radiation Pattern at 900 Mega Cycles

TABLE - II

INPUT IMPEDANCE CALCULATION OF SINGLE ANTENNA

Freq. in Mc/s	Shift in Pos.of min.current in λ		$I_{max.}$ μ amp	$I_{min.}$ μ amp	V_{max} mV	V_{min} mV	VSWR S	$Z_{min.}$	Length of coaxl. cable in λ	Calculated impedance in Ohm.
	Gen.end	Load end.								
250	0.0291		7.0	0.5	1.79	0.15	11.45	4.4	1.540	5-j22.8
300	0.0100		8.8	0.6	2.20	0.20	11.00	4.6	1.850	15+j75
350	0.0700		15.4	0.6	3.75	0.15	25.00	2.0	2.160	2-j31.7
400	0.0400		15.0	0.55	3.66	0.18	20.00	2.5	2.462	3.5+j28
450	0.1725		12.0	0.30	2.95	0.10	29.50	1.7	2.765	3-j31.5
500	0.2150		17.5	1.10	4.24	0.30	14.10	3.6	3.082	7+j48.4
550		0.211	19.0	1.20	4.60	0.34	13.50	3.7	3.390	6.5-j41
600		0.200	24.0	1.00	5.80	0.30	19.60	2.7	3.700	5+j36
650		0.163	13.5	0.99	3.30	0.29	17.40	2.9	4.010	6-j53
700		0.059	23.5	4.50	5.67	1.20	4.74	10.5	4.340	17+j38.5
750		0.025	15.5	0.60	3.86	0.20	19.30	2.6	4.612	6-j53
800		0.0165	17.0	0.50	4.15	0.15	27.7	1.7	4.930	2.3 +j20
850	0.0852		22.5	1.10	5.40	0.30	18.0	2.8	5.210	6-j47
900	0.1000		22.0	1.50	5.32	0.41	13.0	3.9	5.54	45 +j20

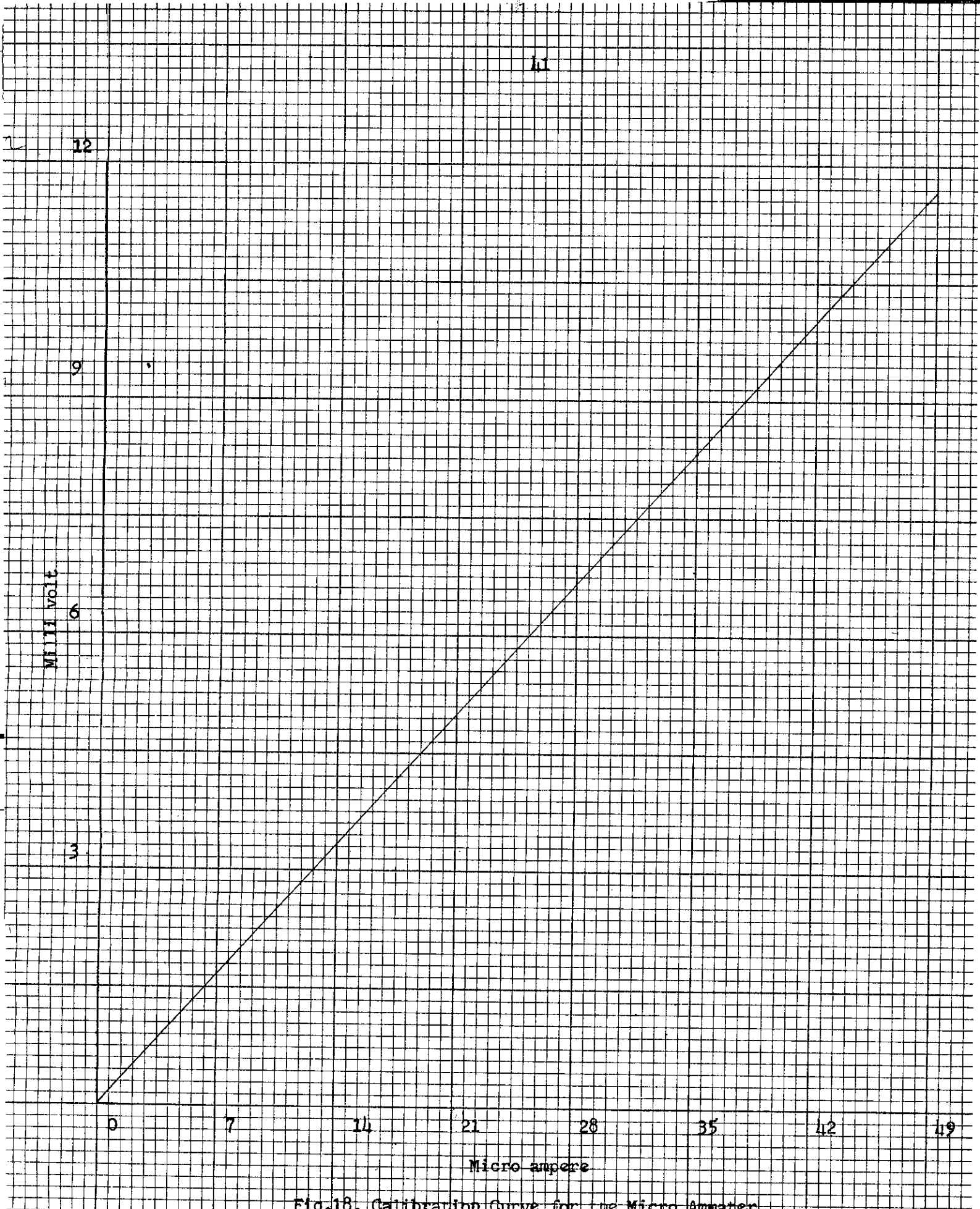

Fig.18. Calibration Curve for the Micro Ammater

TITLE

DATE

IMPEDANCE COORDINATES — 50-OHM CHARACTERISTIC IMPEDANCE

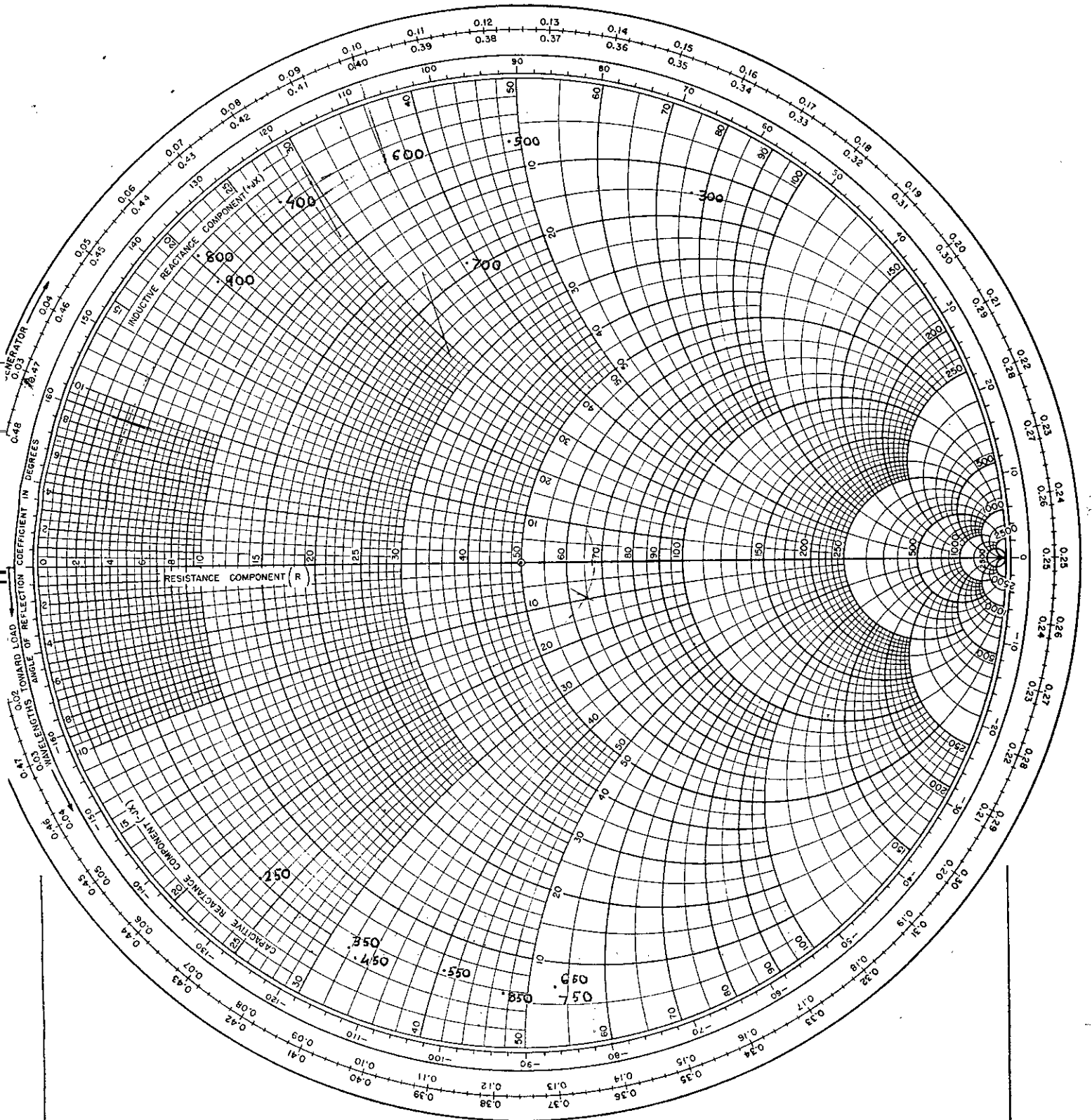

Fig. 19. Calculation of the Input Impedance of the Single Antenna

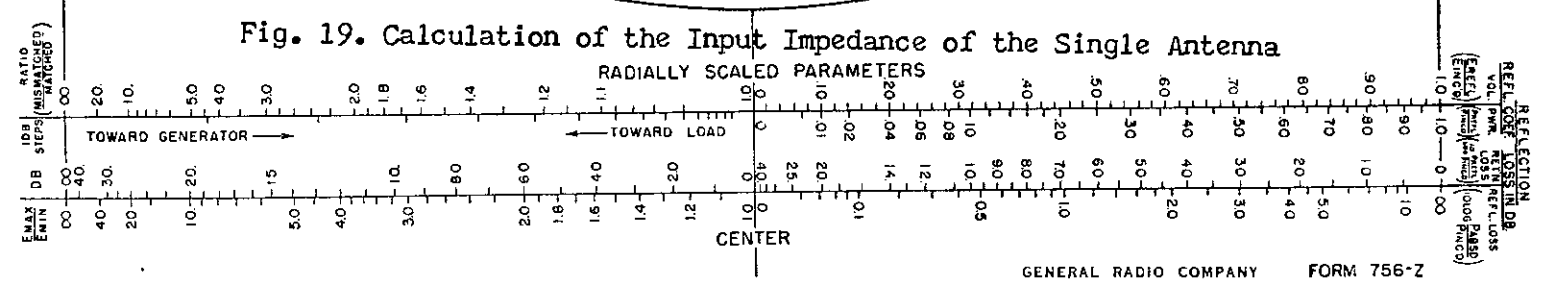

Electronics - VOL. 17, NO. 1, PP. 130-133, 318-325, JAN. 1944

GENERAL RADIO COMPANY
WEST CONCORD, MASS.

FORM 756-Z
Printed in USA

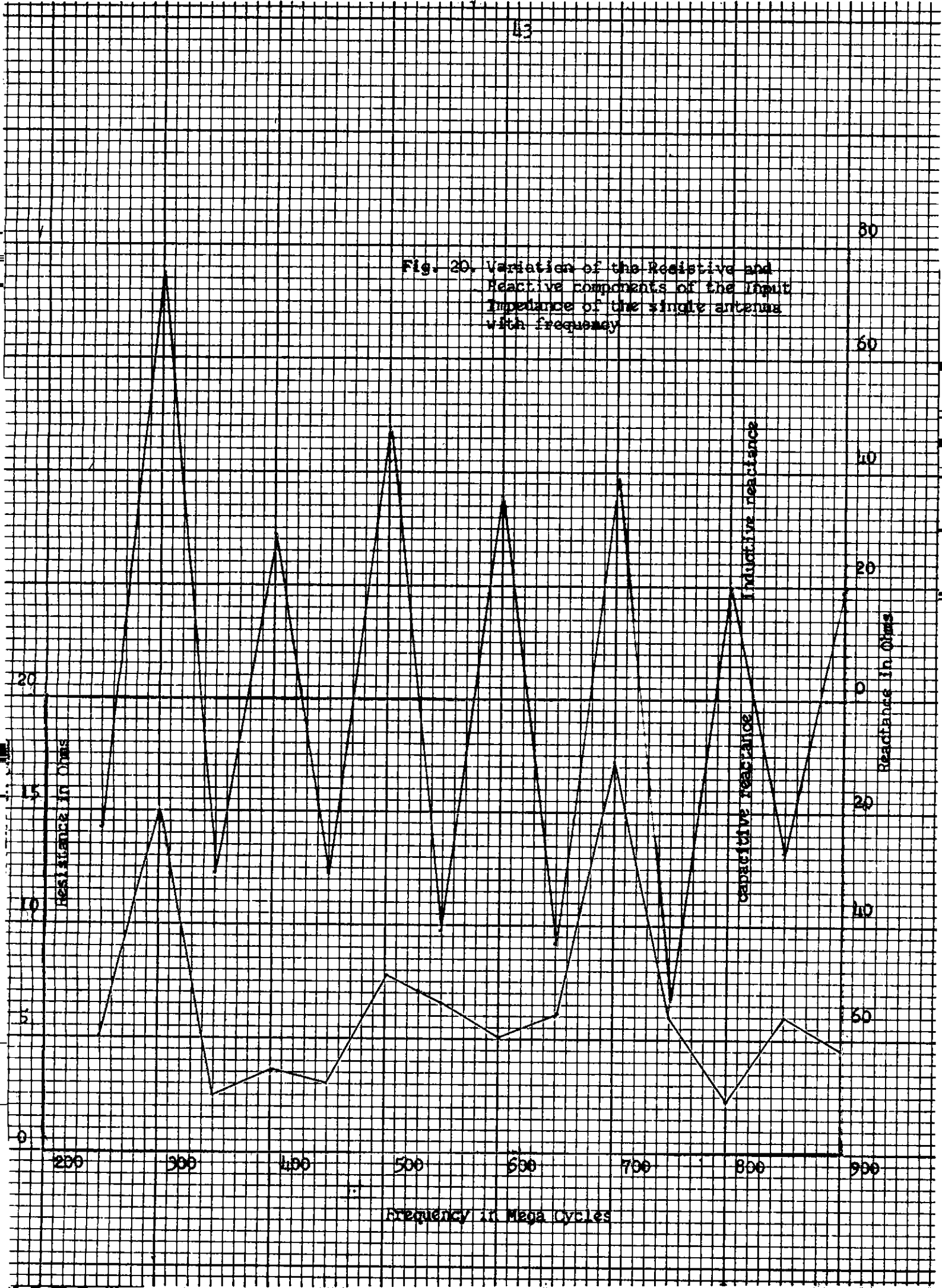

Fig. 20. Variation of the Resistive and Reactive components of the Input Impedance of the single antenna with frequency

B. COMBINATION OF TWO ANTENNAS UNDER INVESTIGATION

Two identical antennas each was as shown in Fig.14 were placed at the two opposite sides of a square base pyramid. One antenna was fed by the inner conductor and the otherwas fed by the outer conductor of the co-axial cable from the same signal generator. The other procedure of the experiment was identical as in 'A'. The measured values of the radiation intensities for the antenna axis horizontal is shown in table III and the radiation patterns are shown in Figs. 21a,21b,21c,21d,21e,21f,21g,21h.

For the vertical position of the antenna axis the measured values of the radiation intensities are shown in the table IV and the radiation patterns are shown in Figs. 22a,22b,22c.

The input impedances were calculated from a Smith Chart as shown in Fig.23. The values of the input impedance is shown in table V. The impedance vs. frequency curve is shown in Fig. 24.

TABLE - III

MEASUREMENT OF RADIATION INTENSITIES

TWO ANTENNAS COMBINED

AXIS HORIZONTAL

250 MEGA CYCLES

Pos.in deg.	Radiation in db.	Pos. in deg.	Radiation in db.	Pos.in deg.	Radiation in db.
0	34.0	120	11.0	240	19.0
10	39.0	130	21.0	250	24.0
20	39.0	140	23.0	260	25.0
30	37.0	150	24.0	270	25.0
40	33.0	160	24.0	280	22.0
50	28.0	170	20.0	290	23.0
60	22.0	180	19.0	300	27.0
70	22.0	190	20.0	310	28.0
80	26.0	200	21.0	320	26.0
90	26.0	210	18.0	330	30.0
100	25.0	220	20.0	340	33.0
110	22.0	230	18.0	350	26.0

300 MEGA CYCLES

0	32.0	120	14.0	240	19.0
10	40.0	130	21.0	250	20.0
20	39.0	140	21.0	260	24.0
30	36.0	150	20.5	270	25.0
40	28.0	160	20.0	280	25.0
50	23.0	170	13.0	290	24.0
60	20.0	180	13.0	300	25.0
70	28.0	190	16.0	310	26.0
80	29.0	200	18.0	320	28.0
90	25.0	210	16.0	330	35.0
100	23.0	220	18.0	340	36.0
110	19.0	230	18.0	350	27.0

400 MEGA CYCLES

Pos.in deg.	Radiation in db.	Pos.in deg.	Radiation in db.	Pos. in deg.	Radiation in db.
0	32.0	120	8.0	240	20.0
10	38.0	130	22.0	250	29.0
20	39.0	140	26.0	260	28.0
30	34.0	150	29.0	270	26.0
40	38.0	160	28.0	280	20.0
50	33.0	170	27.0	290	22.0
60	28.0	180	26.0	300	30.0
70	20.0	190	24.0	310	31.0
80	23.0	200	24.0	320	24.0
90	27.0	210	20.0	330	30.0
100	28.0	220	22.0	340	34.0
110	26.0	230	19.0	350	24.0

500 MEGA CYCLES

0	32.0	120	13.0	240	14.0
10	33.0	130	12.0	250	14.0
20	31.5	140	15.0	260	19.0
30	30.0	150	17.5	270	17.0
40	26.0	160	22.0	280	23.5
50	25.0	170	19.5	290	14.0
60	23.0	180	18.0	300	23.0
70	23.0	190	20.0	310	28.0
80	24.0	200	12.0	320	22.0
90	22.0	210	13.0	330	20.0
100	20.0	220	10.0	340	26.0
110	15.0	230	13.0	350	28.0

600 MEGA CYCLES

Pos.in deg.	Radiation in db.	Pos. in deg.	Radiation in db.	Pos. in deg.	Radiation in db.
0	32.0	120	15.5	240	16.0
10	31.0	130	16.0	250	13.0
20	36.0	140	17.0	260	21.0
30	30.0	150	15.0	270	17.0
40	22.0	160	14.0	280	23.0
50	26.0	170	14.0	290	26.0
60	24.0	180	17.0	300	23.0
70	12.0	190	6.0	310	27.0
80	23.5	200	14.0	320	30.0
90	26.0	210	13.5	330	32.0
100	15.0	220	23.0	340	33.0
110	16.0	230	16.0	350	34.0

700 MEGA CYCLES

0	24.0	120	5.0	240	10.0
10	26.0	130	9.0	250	9.0
20	23.0	140	6.0	260	10.0
30	19.0	150	14.0	270	12.0
40	16.0	160	9.0	280	13.0
50	13.0	170	10.0	290	15.0
60	11.0	180	10.0	300	18.0
70	10.0	190	14.0	310	13.0
80	10.0	200	15.0	320	17.0
90	12.0	210	13.0	330	19.0
100	11.0	220	11.0	340	20.5
110	8.0	230	8.0	350	22.0

800 MEGA CYCLES

Pos.in deg.	Radiation in db.	Pos.in deg.	Radiation in db.	Pos. in deg.	Radiation in db.
0	26.0	120	10.0	240	9.0
10	22.0	130	11.0	250	13.0
20	14.0	140	9.0	260	5.0
30	16.5	150	5.0	270	13.0
40	13.	160	5.0	280	12.0
50	5.0	170	12.0	290	15.0
60	10.	180	8.0	300	12.0
70	8.0	190	11.0	310	14.0
80	8.0	200	10.0	320	20.0
90	11.0	210	11.0	330	16.0
100	10.	220	6.0	340	20.5
110	13.	230	7.0	350	24.0

900 MEGA CYCLES

0	27.	120	8.0	240	8.0
10	29.5	130	9.0	250	15.0
20	28.0	140	19.0	260	13.0
30	24.5	150	13.0	270	12.0
40	23.0	160	7.0	280	5.0
50	14.0	170	11.0	290	16.0
60	16.0	180	12.0	300	23.0
70	10.0	190	10.0	310	20.0
80	17.0	200	14.0	320	23.0
90	14.0	210	14.0	330	16.0
100	18.0	220	15.0	340	18.0
110	13.0	230	12.0	350	23.0

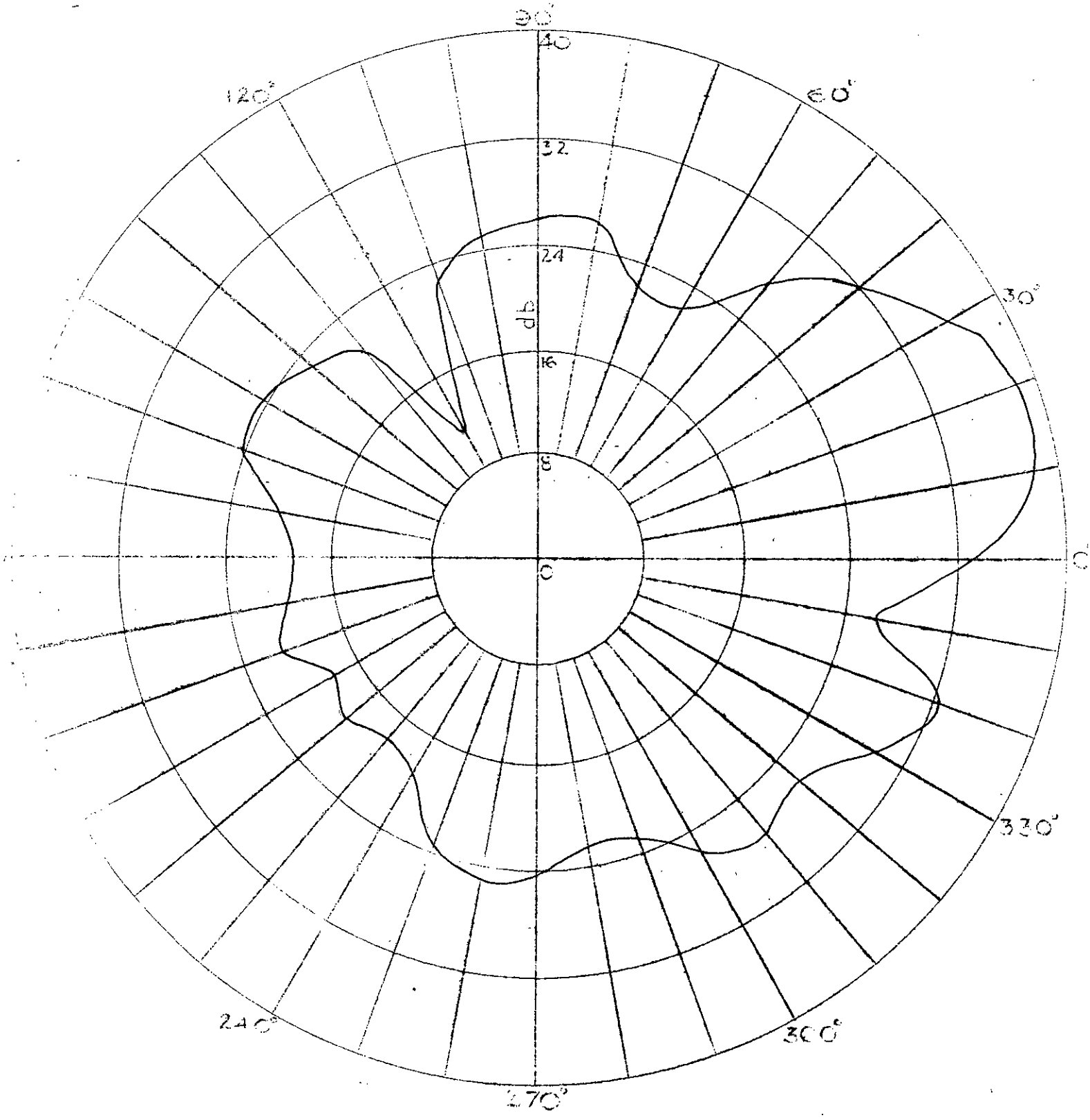

Fig. 21a Radiation Pattern at 250 Mega Cycles

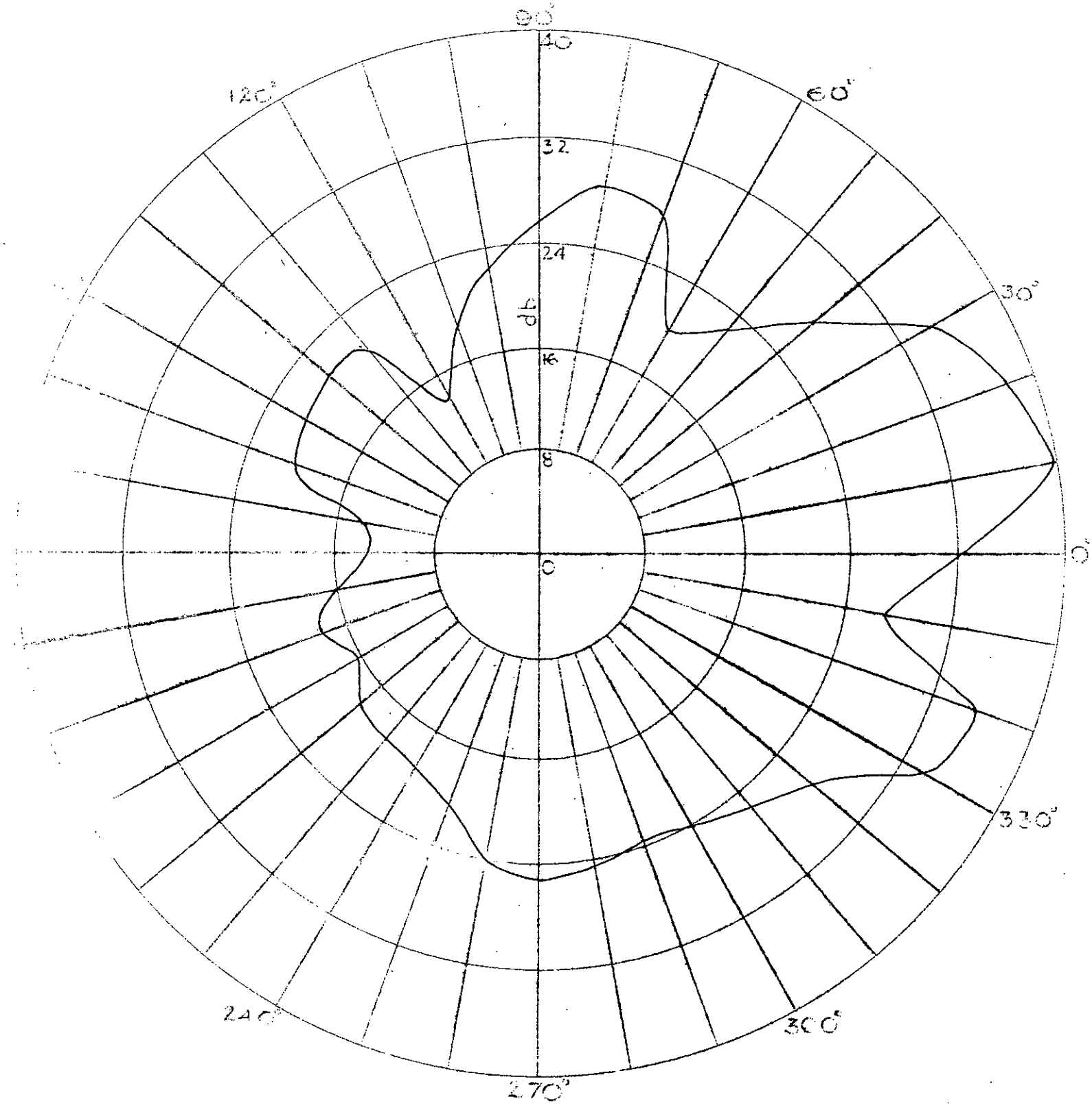

Fig. 21b Radiation Pattern a 300 Mega Cycles

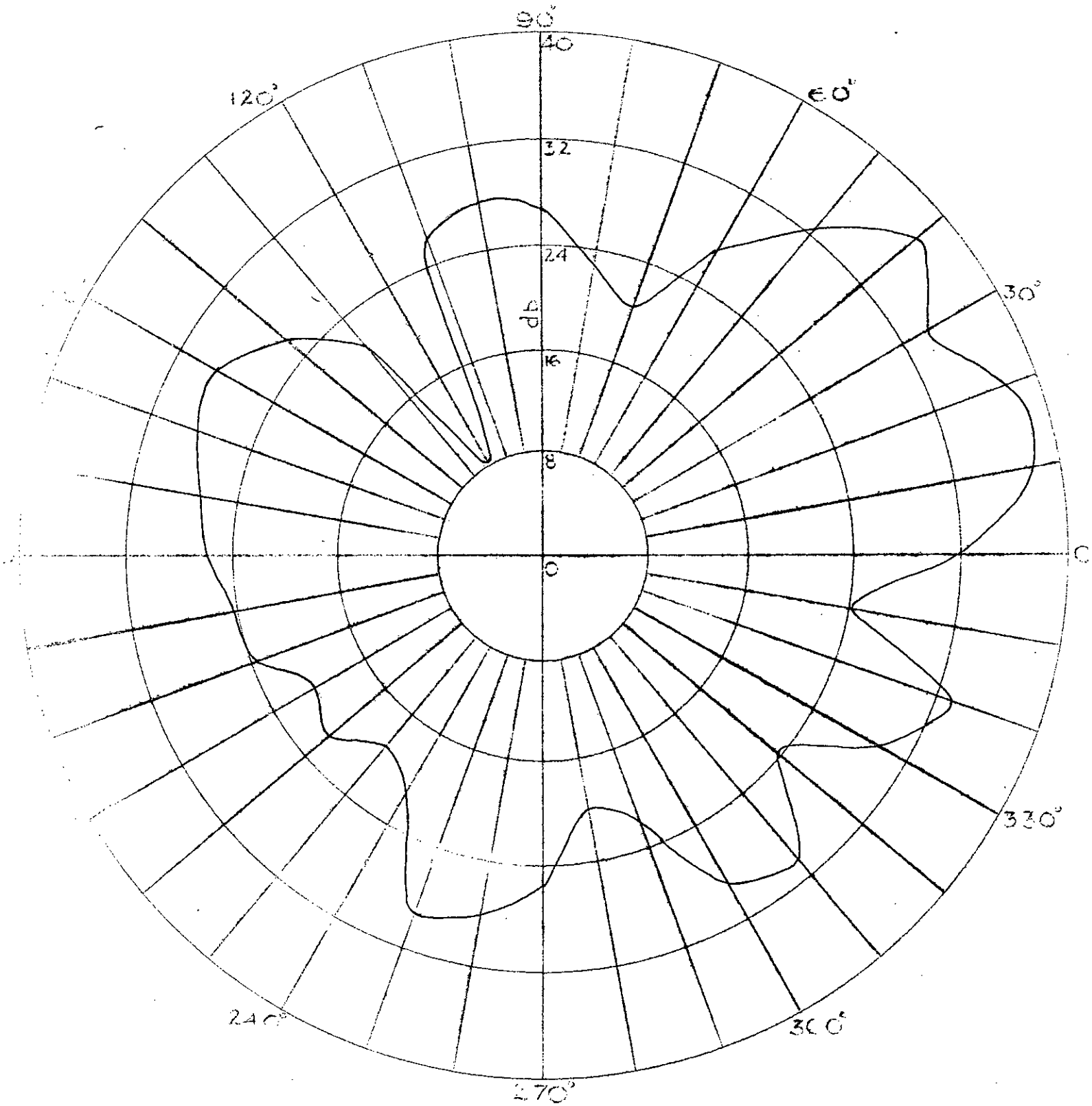

Fig. 21c Radiation Pattern at 400 Mega Cycles

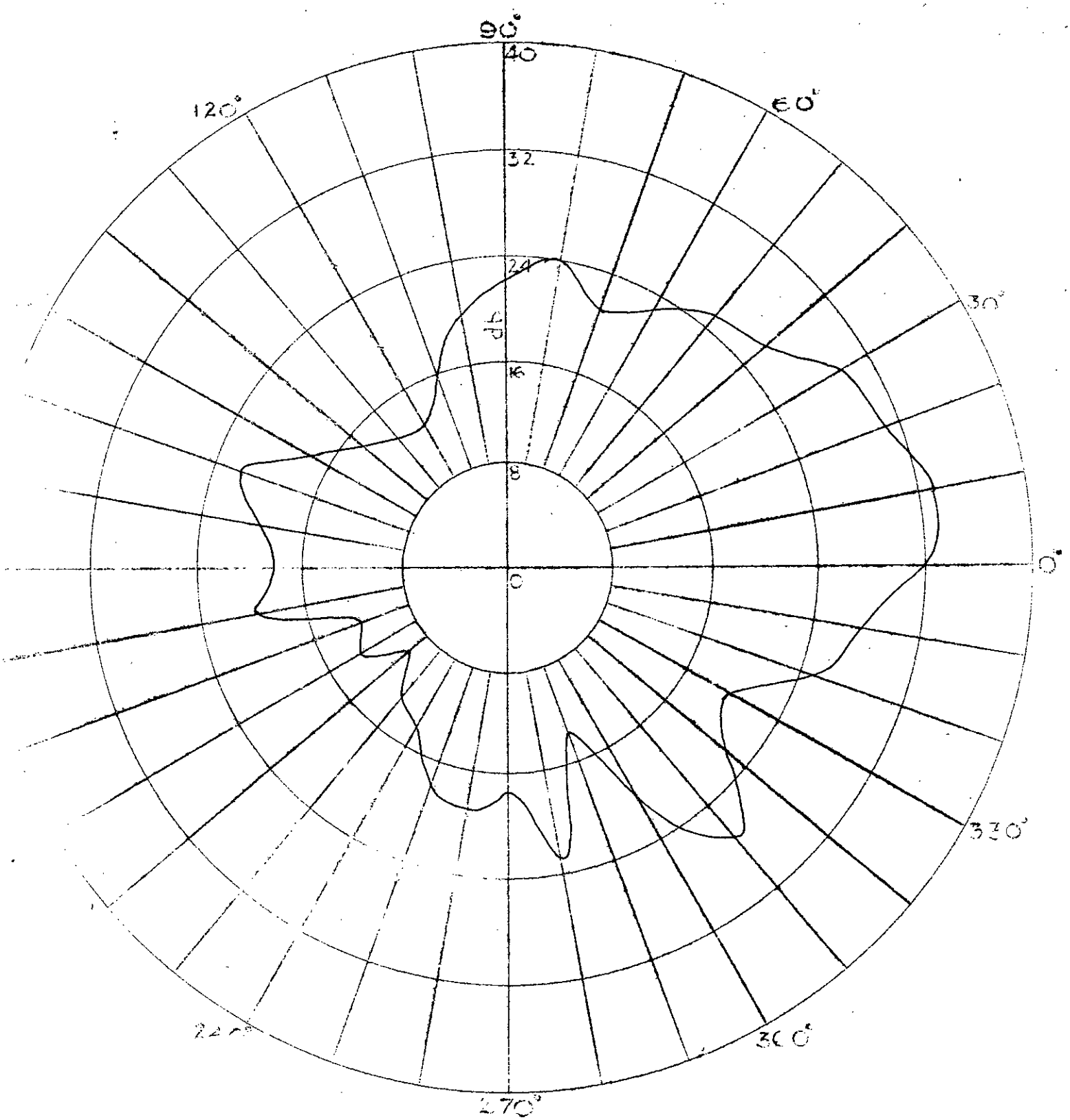

Fig. 21d Radiation Pattern at 500 Mega Cycles

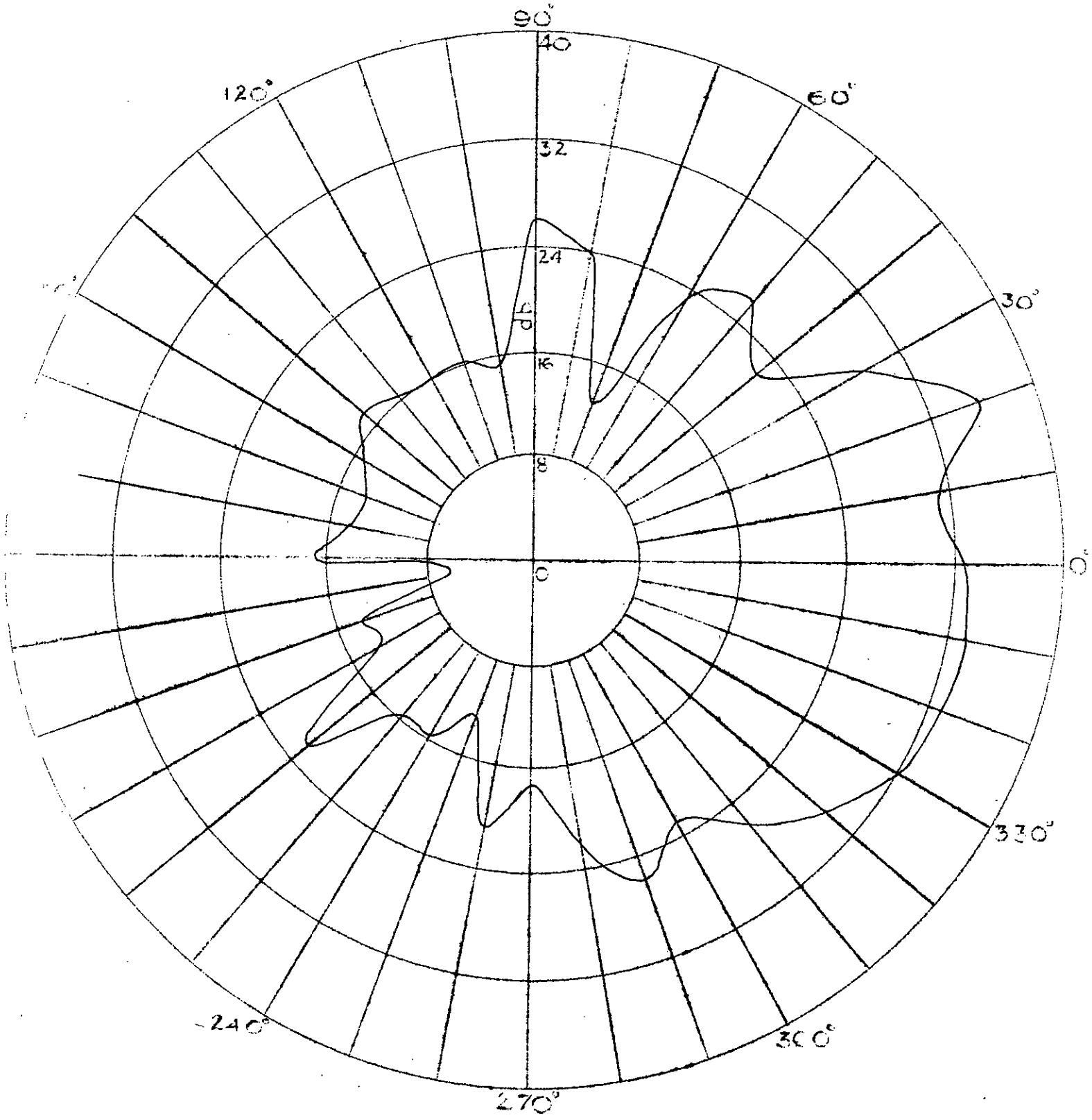

Fig. 21e Radiation Pattern at 600 Mega Cycles

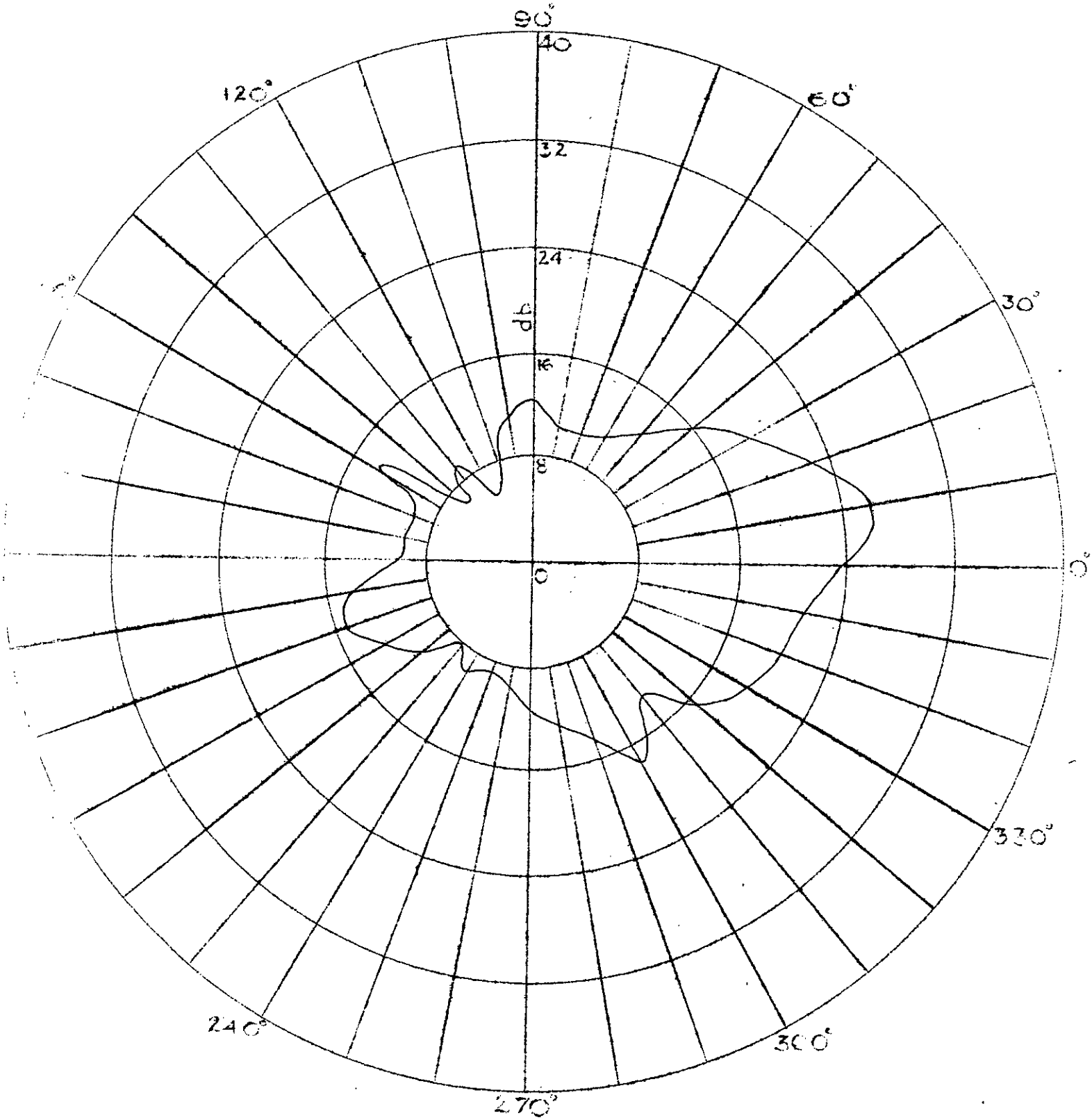

Fig. 21f Radiation Pattern at 700 Mega Cycles

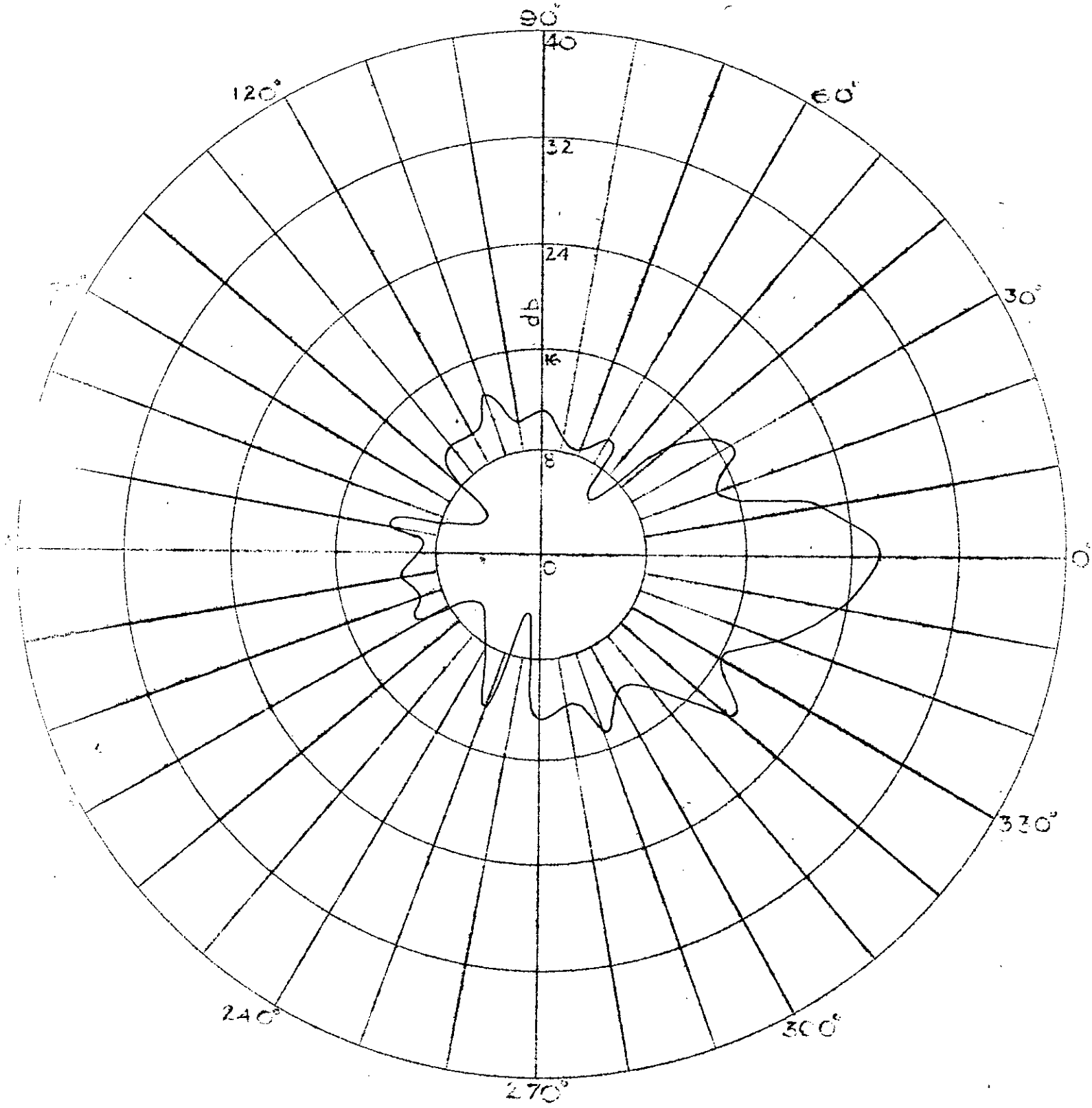

Fig. 21g Radiation Pattern at 800 Mega Cycles

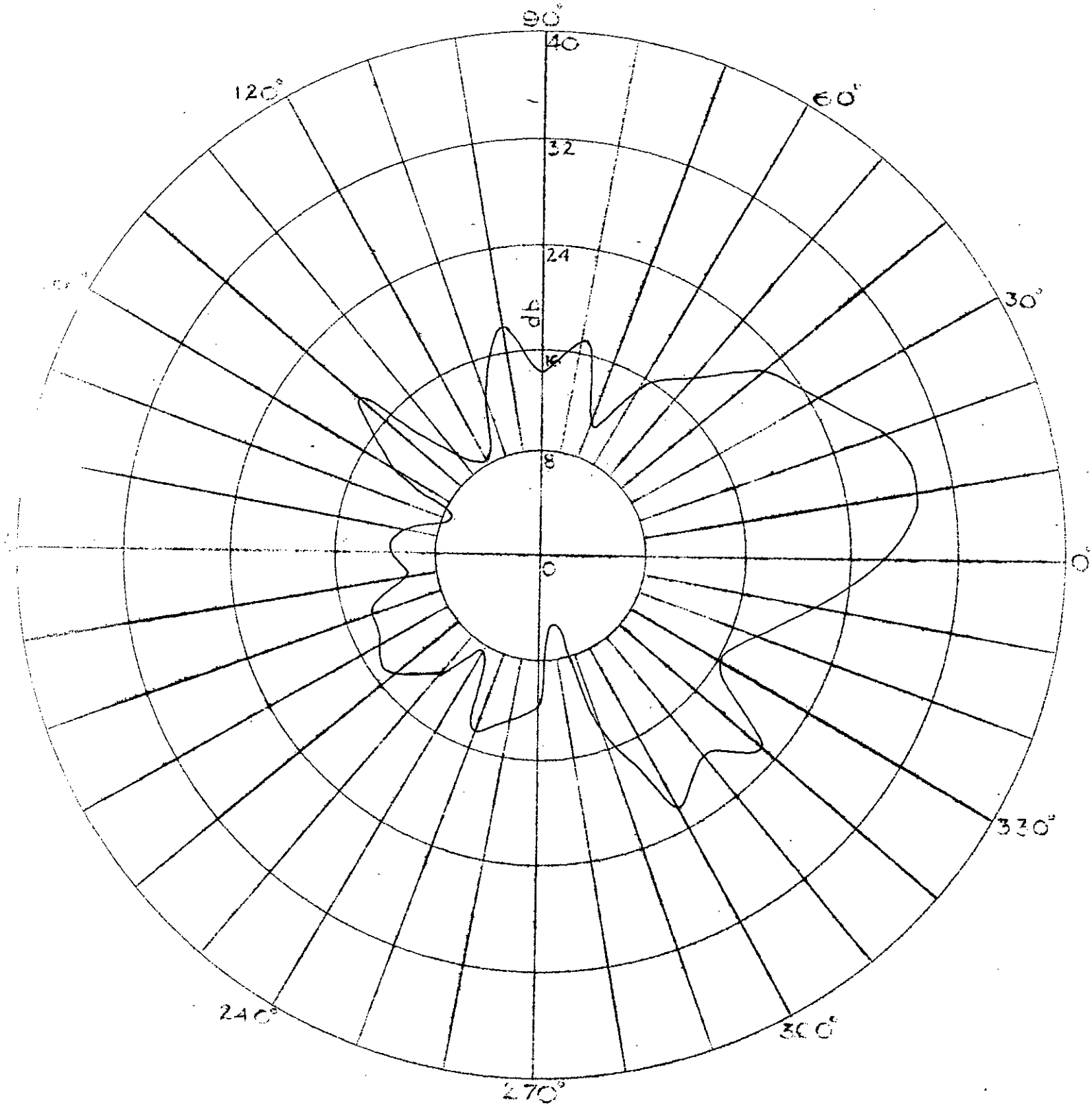

Fig. 21h Radiation Pattern at 900 Mega Cycles

TABLE - IV

MEASUREMENT OF RADIATION INTENSITIES

TWO ANTENNAS COMBINED

AXIS VERTICAL

300 MEGA CYCLES

Pos.in deg.	Radiation in db.	Pos.in deg.	Radiation in db.	Pos.in deg.	Radiation in db.
0	22.5	120	15.0	240	11.0
10	20.0	130	21.0	250	14.0
20	18.0	140	6.0	260	16.0
30	19.0	150	7.0	270	15.0
40	21.0	160	14.0	280	12.0
50	19.0	170	14.0	290	17.0
60	13.0	180	8.0	300	8.0
70	10.0	190	10.0	310	14.0
80	10.0	200	14.0	320	12.0
90	17.0	210	10.0	330	18.0
100	15.0	220	3.0	340	16.0
110	13.0	230	120	350	19.5

600 MEGA CYCLES

0	18.0	120	21.5	240	14.0
10	23.0	130	22.0	250	19.0
20	19.0	140	19.5	260	19.0
30	21.0	150	27.5	270	19.0
40	15.0	160	27.0	280	10.0
50	10.0	170	24.0	290	15.0
60	7.0	180	21.0	300	18.0
70	20.0	190	13.0	310	15.0
80	24.0	200	12.0	320	22.0
90	18.0	210	7.0	330	20.0
100	17.0	220	3.0	340	22.0
110	14.0	230	13.0	350	21.0

900 MEGA CYCLES

Pos.in deg.	Radiation in db.	Pos.in deg.	Radiation in db.	Pos. in deg.	Radiation in db.
0	14.0	120	14.0	240	12.0
10	7.0	130	16.0	250	13.0
20	6.0	140	13.0	260	19.0
30	7.0	150	12.0	270	19.0
40	8.0	160	11.0	280	17.0
50	3.0	170	14.0	290	10.0
60	6.0	180	16.0	300	10.0
70	5.0	190	17.0	310	9.0
80	16.0	200	11.0	320	8.0
90	15.0	210	7.0	330	9.0
100	17.0	220	6.0	340	10.0
110	17.0	230	5.0	350	16.0

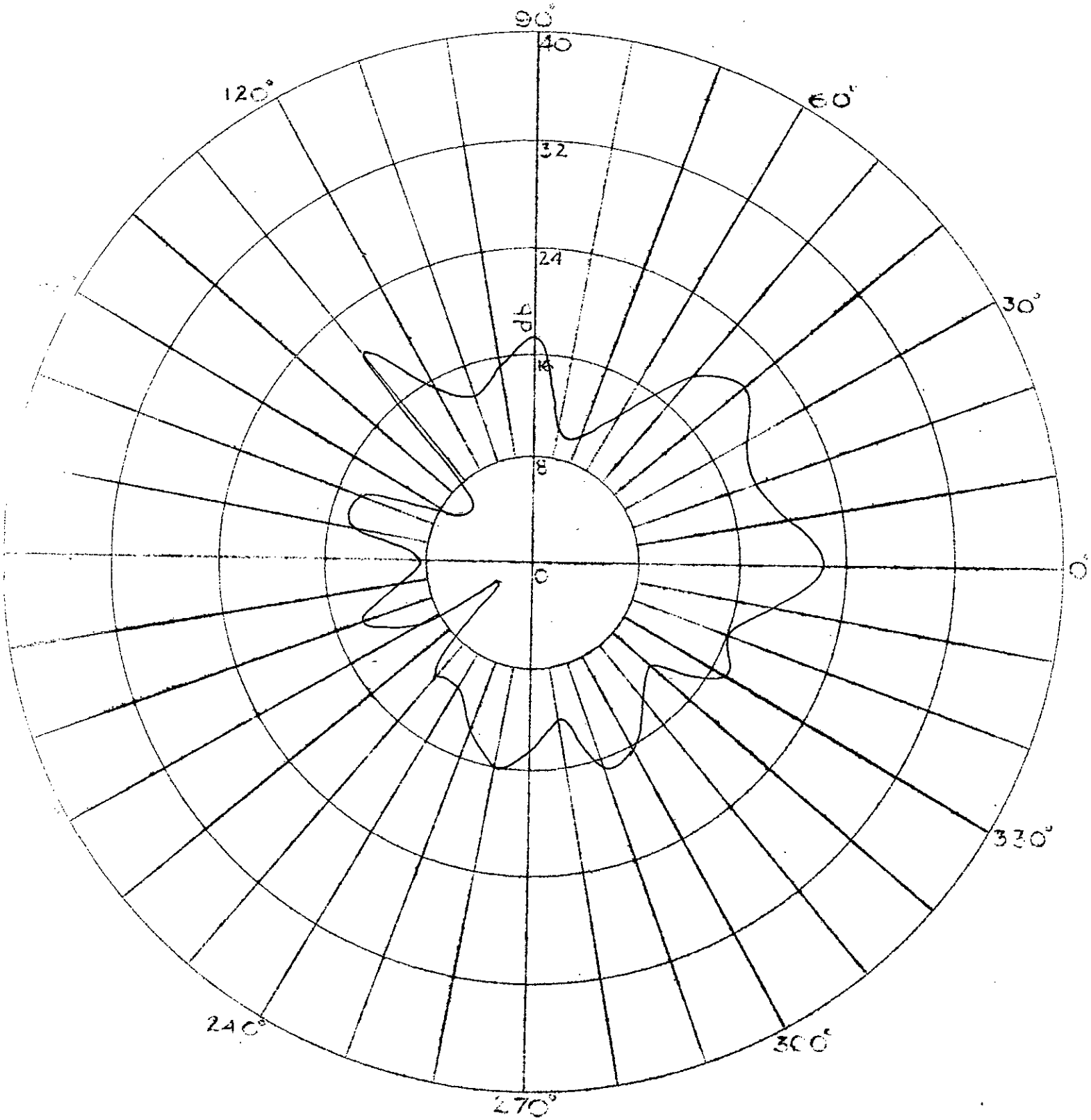

Fig. 22a Radiation Pattern at 300 Mega Cycles

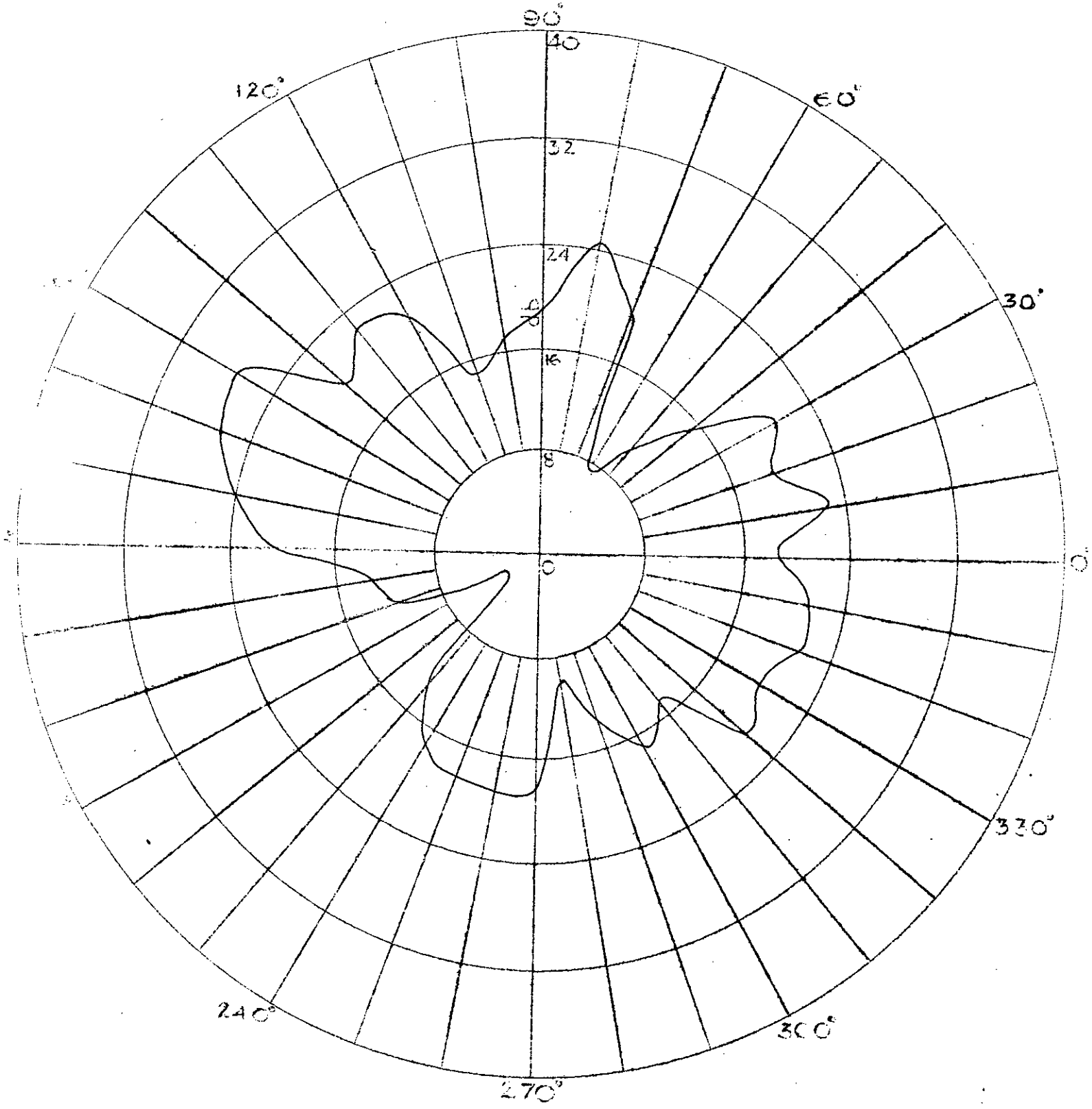

Fig.22b Radiation Pattern at 600 Mega Cycles

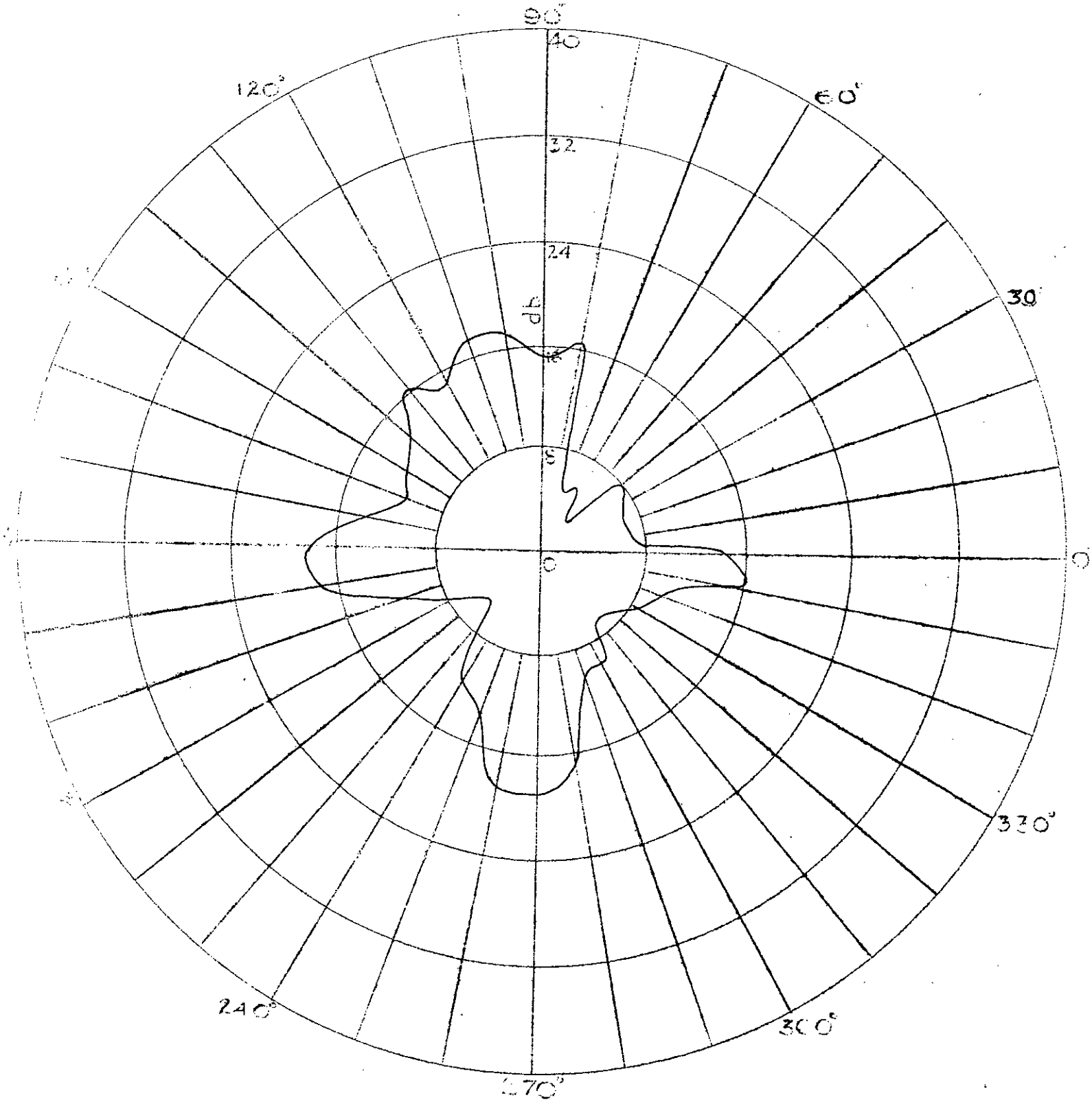

Fig. 22c Radiation Pattern at 900 Mega Cycles

1.12

TABLE - V

INPUT IMPEDANCE CALCULATION OF TWO ANTENNAS COMBINED

Freq. in Mc/s	Shift in Pos.of min.current in λ		$I_{max.}$ μ amp.	$I_{min.}$ μ amp.	$V_{max.}$ mV	$V_{min.}$ mV	VSWR S	Z_{0in}	Length of coaxl. cable in λ	Calculated impedance in Ohm.
	Gen.end	Load end.								
250		0.183	6.0	0.5	1.55	0.15	10.30	4.9	2.379	5.5-j20
300	0.125		8.0	1.3	2.00	0.35	7.20	6.9	2.850	150-j185
350		0.065	16.5	2.0	3.30	0.56	5.90	8.5	3.330	13+j37
400	0.233		19.5	3.4	4.70	0.91	5.16	9.8	3.800	11.5-j21.5
450	0.045		13.0	2.2	3.19	0.60	5.32	9.4	4.270	165-j135
500	0.340		38.0	4.5	8.90	1.20	7.42	6.8	4.750	9.5+j31
550		0.312	33.0	5.0	7.80	1.30	6.00	8.3	5.230	8.8-j13
600		0.010	24.0	4.0	5.78	1.05	5.50	9.1	5.700	100-j130
650		0.217	21.0	3.0	5.09	0.80	6.35	7.9	6.200	10.5+j28.5
700	0.117		23.2	2.5	5.55	0.69	8.05	6.2	6.680	7.5-j2055
750		0.100	14.5	2.0	3.51	0.56	6.27	7.9	7.135	240-j150
800		0.320	7.5	1.0	1.90	0.28	6.80	7.4	7.600	10.5+j31
850	0.028		16.5	2.3	4.00	0.61	6.55	7.6	8.080	8.8-j13
900		0.495	14.5	2.2	3.51	0.61	5.87	8.5	8.560	9.5-j17.5

TITLE

DATE

IMPEDANCE COORDINATES—50-OHM CHARACTERISTIC IMPEDANCE

A-5650

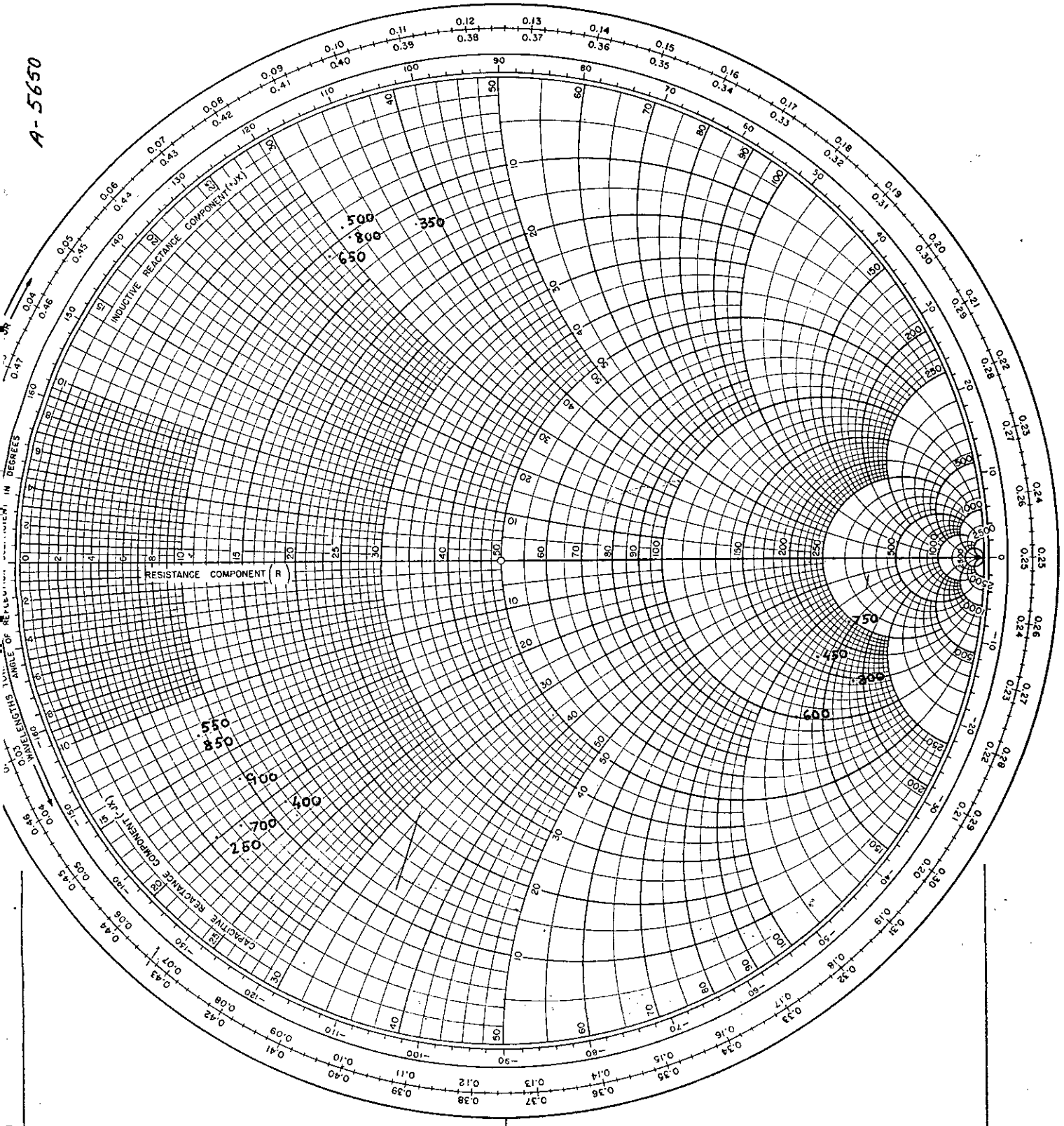

Fig.23. Calculation of the Input Impedance of the combination of Two Antennas

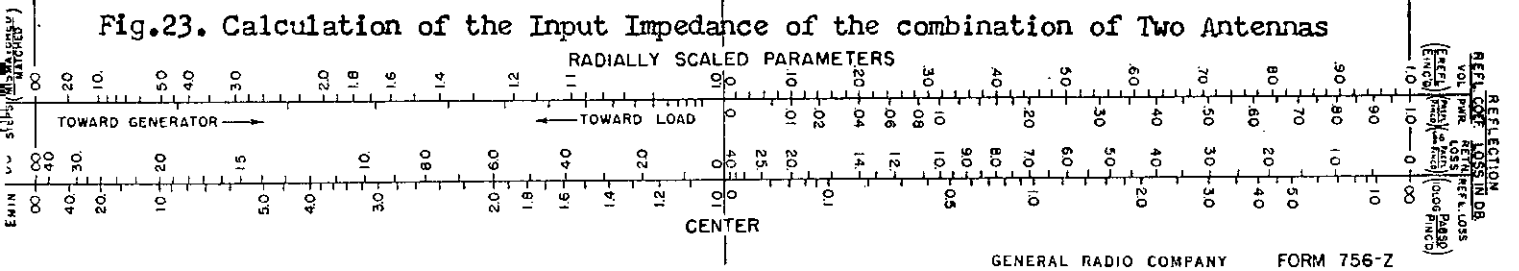

Electronics - VOL. 17, NO. 1, PP. 130-133, 318-325, JAN. 1944

GENERAL RADIO COMPANY
WEST CONCORD, MASS.

FORM 756-Z
Printed in USA

Fig.24. Variation of the Resistive and Reactive components of the Input Impedance of the combination of two antennas with frequency.

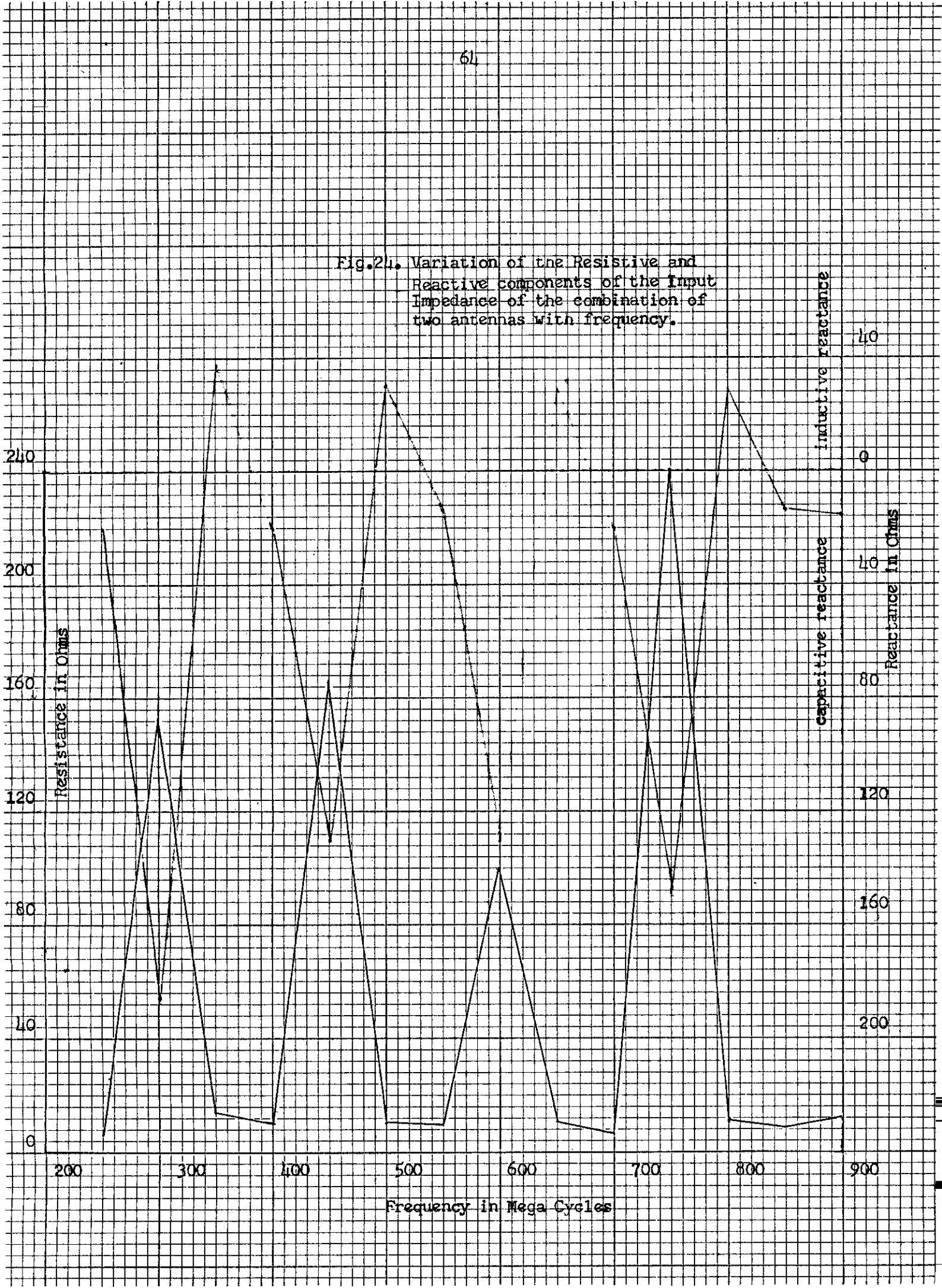

C. COMBINATION OF FOUR ANTENNAS UNDER INVESTIGATION

Four identical antennas each was as shown in Fig.14 were placed at the four sides of a square base pyramid. Two antennas at the opposite sides were shorted at the smaller ends. One pair of the shorted antenna was fed by the inner conductor and other pair was fed by the outer conductor of the co-axial cable from the same signal generator. The experiment was identical as in 'B'. The measured values of radiation intensities for the antenna axis horizontal is shown in table VI and the radiation patterns are shown in Figs. 26a,26b,26c,26d,26e,26f,26g,26h.

For the vertical position of the antenna axis the measured values of the radiation intensities are shown in table VII and the radiation patterns are shown in the Figs. 27a,27b,27c,27d,27e,27f,27g,27h.

The values of the input impedance were calculated from a Smith Chart as shown in Fig. 28. Calculated values of the input impedance are shown in table VIII. The impedance vs frequency curve is shown in Fig.29.

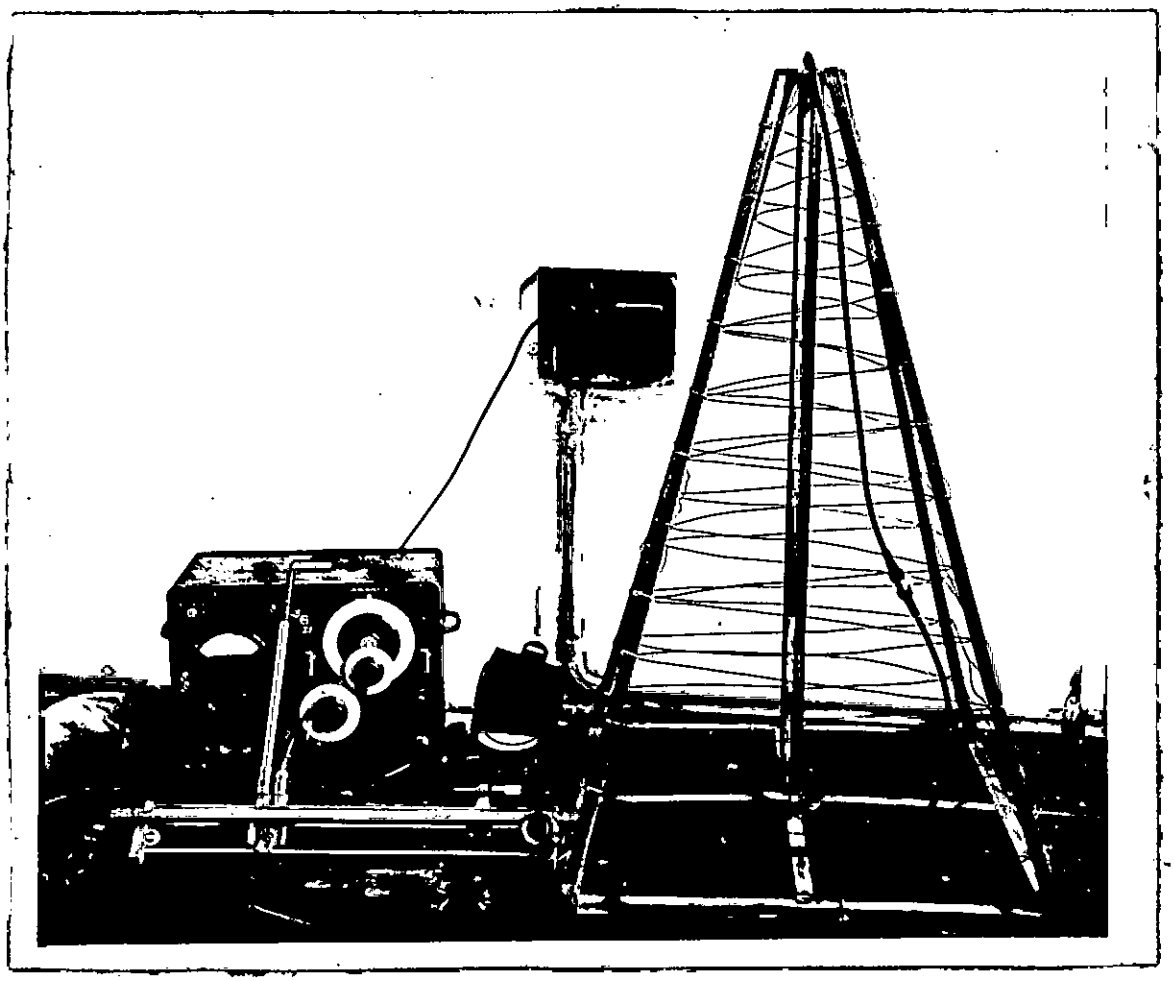

Fig. 25. Experimental set up for the
Measurement of Input Impedance

TABLE - VI

MEASUREMENT OF RADIATION INTENSITIES

FOUR ANTENNAS COMBINED

AXIS HORIZONTAL

250 MEGA CYCLES

Pos.in deg.	Radiation in db.	Pos.in deg.	Radiation in db.	Pos.in deg.	Radiation in db.
0	24.0	120	20.5	240	5.0
10	24.0	130	10.5	250	10.0
20	30.0	140	20.0	260	22.0
30	35.5	150	22.0	270	25.5
40	36.0	160	24.0	280	30.0
50	34.0	170	24.5	290	31.5
60	34.5	180	22.0	300	34.0
70	32.0	190	22.0	310	35.0
80	31.5	200	20.0	320	34.0
90	29.5	210	18.5	330	31.0
100	25.5	220	16.5	340	28.0
110	22.5	230	16.0	350	22.0

300 MEGA CYCLES

0	30.0	120	28.0	240	22.0
10	32.0	130	27.5	250	16.0
20	31.5	140	20.0	260	25.0
30	33.5	150	15.0	270	28.0
40	35.5	160	7.5	280	32.5
50	35.0	170	19.5	290	30.5
60	35.0	180	18.0	300	30.0
70	29.0	190	20.0	310	31.5
80	27.5	200	23.5	320	33.0
90	25.0	210	26.0	330	28.5
100	23.5	220	22.0	340	27.5
110	29.0	230	26.5	350	24.0

400 MEGA CYCLES

Pos.in deg.	Radiation in db.	Pos.in deg.	Radiation in db.	Pos.in deg.	Radiation in db.
0	32.0	120	30.0	240	10.0
10	32.0	130	25.5	250	14.0
20	32.0	140	31.0	260	23.5
30	32.0	150	4.0	270	24.0
40	33.0	160	9.0	280	27.0
50	39.0	170	22.0	290	33.0
60	40.0	180	10.0	300	33.0
70	39.0	190	8.0	310	35.0
80	32.0	200	7.0	320	32.0
90	28.0	210	8.0	330	37.0
100	33.0	220	26.0	340	37.0
110	31.5	230	17.0	350	34.0

500 MEGA CYCLES

0	33.0	120	30.0	240	24.5
10	32.5	130	31.0	250	26.0
20	30.0	140	24.0	260	19.5
30	33.0	150	22.0	270	18.0
40	36.0	160	25.0	280	25.5
50	37.0	170	20.0	290	29.5
60	39.5	180	17.0	300	37.0
70	37.0	190	22.0	310	36.0
80	35.5	200	20.0	320	36.0
90	35.5	210	21.0	330	37.0
100	32.5	220	27.0	340	37.5
110	31.0	230	30.0	350	39.0

600 MEGA CYCLES

Pos.in deg.	Radiation in db.	Pos.in deg.	Radiation in db.	Pos. in deg.	Radiation in db.
0	27.5	120	0.0	240	24.0
10	16.0	130	14.0	250	19.5
20	20.0	140	20.0	260	27.0
30	21.0	150	24.0	270	29.0
40	19.5	160	26.0	280	25.0
50	21.0	170	22.0	290	34.0
60	18.0	180	15.0	300	37.5
70	12.0	190	3.0	310	39.0
80	15.5	200	18.0	320	39.5
90	12.0	210	17.5	330	38.5
100	2.0	220	17.5	340	38.0
110	5.0	230	20.0	350	38.0

700 MEGA CYCLES

0	21.0	120	12.0	240	17.0
10	20.0	130	4.0	250	19.5
20	20.0	140	9.0	260	19.5
30	25.0	150	12.0	270	22.0
40	27.5	160	10.0	280	23.0
50	24.0	170	6.0	290	28.5
60	26.0	180	4.0	300	29.0
70	24.0	190	7.0	310	30.0
80	22.0	200	12.5	320	27.5
90	23.0	210	12.0	330	28.0
100	19.0	220	10.0	340	29.0
110	17.5	230	10.0	350	25.0

800 MEGA CYCLES

Pos.in deg.	Radiation in db.	Pos.in deg.	Radiation in db.	Pos. in deg.	Radiation in db.
0	26.0	120	15.5	240	15.0
10	20.0	130	14.0	250	12.0
20	20.0	140	14.0	260	17.0
30	22.0	150	10.0	270	12.0
40	22.0	160	8.5	280	21.0
50	22.0	170	8.5	290	19.0
60	23.0	180	13.5	300	20.0
70	22.0	190	11.0	310	19.0
80	15.0	200	12.5	320	18.0
90	16.5	210	12.0	330	10.0
100	16.0	220	7.0	340	16.0
110	11.5	230	14.5	350	20.0

900 MEGA CYCLES

0	17.0	120	13.5	240	10.0
10	17.0	130	14.0	250	11.5
20	15.5	140	8.5	260	16.0
30	19.0	150	15.5	270	15.5
40	19.0	160	15.5	280	13.0
50	21.0	170	12.5	290	14.0
60	24.0	180	10.3	300	13.0
70	20.0	190	11.0	310	23.0
80	20.0	200	8.0	320	19.5
90	20.0	210	3.0	330	18.5
100	17.0	220	4.0	340	13.5
110	8.0	230	6.0	350	17.5

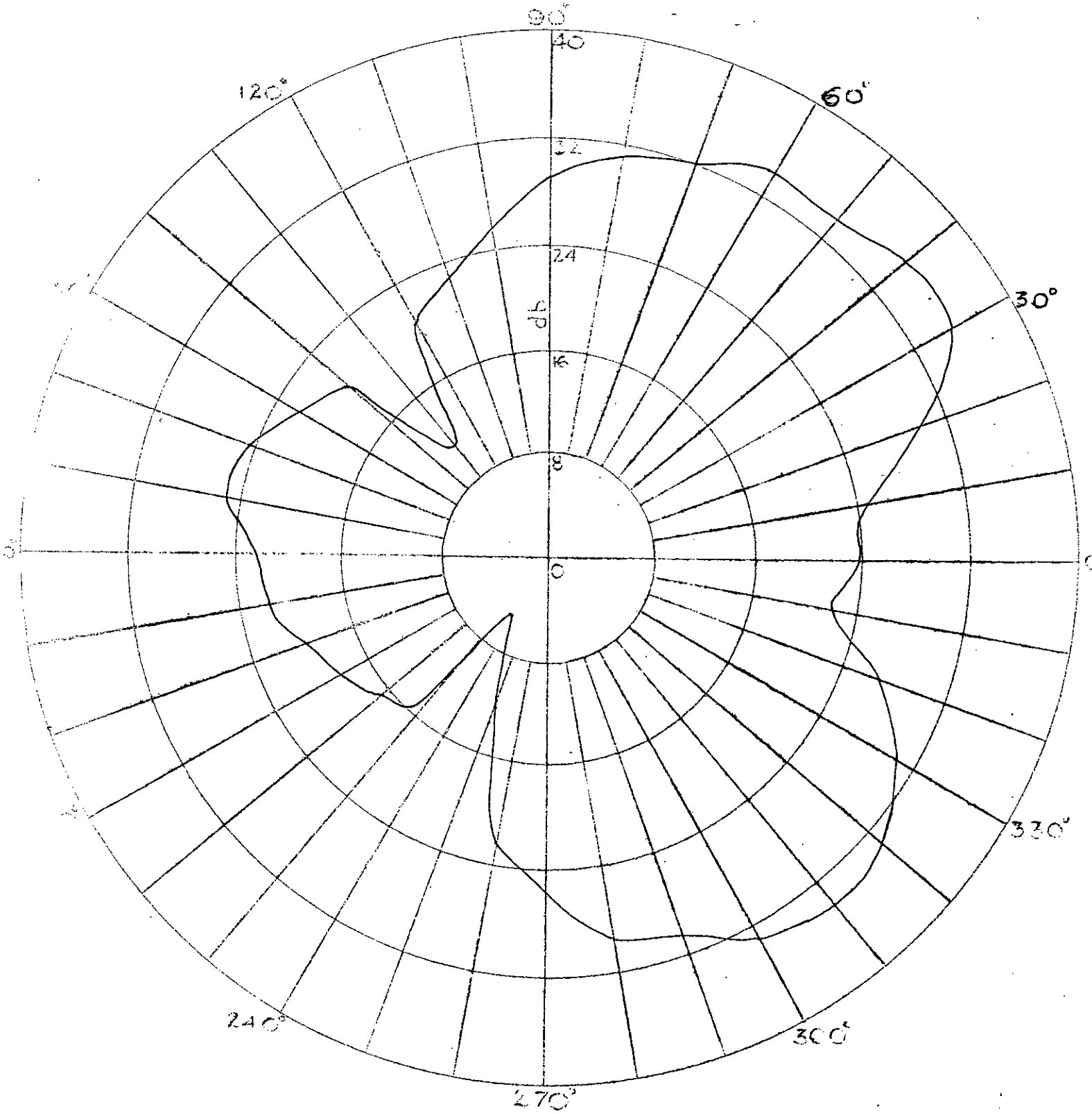

Fig. 26a Radiation Pattern at 250 Mega Cycles

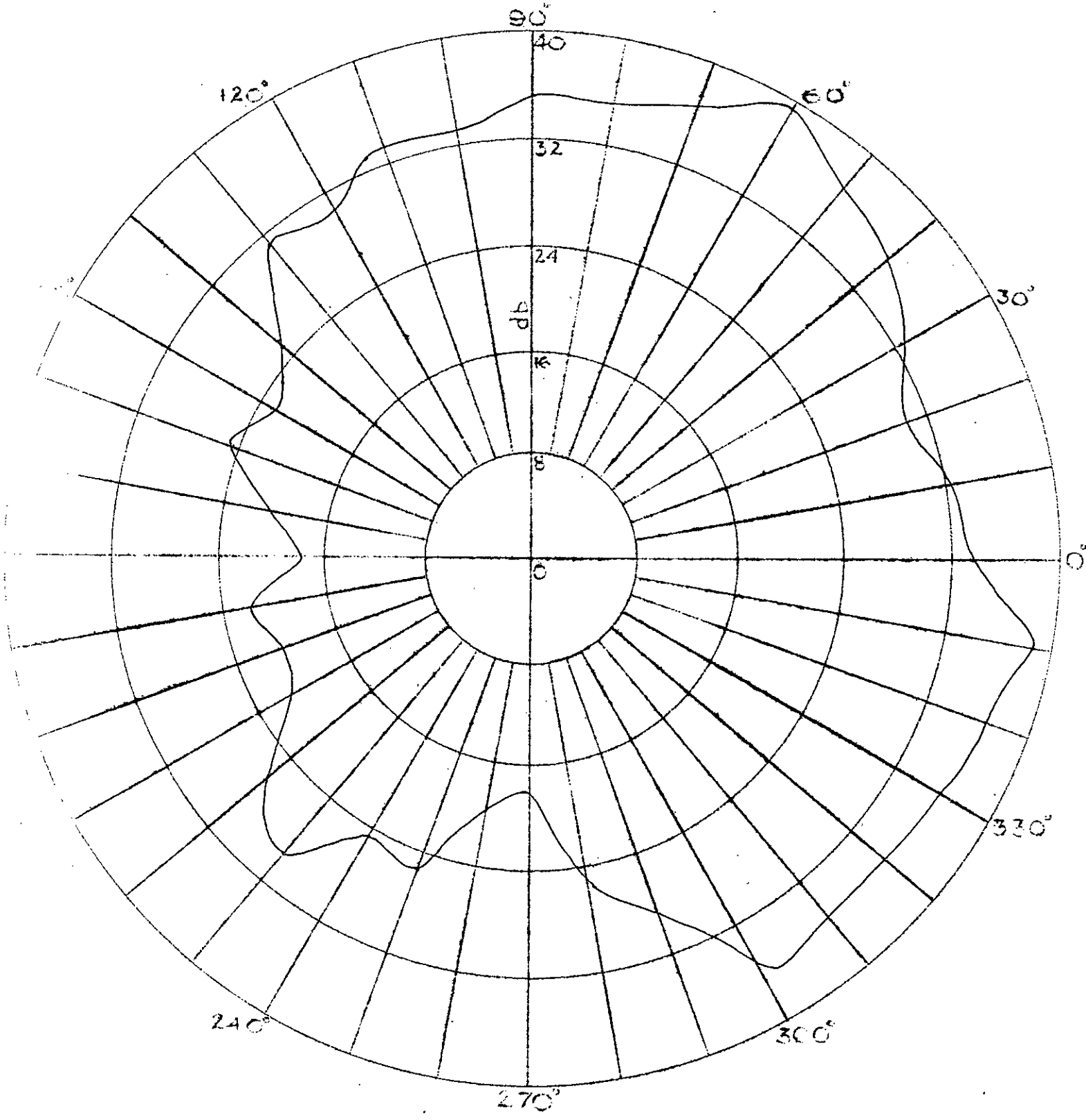

Fig. 26b Radiation Pattern at 300 Mega Cycles

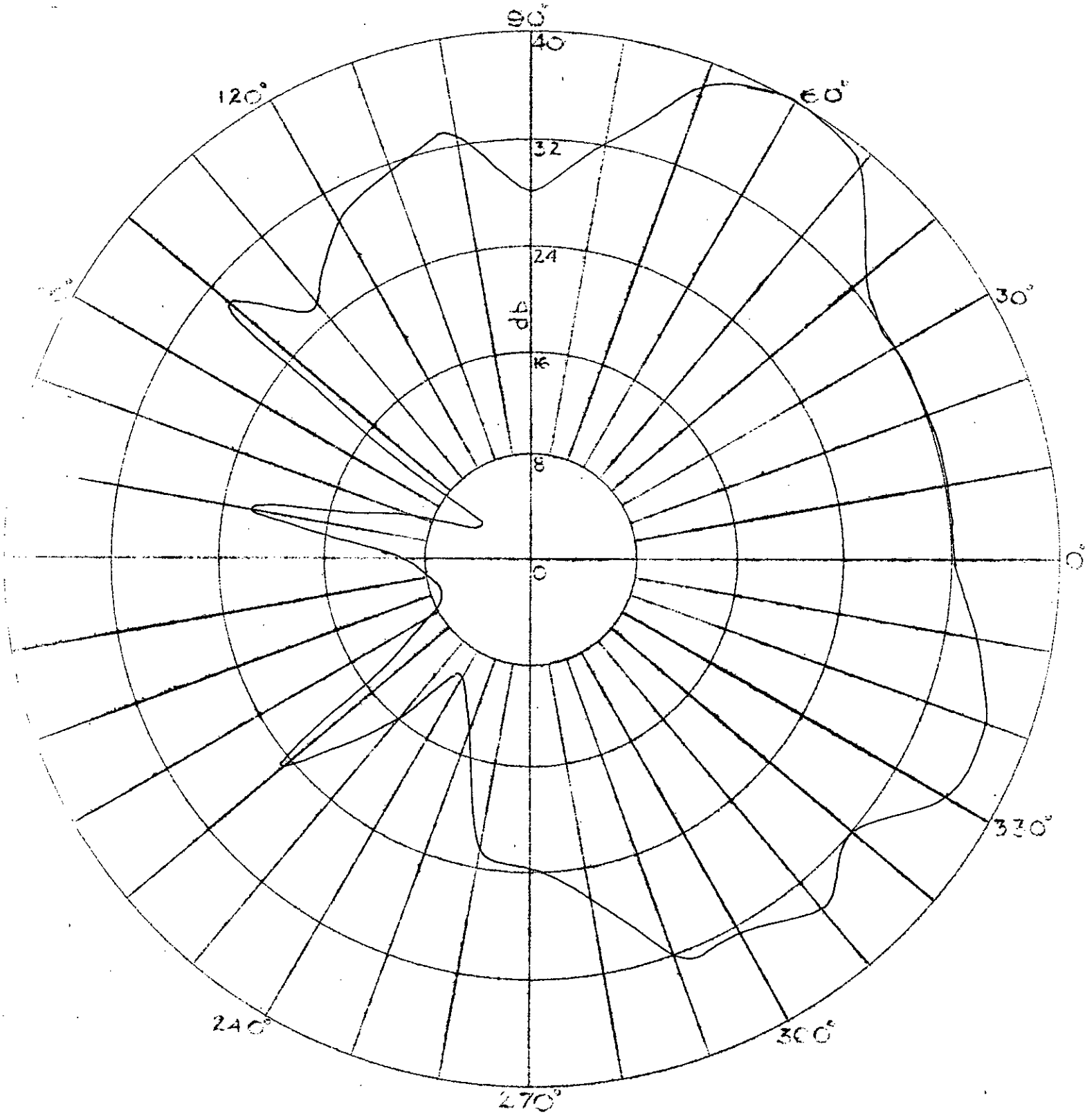

Fig. 26c Radiation Pattern at 400 Mega Cycles

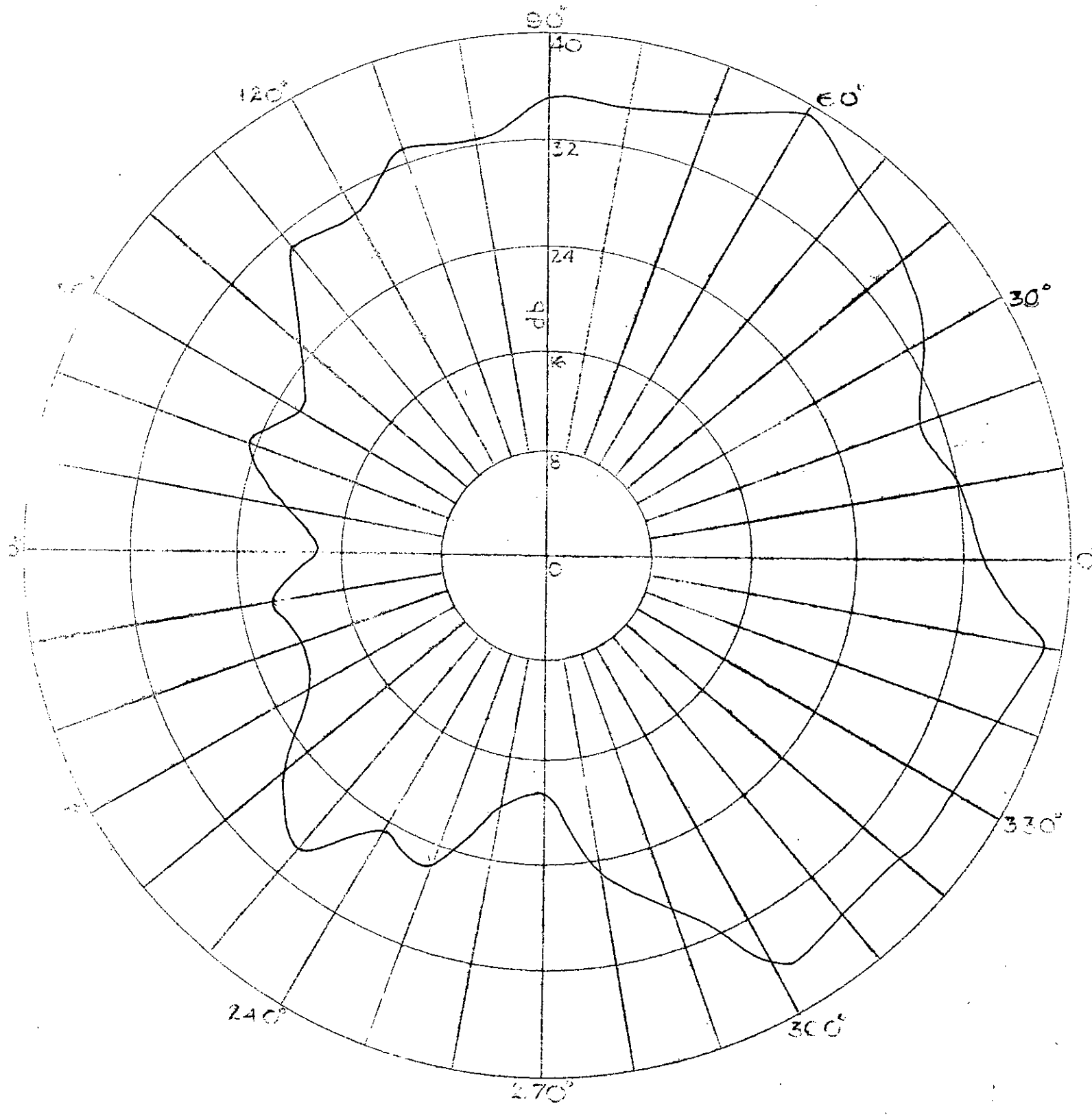

Fig. 26d Radiation Pattern at 500 Mega Cycles

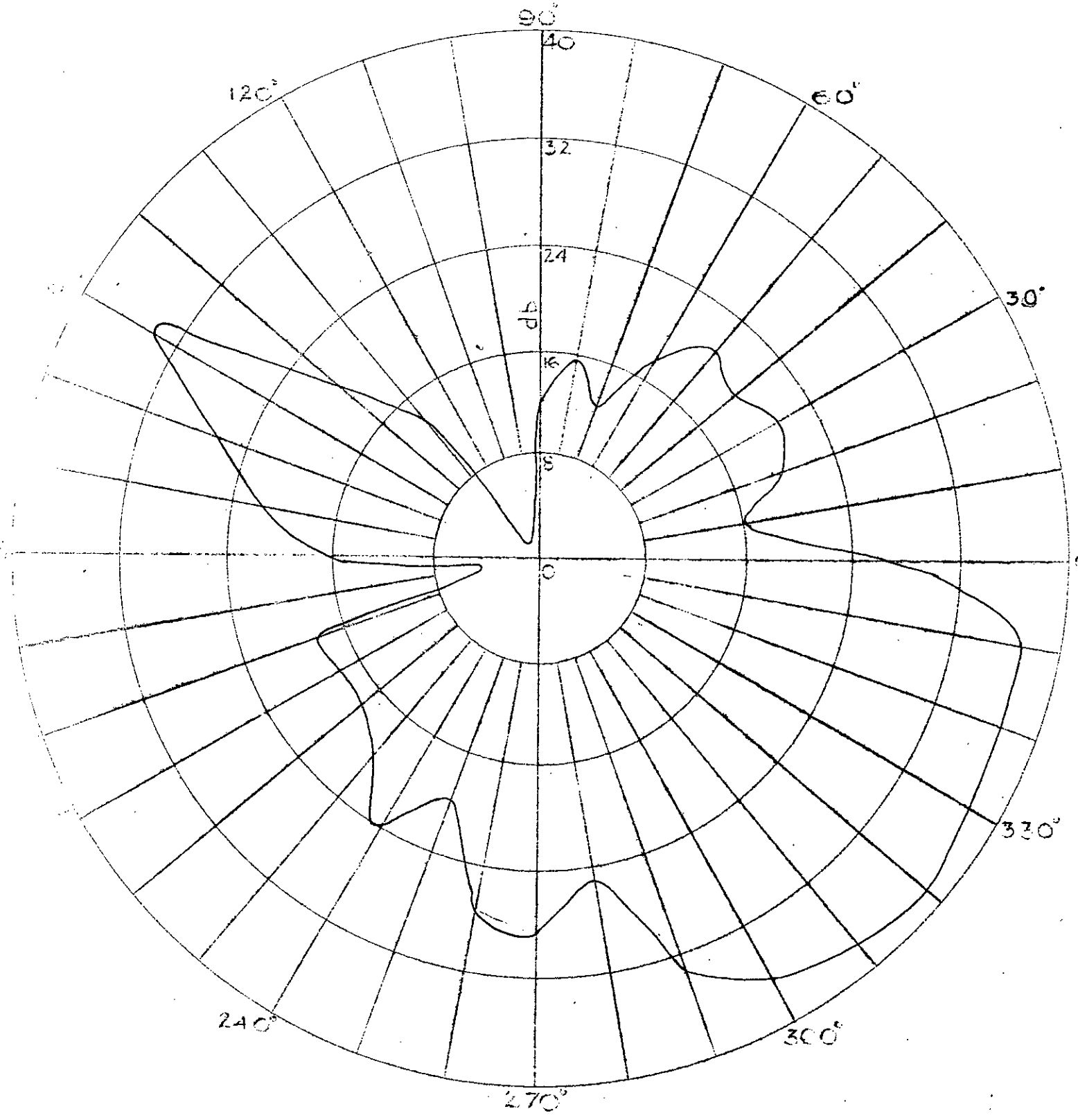

Fig. 26e Radiation Pattern at 600 Mega Cycles

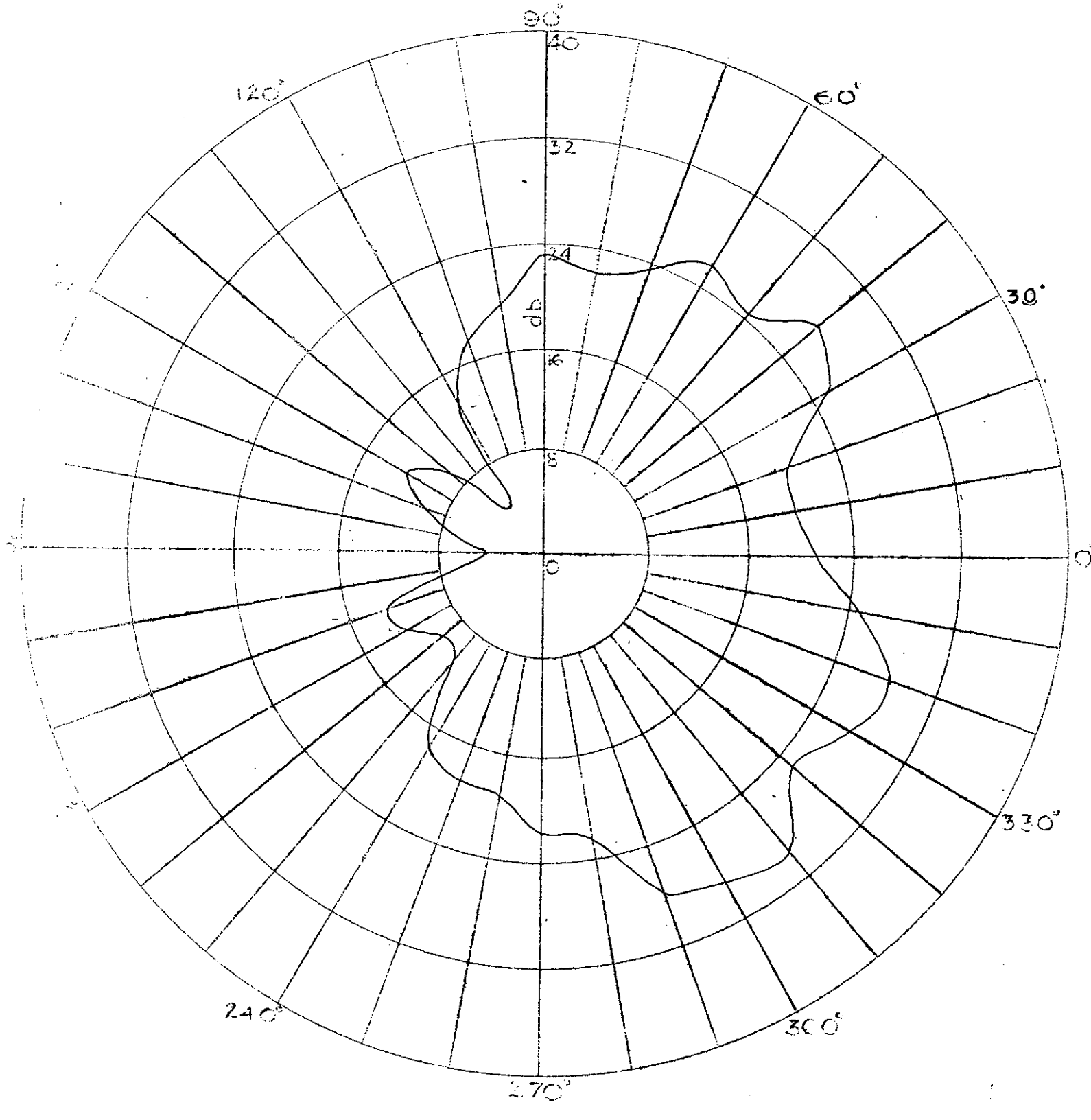

Fig. 26f Radiation Pattern at 700 Mega Cycles

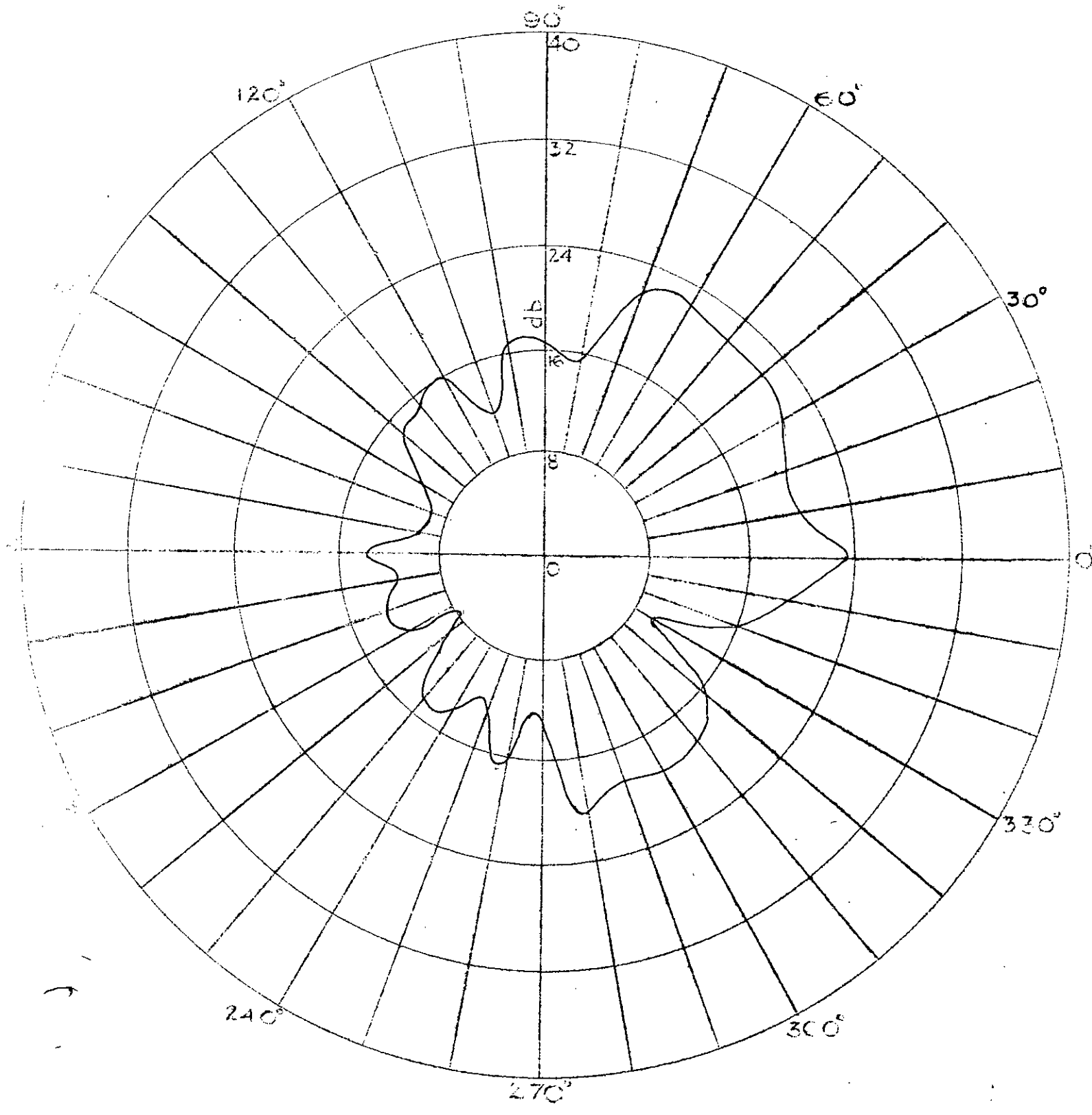

Fig. 26g Radiation Pattern at 800 Mega Cycles

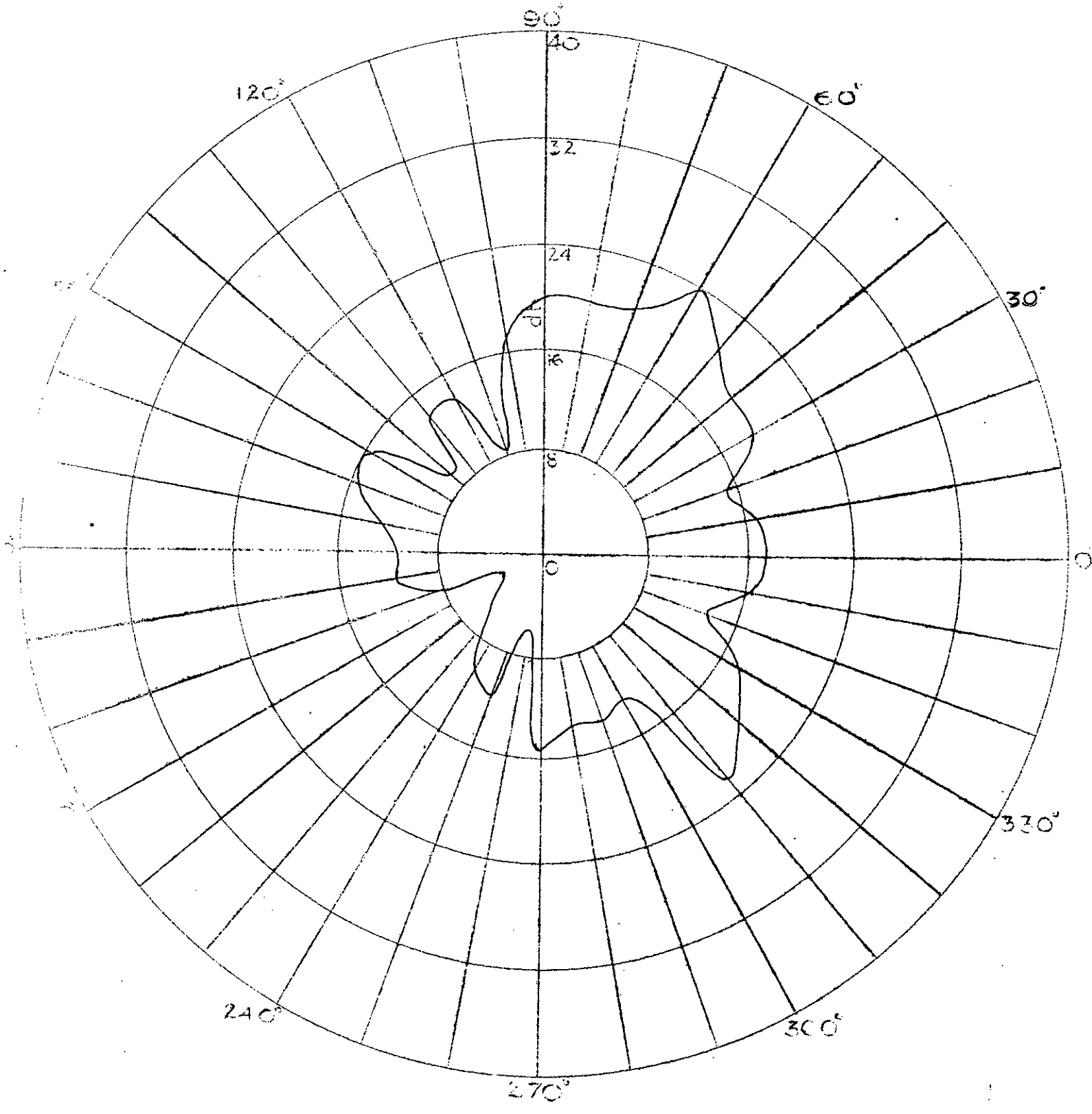

Fig. 26h Radiation Pattern at 900 Mega Cycles

TABLE - VII

MEASUREMENT OF RADIATION INTENSITIES
FOUR ANTENNAS COMBINED
ANTENNA AXIS VERTICAL
250 MEGA CYCLES

Pos.in deg.	Radiation in db.	Pos.in deg.	Radiation in db.	Pos.in deg.	Radiation in db.
0	20.0	120	22.0	240	25.5
10	22.0	130	17.0	250	18.0
20	25.0	140	2300	260	10.0
30	24.0	150	20.0	270	18.0
40	24.0	160	24.0	280	20.0
50	25.5	170	24.0	290	25.0
60	22.5	180	25.5	300	19.0
70	24.0	190	26.0	310	11.0
80	25.0	200	26.0	320	10.0
90	26.0	210	25.0	330	18.5
100	23.0	220	24.0	340	17.5
110	20.0	230	24.5	350	12.0

300 MEGA CYCLES

0	30.0	120	29.0	240	28.0
10	29.0	130	29.0	250	29.0
20	29.0	140	28.0	260	26.0
30	28.0	150	27.0	270	27.0
40	26.5	160	28.0	280	29.0
50	28.0	170	28.5	290	31.0
60	29.0	180	28.5	300	31.0
70	27.0	190	29.0	310	32.0
80	27.0	200	28.5	320	30.0
90	22.0	210	28.5	330	30.0
100	23.0	220	28.0	340	30.0
110	28.0	230	29.0	350	32.0

400 MEGA CYCLES

Pos.in deg.	Radiation in db.	Pos.in deg.	Radiation in db.	Pos.in deg.	Radiation in db.
0	29.0	120	30.0	240	28.0
10	33.0	130	28.5	250	29.0
20	40.0	140	28.0	260	25.0
30	34.0	150	33.0	270	28.5
40	34.5	160	30.0	280	23.0
50	34.0	170	32.0	290	29.0
60	36.0	180	31.0	300	21.0
70	35.0	190	31.0	310	25.0
80	32.0	200	31.0	320	25.0
90	31.0	210	31.0	330	24.0
100	33.0	220	30.0	340	29.0
110	35.0	230	21.0	350	28.0

500 MEGA CYCLES

0	24.5	120	28.1	240	27.0
10	20.0	130	28.0	250	25.0
20	22.0	140	30.0	260	23.0
30	26.0	150	28.0	270	29.0
40	20.0	160	27.0	280	27.0
50	26.0	170	28.0	290	28.0
60	20.0	180	28.0	300	25.0
70	26.0	190	27.0	310	25.0
80	21.0	200	26.0	320	29.0
90	25.0	210	32.0	330	28.5
100	25.0	220	35.0	340	27.0
110	28.5	230	25.0	350	26.0

600 MEGA CYCLES

Pos. in deg.	Radiation in db.	Pos.in deg.	Radiation in db.	Pos.in deg.	Radiation in db.
0	26.0	120	23.0	240	28.5
10	25.5	130	21.5	250	24.0
20	25.0	140	24.0	260	23.5
30	22.0	150	25.0	270	22.0
40	21.0	160	24.0	280	20.5
50	23.0	170	27.0	290	25.0
60	22.0	180	28.0	300	24.0
70	23.0	190	25.0	310	27.0
80	21.0	200	28.5	320	22.0
90	20.0	210	29.0	330	27.0
100	20.0	220	25.0	340	28.5
110	20.0	230	28.5	350	31.0

700 MEGA CYCLES

0	21.0	120	20.0	240	24.0
10	22.0	130	21.0	250	22.0
20	21.0	140	23.0	260	24.0
30	21.0	150	24.0	270	19.0
40	21.0	160	22.0	280	21.0
50	24.0	170	25.0	290	25.5
60	22.0	180	25.0	300	25.0
70	20.0	190	25.0	310	25.0
80	23.0	200	25.0	320	22.0
90	20.0	210	26.5	330	25.0
100	22.0	220	24.5	340	24.0
110	22.0	230	23.5	350	25.0

800 MEGA CYCLES

Pos.in deg.	Radiation in db.	Pos.in deg.	Radiation in db.	Pos.in deg.	Radiation in db.
0	6.0	120	12.0	240	8.0
10	2.0	130	13.5	250	13.0
20	5.0	240	14.5	260	17.0
30	10.0	150	14.0	270	19.0
40	12.0	160	12.0	280	17.5
50	12.0	170	13.0	290	17.0
60	12.0	180	15.0	300	16.0
70	11.0	190	13.0	310	17.0
80	15.0	200	12.5	320	8.0
90	11.0	210	7.0	330	13.0
100	7.5	220	13.0	340	4.0
110	6.0	230	15.5	350	22.0

900 MEGA CYCLES

0	21.0	120	14.0	240	21.0
10	22.0	130	14.5	250	20.0
20	24.5	140	14.5	260	22.0
30	21.5	150	16.0	270	20.0
40	24.5	160	19.0	280	14.0
50	25.0	170	14.0	290	11.0
60	24.0	180	9.0	300	11.0
70	25.0	190	11.0	310	15.0
80	19.5	200	16.0	320	12.0
90	18.0	210	19.0	330	18.0
100	17.0	220	18.0	340	20.0
110	8.0	230	19.0	350	21.0

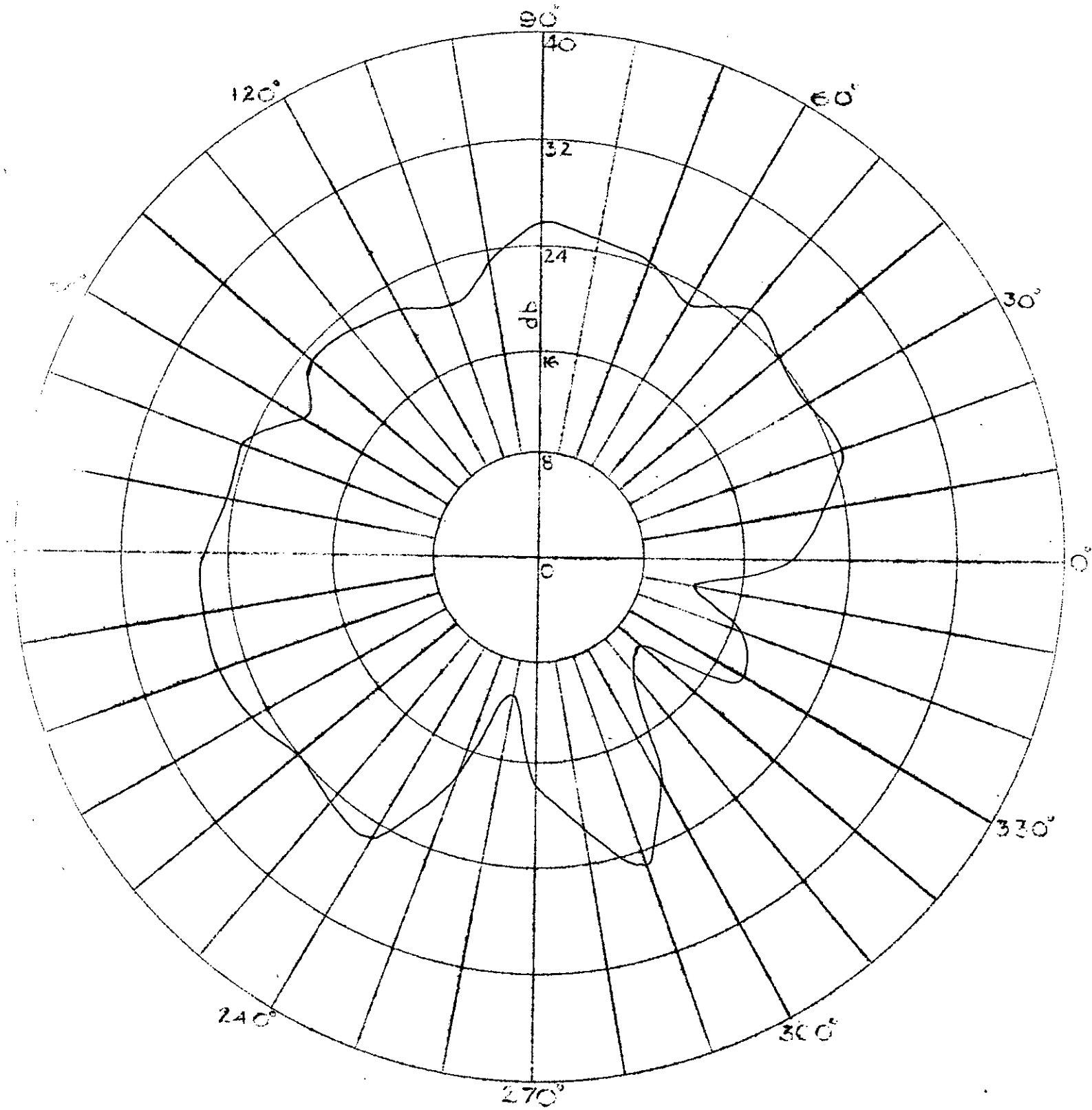

Fig. 27a Radiation Pattern at 250 Mega Cycles

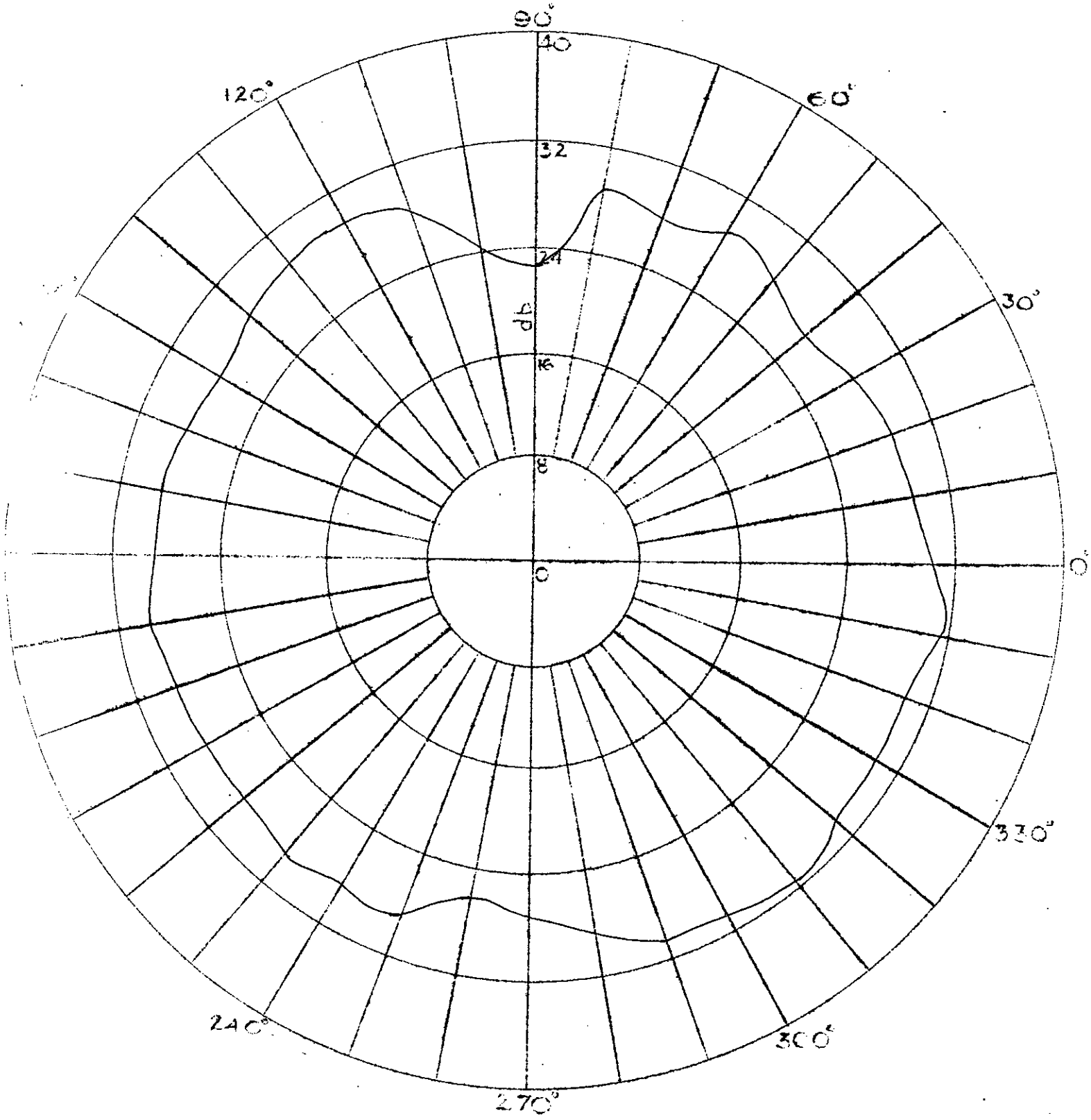

Fig. 27b Radiation Pattern at 300 Mega Cycles

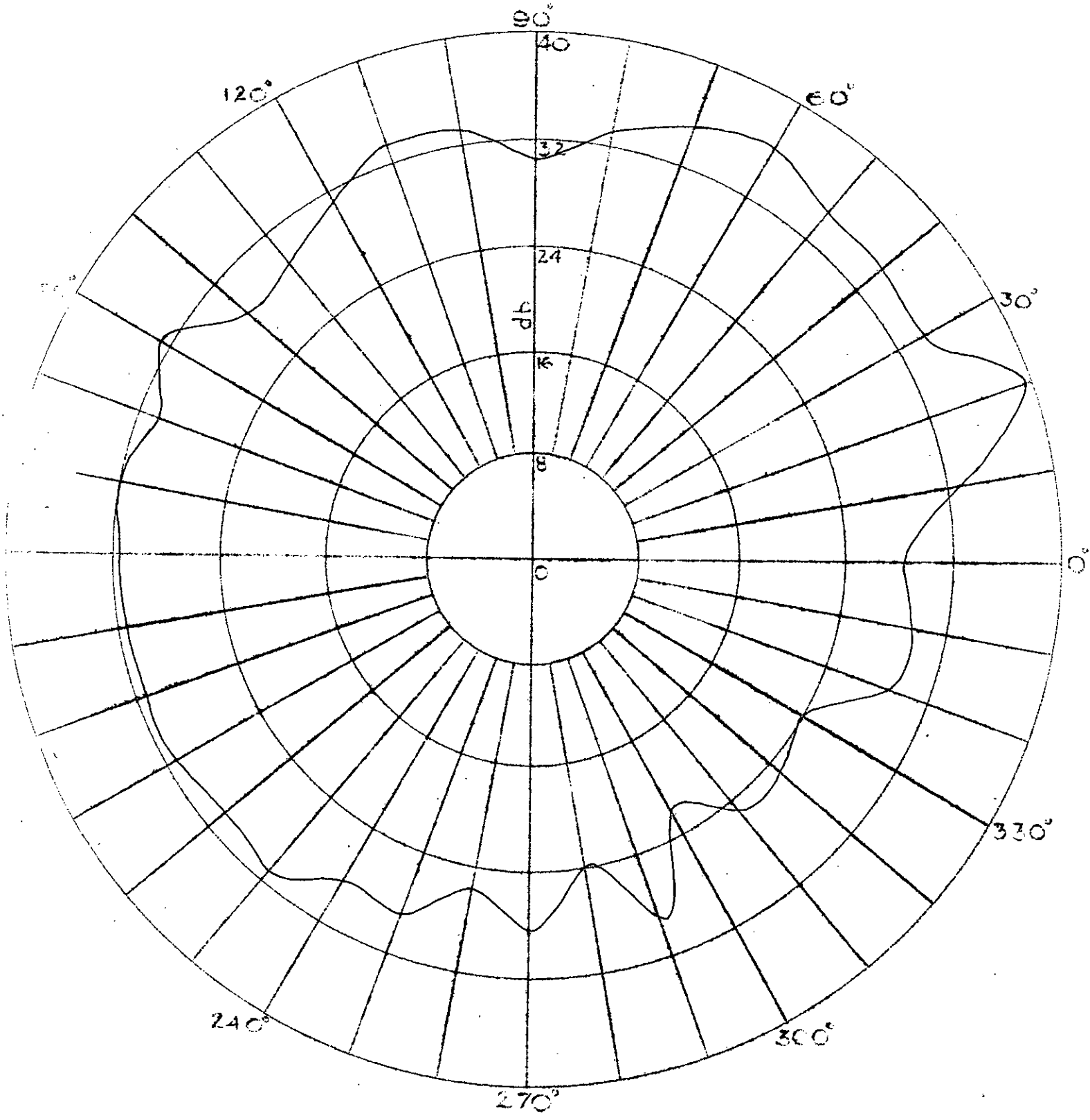

Fig. 27c Radiation Pattern at 400 Mega Cycles

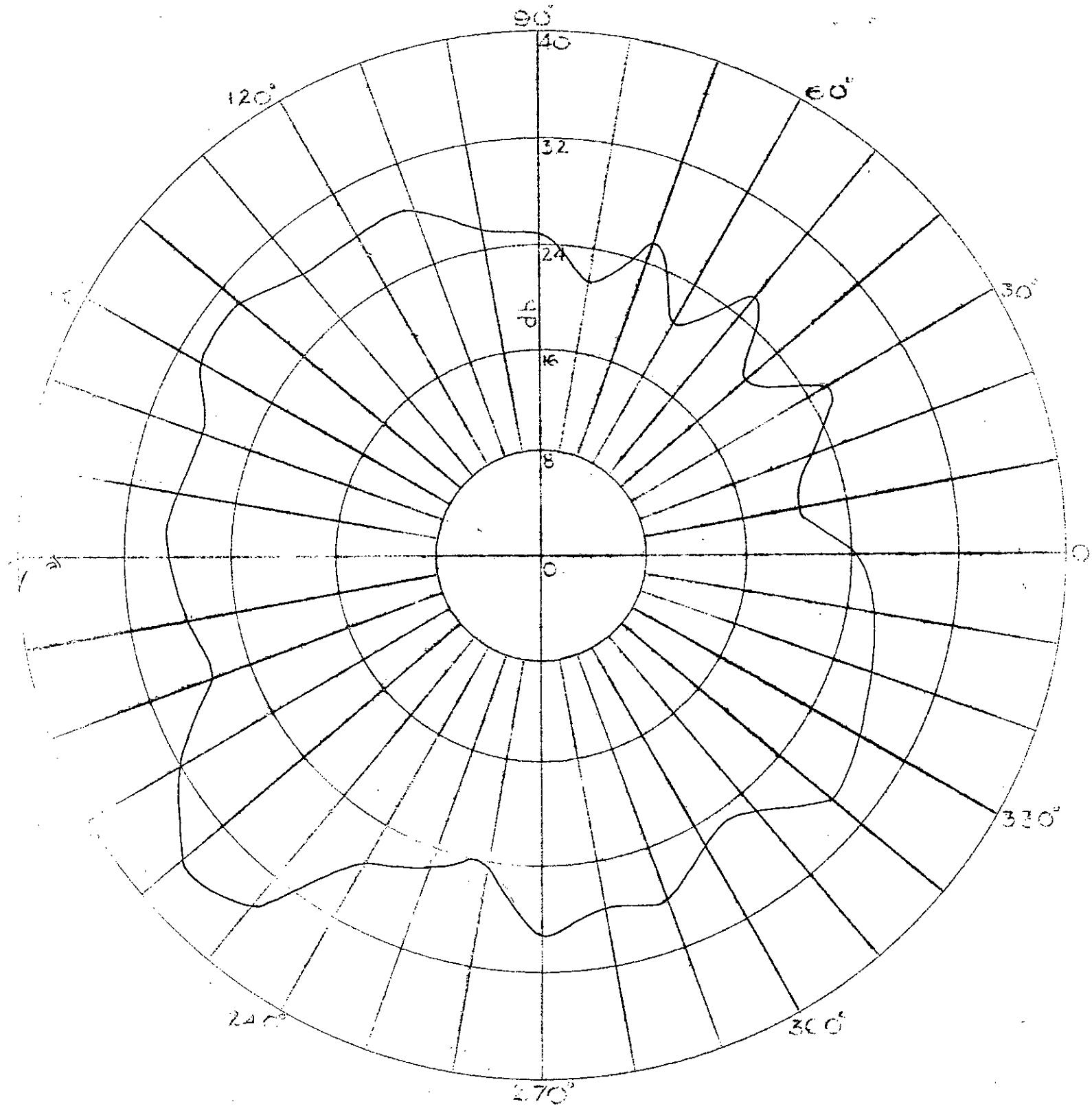

Fig. 27d Radiation Pattern at 500 Mega Cycles

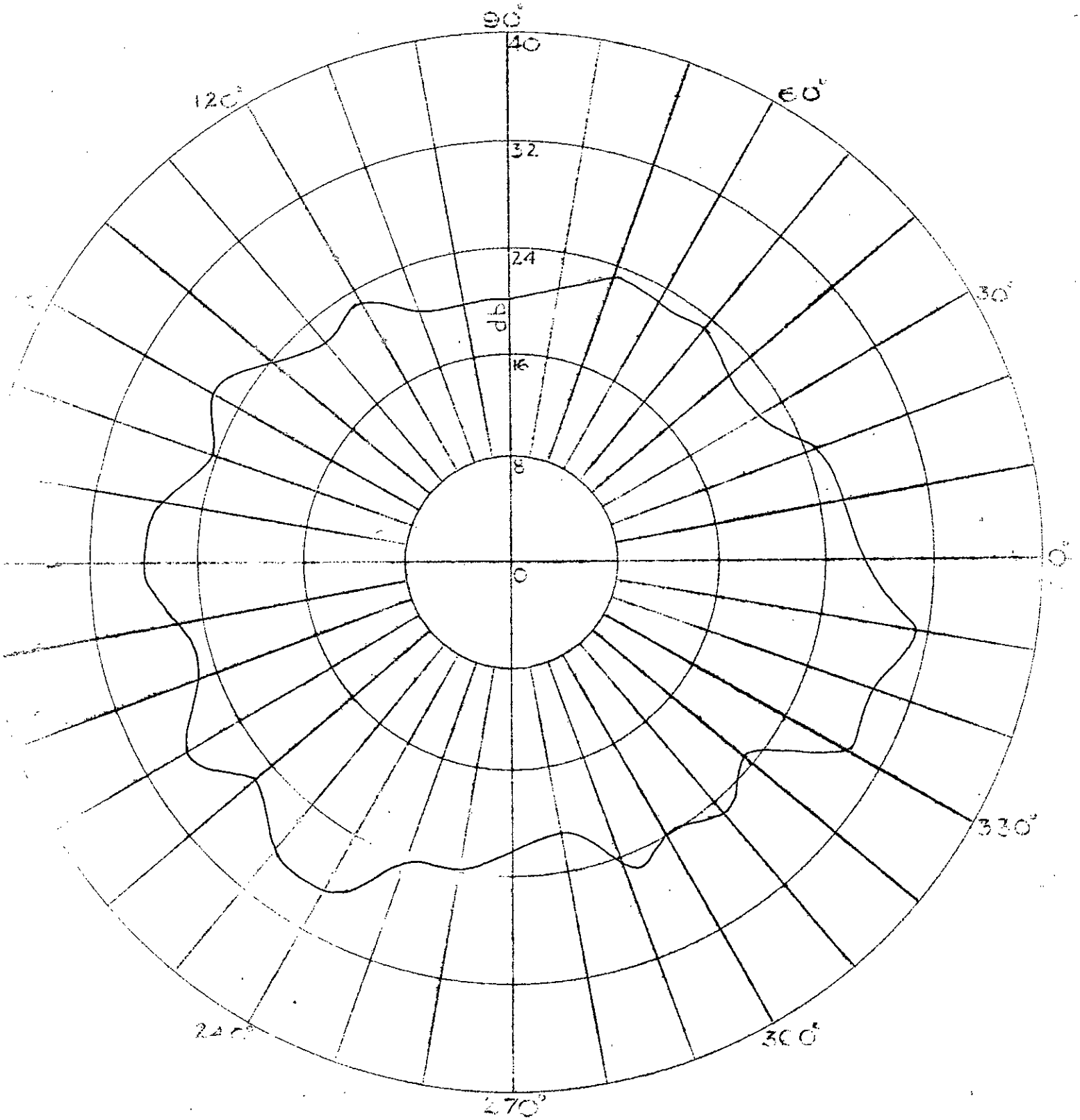

Fig.27e Radiation Pattern at 600 Mega Cycles

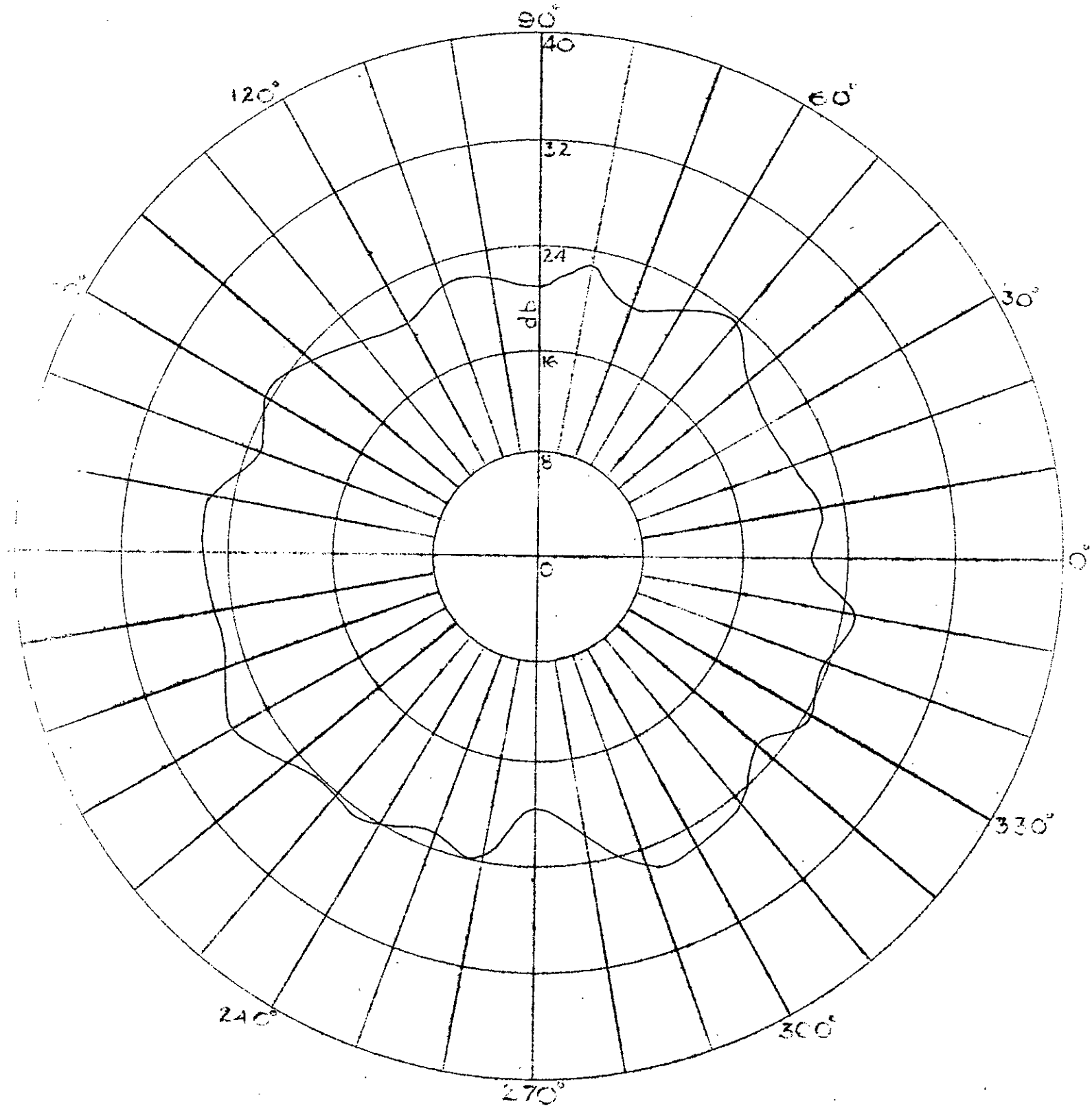

Fig. 27f Radiation Pattern at 700 Mega Cycles

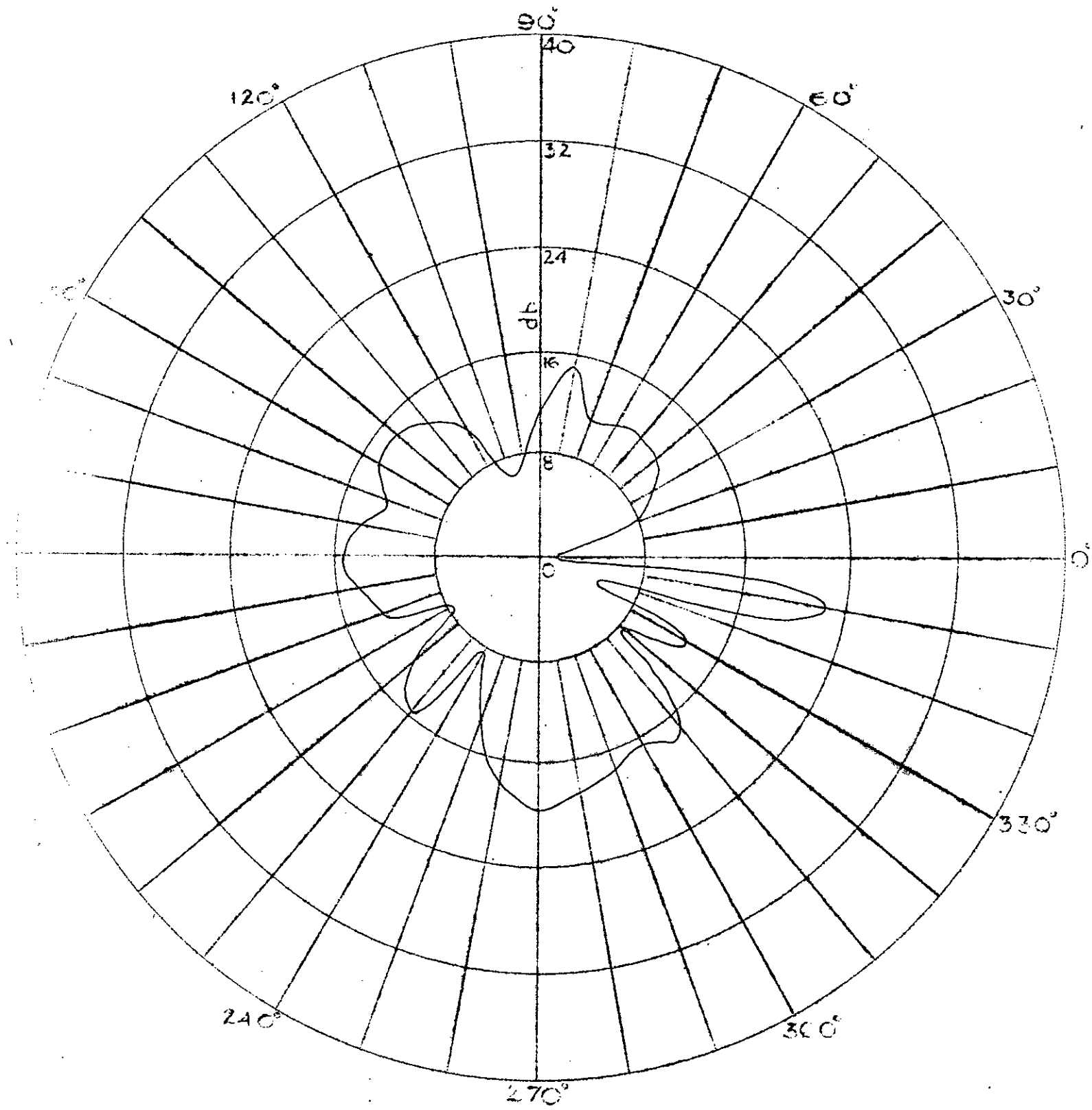

Fig.27g Radiation Pattern at 800 Mega Cycles

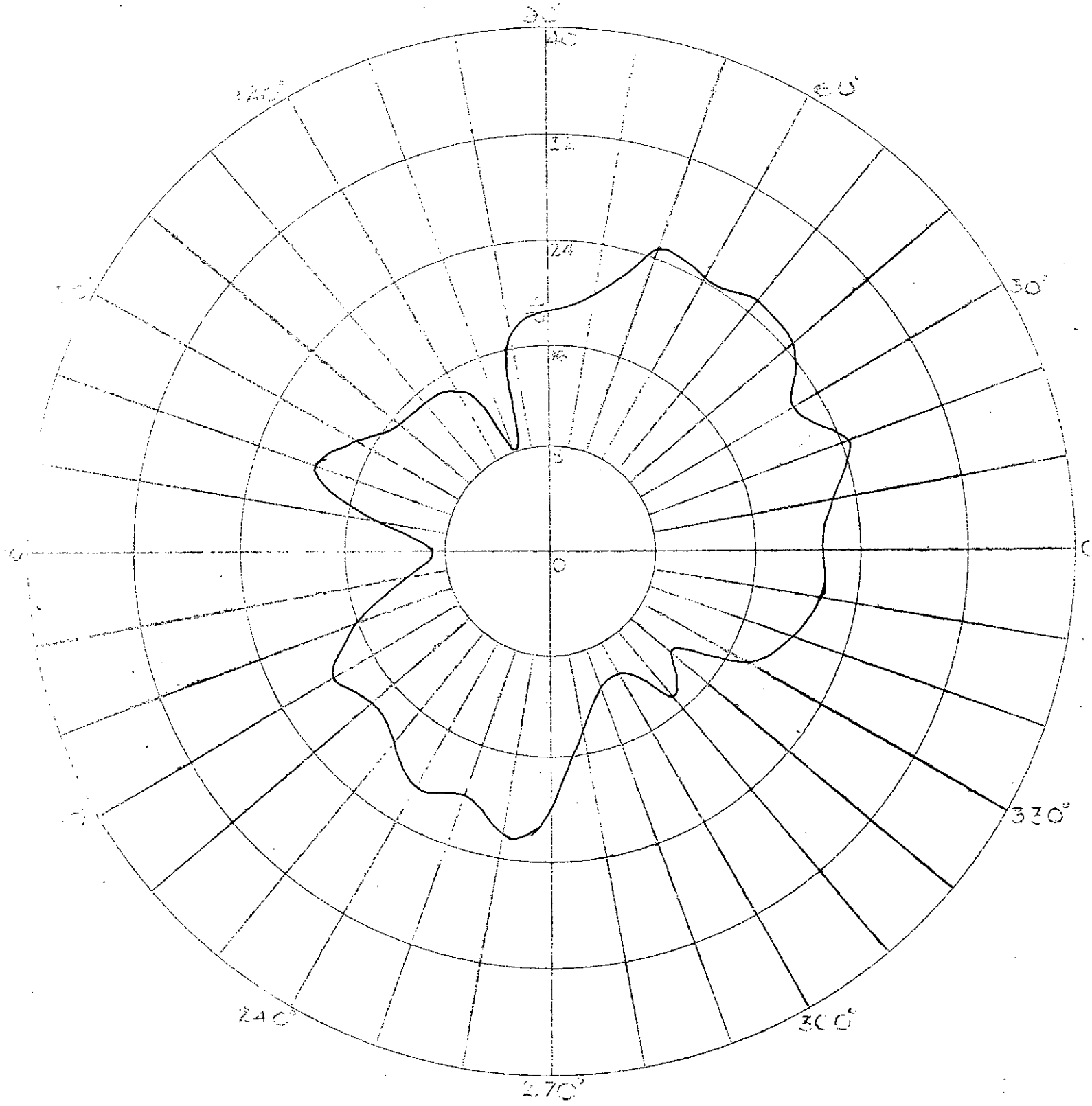

Fig. 27h Radiation Pattern at 900 Mega Cycles

TABLE - VIII

INPUT IMPEDANCE CALCULATION OF FOUR ANTENNAS COMBINED

Freq. in Mc/s	Shift in Pos. of min.current ~~of~~ in λ		$I_{max.}$ μamp	$I_{min.}$ μamp	$V_{max.}$ mV	$V_{min.}$ mV	VSWR S	Z_{min}	Length of coaxl. cable in λ	Calculated impedance in Ohm.
	Gen.end	Load end								
250		0.010	4.0	3.0	1.05	0.80	1.31	38.2	2.363	48+j14
300		0.325	3.4	1.5	0.90	0.41	2.20	22.8	2.840	55-j43
350		0.064	3.5	1.5	0.91	0.41	2.21	22.5	2.315	36+j32
400		0.253	4.5	0.65	1.18	0.20	5.10	8.5	3.785	8-j10
450	0.015		3.1	0.6	0.81	0.17	4.77	10.5	4.250	100-j85
500	0.383		4.5	0.5	1.18	0.15	3.47	14.4	4.740	35+j55
550		0.377	7.2	4.5	1.80	1.18	1.53	32.8	5.210	42-j15
600		0.010	8.0	1.7	2.00	0.48	4.16	12.0	5.680	65-j85
650		0.210	4.5	1.2	1.18	0.34	3.48	14.4	6.170	25+j40
700	0.163		15.0	5.0	3.61	1.30	2.78	17.3	6.660	17+j1
750		0.050	11.0	1.1	2.71	0.38	7.10	7.1	7.100	20-j65
800		0.240	2.4	0.2	0.62	0.05	12.40	4.2	7.570	30+j120
850	0.128		7.0	0.0	1.75	0.00		0.0	8.050	0+j105
900		0.167	15.5	1.0	3.75	0.27	13.9	3.6	8.530	5-j27

IMPEDANCE COORDINATES—50-OHM CHARACTERISTIC IMPEDANCE

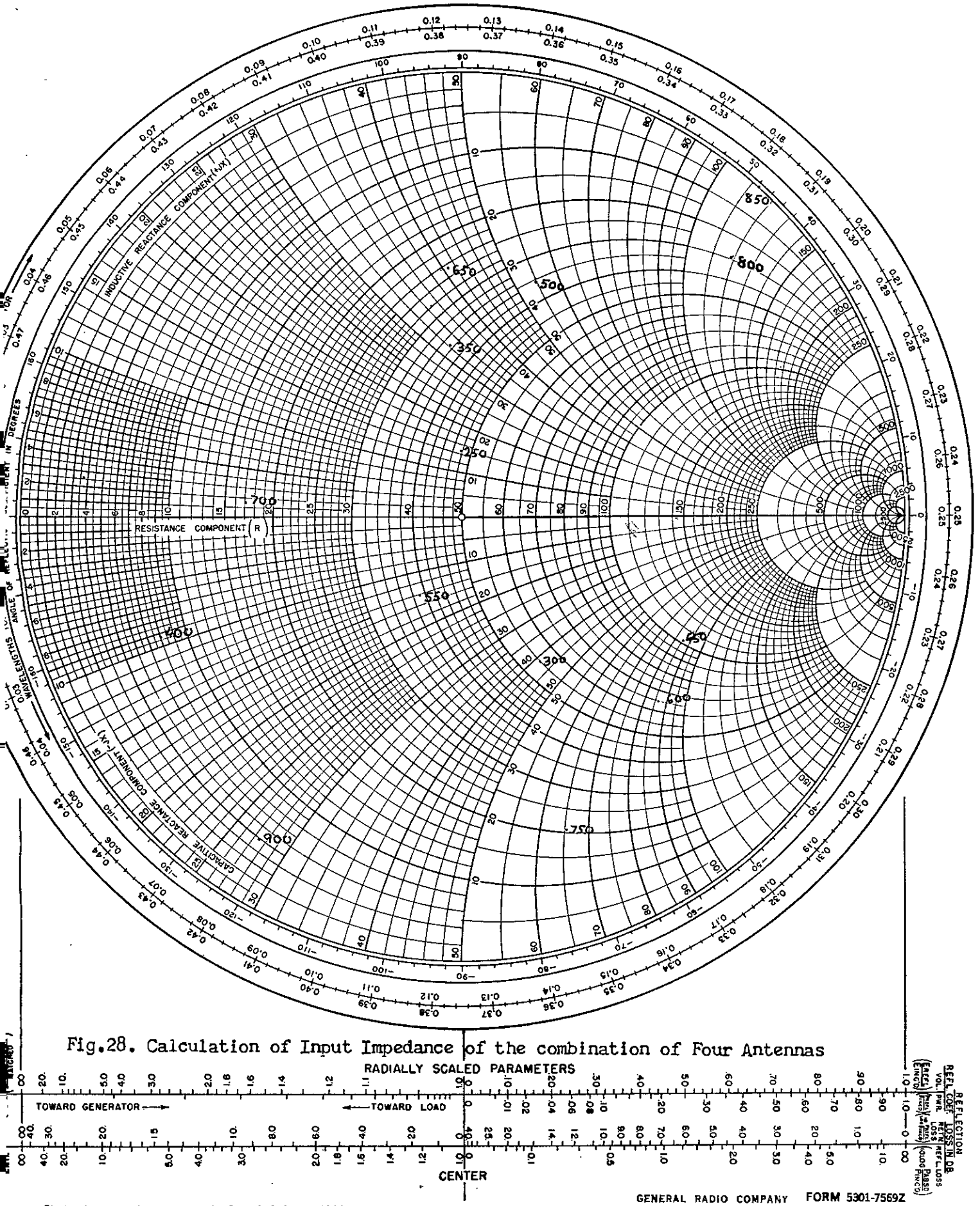

Fig.28. Calculation of Input Impedance of the combination of Four Antennas

Fig. 29. Variation of the Resistive and Reactive components of the Input Impedance of the combination of four antennas with frequency.

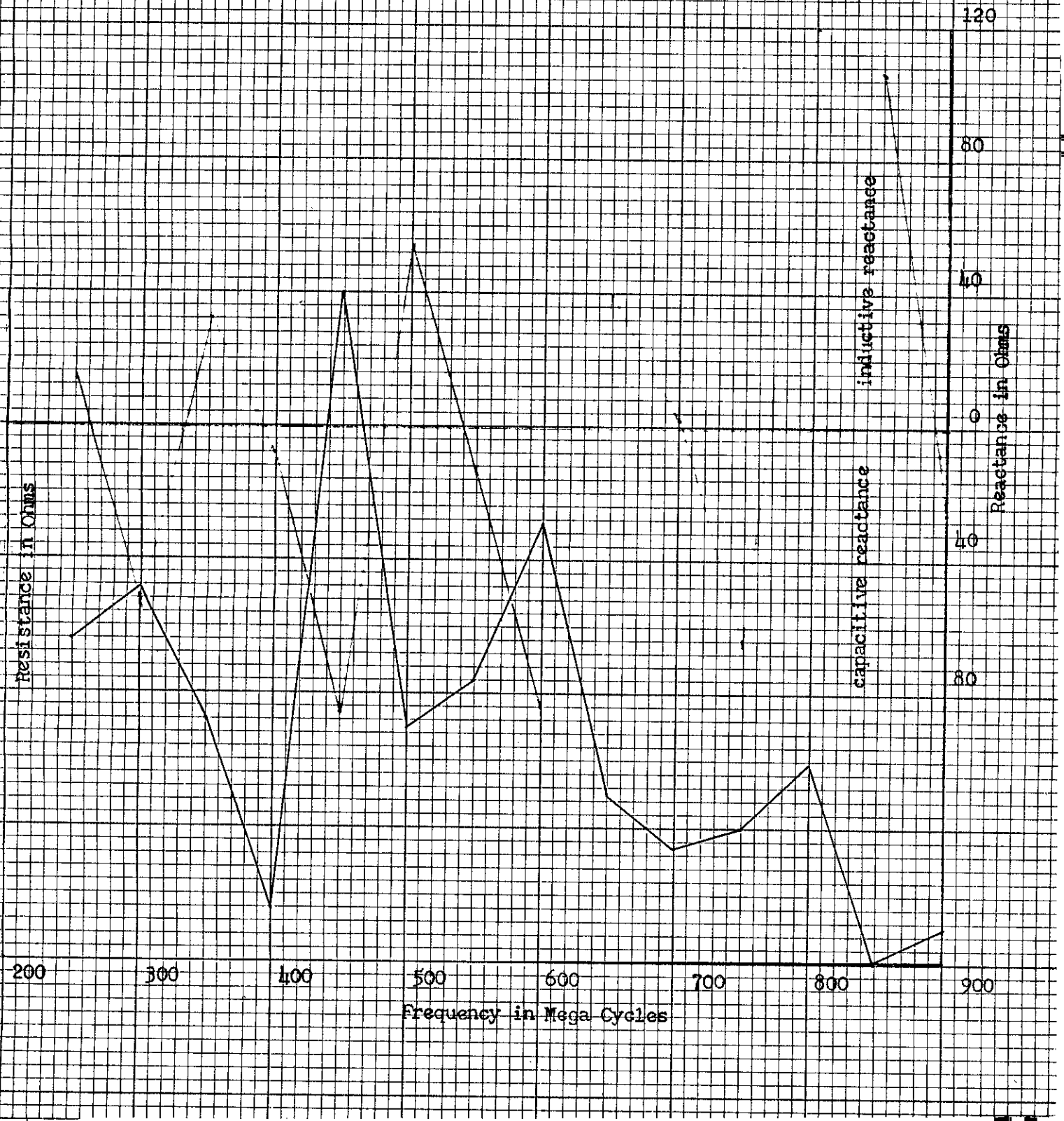

D. COMBINATION OF FOUR LOG-PERIODIC ANTENNAS UNDER INVESTIGATION

Four identical antennas each was as shown in Fig. 30 were placed at the four sides of a square base pyramid. This time the separation between the conductors were in Log. Antennas at the opposite sides were shorted at the smaller ends. One pair of the shorted antennas was fed by the inner conductor and the other pair was fed by the outer conductor of the co-axial cable from the same signal generator. The experiment was identical as in 'C'. The measured values of the radiation intensities for the antenna axis horizontal is shown in table IX and the radiation patterns are shown in Figs. 31a, 31b, 31c, 31d, 31e, 31f,31g.

For the vertical position of the antenna axis the measured values of the radiation intensities are shown in table X and the radiation patterns are shown in Figs. 32a, 32b, 32c, 32d, 32e, 32f, 32g.

The values of the input impedance were calculated from a Smith Chart as shown in Fig. 33. Calculated values are shown in table XI. The impedance vs frequency curve is shown in Fig. 34.

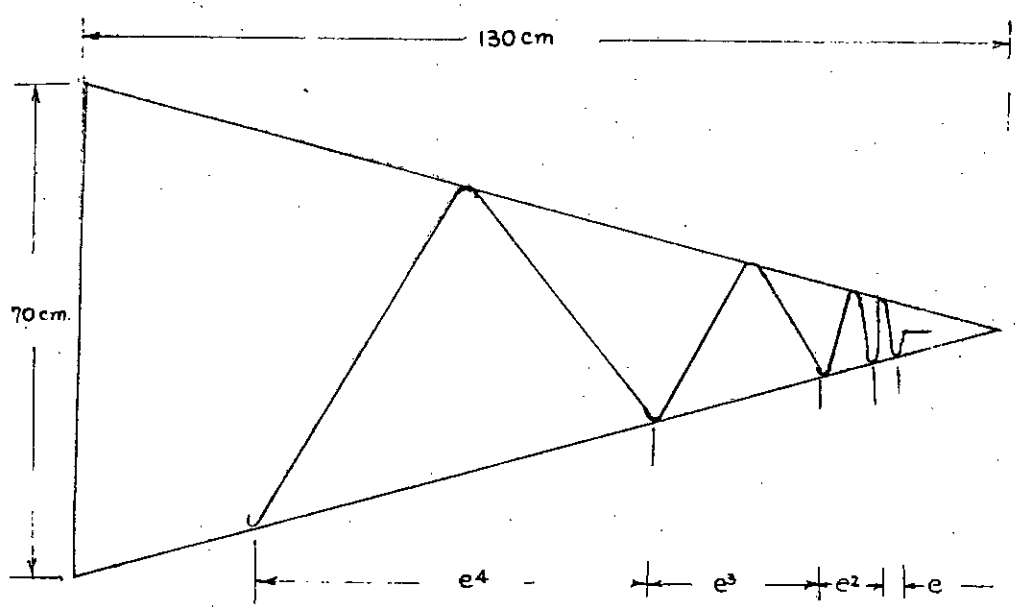

FIG. 30. ONE FACE OF THE LOG-PERIODIC ANTENNA UNDER INVESTIGATION

TABLE - IX

MEASUREMENT OF RADIATION INTENSITIES

FOUR LOG-PERIODIC ANTENNAS COMBINED

AXIS HORIZONTAL

300 MEGA CYCLES

Pos.in deg.	Radiation in db.	Pos. in deg.	Radiation in db.	Pos.in deg.	Radiation in db.
0	29.0	120	27.5	240	27.0
10	23.0	130	21.0	250	32.0
20	31.0	140	17.0	260	29.0
30	31.0	150	11.0	270	28.0
40	29.0	160	13.0	280	27.0
50	29.0	170	17.0	290	22.0
60	30.0	180	20.0	300	24.0
70	32.0	190	21.0	310	25.0
80	30.0	200	20.0	320	28.0
90	29.0	210	18.0	330	29.0
100	29.0	220	24.0	340	28.0
110	27.0	230	26.0	350	29.0

400 MEGA CYCLES

0	32.0	120	27.0	240	28.0
10	30.0	130	23.0	250	27.0
20	34.0	140	18.0	260	28.0
30	35.0	150	21.0	270	28.0
40	30.0	160	17.0	280	32.0
50	34.0	170	24.0	290	29.0
60	35.0	180	24.0	300	30.0
70	35.0	190	23.0	310	30.0
80	35.0	200	27.0	320	29.0
90	35.0	210	26.0	330	25.0
100	30.0	220	29.0	340	25.0
110	27.0	230	28.0	350	28.0

500 MEGA CYCLES

Pos.in deg.	Radiation in db.	Pos.in deg.	Radiation in db.	Pos. in deg.	Radiation in db.
0	35.0	120	28.0	240	30.0
10	38.0	130	29.0	250	22.0
20	36.0	140	20.0	260	27.0
30	38.0	150	31.0	270	28.0
40	33.0	160	22.0	280	37.0
50	40.0	170	32.0	290	30.0
60	40.0	180	28.0	300	37.0
70	38.0	190	26.0	310	36.0
80	40.0	200	34.0	320	30.0
90	39.0	210	35.0	330	22.0
100	32.0	220	35.0	340	22.0
110	27.0	230	32.0	350	26.0

600 MEGA CYCLES

0	27.0	120	20.0	240	22.0
10	32.0	130	22.0	250	18.0
20	30.0	140	18.0	260	20.0
30	29.5	150	24.0	270	20.0
40	32.0	160	19.0	280	32.0
50	32.0	170	23.0	290	29.0
60	30.0	180	20.0	300	30.0
70	27.0	190	16.0	310	29.0
80	27.0	200	15.5	320	28.0
90	26.0	210	24.0	330	23.0
100	22.0	220	25.0	340	24.0
110	28.0	230	22.0	350	23.0

700 MEGA CYCLES

Pos.in deg.	Radiation in db.	Pos.in deg.	Radiation in db.	Pos. in deg.	Radiation in db.
0	21.0	120	13.5	240	14.0
10	21.0	130	16.0	250	16.0
20	22.0	140	17.0	260	14.0
30	26.0	150	18.0	270	11.0
40	27.0	160	16.0	280	24.0
50	25.0	170	14.0	290	20.0
60	21.0	180	13.0	300	23.0
70	14.0	190	7.5	310	23.0
80	15.0	200	7.0	320	26.0
90	14.0	210	14.0	330	28.0
100	15.0	220	16.0	340	26.0
110	10.0	230	13.0	350	21.0

800 MEGA CYCLES

0	19.0	120	11.0	240	12.0
10	20.0	130	12.0	250	13.0
20	23.0	140	10.0	260	14.0
30	26.0	150	11.0	270	10.0
40	26.0	160	10.0	280	17.0
50	21.0	170	11.5	290	18.5
60	20.0	180	10.0	300	25.0
70	11.0	190	8.0	310	23.0
80	12.5	200	7.0	320	26.5
90	12.0	210	11.5	330	27.0
100	9.0	220	12.0	340	27.0
110	12.5	230	11.5	350	24.0

900 MEGA CYCLES

Pos.in deg.	Radiation in db.	Pos.in deg.	Radiation in db.	Pos.in deg.	Radiation in db.
0	22.0	120	10.0	240	12.0
10	21.0	130	12.0	250	10.0
20	24.0	140	5.0	260	14.0
30	27.0	150	4.0	270	10.0
40	26.0	160	3.0	280	11.0
50	17.0	170	11.0	290	18.0
60	20.0	180	10.0	300	22.0
70	8.0	190	9.0	310	23.0
80	12.0	200	7.0	320	27.0
90	9.0	210	8.0	330	24.0
100	3.0	220	8.0	340	28.0
110	14.0	230	11.0	350	28.0

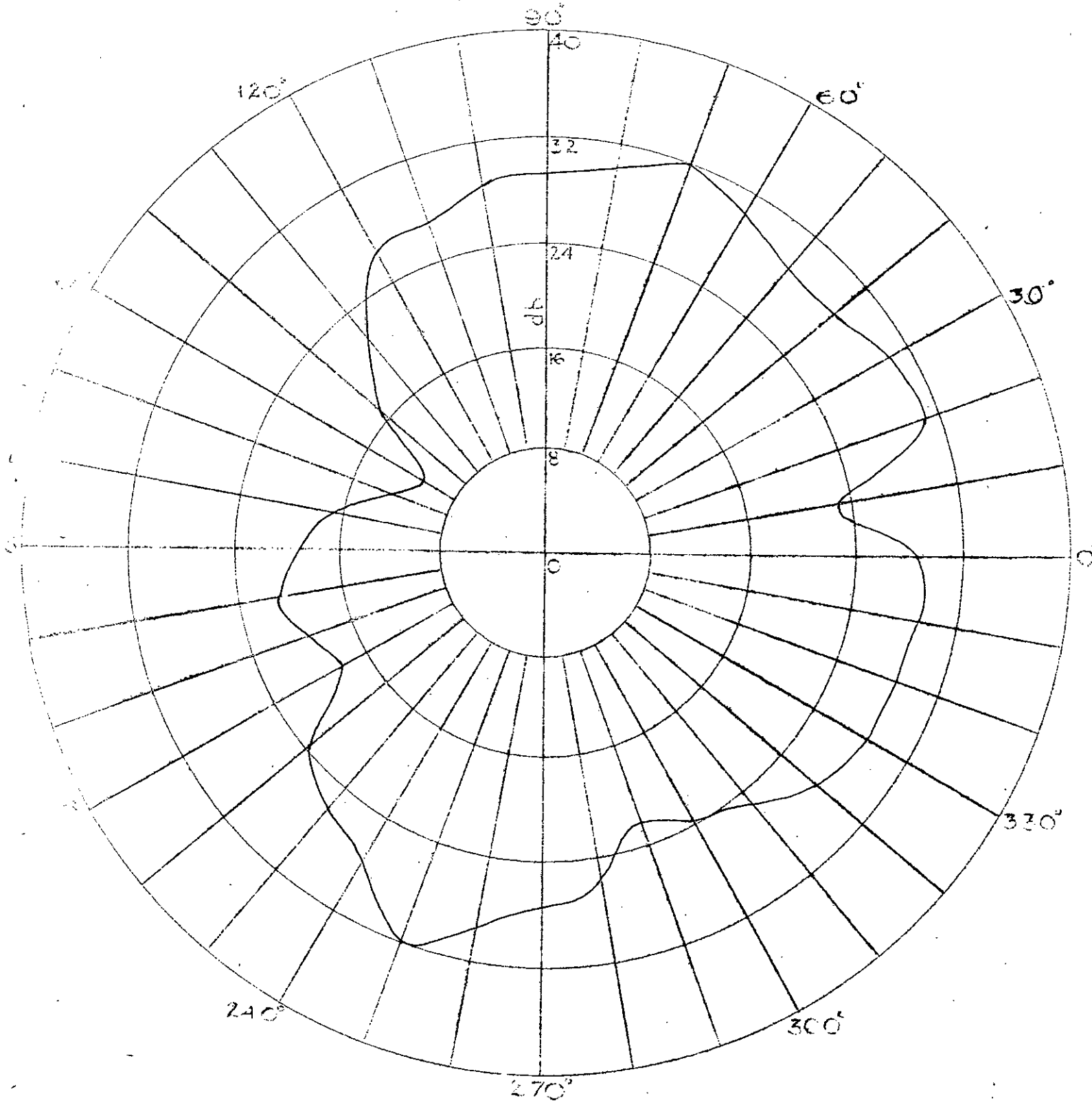

Fig.31a Radiation Pattern at 300 Mega Cycles

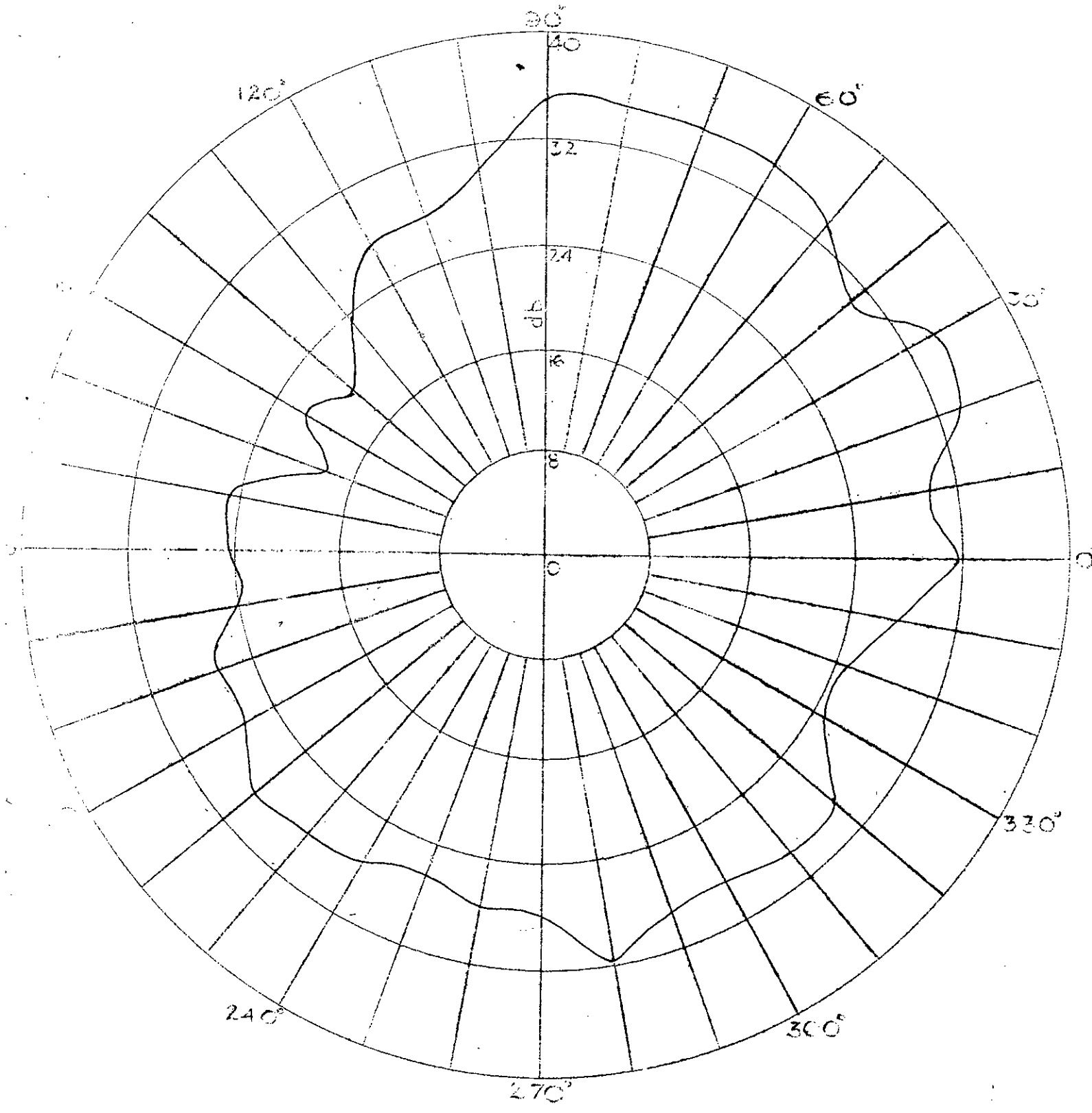

Fig. 31b Radiation Pattern at 400 Mega Cycles

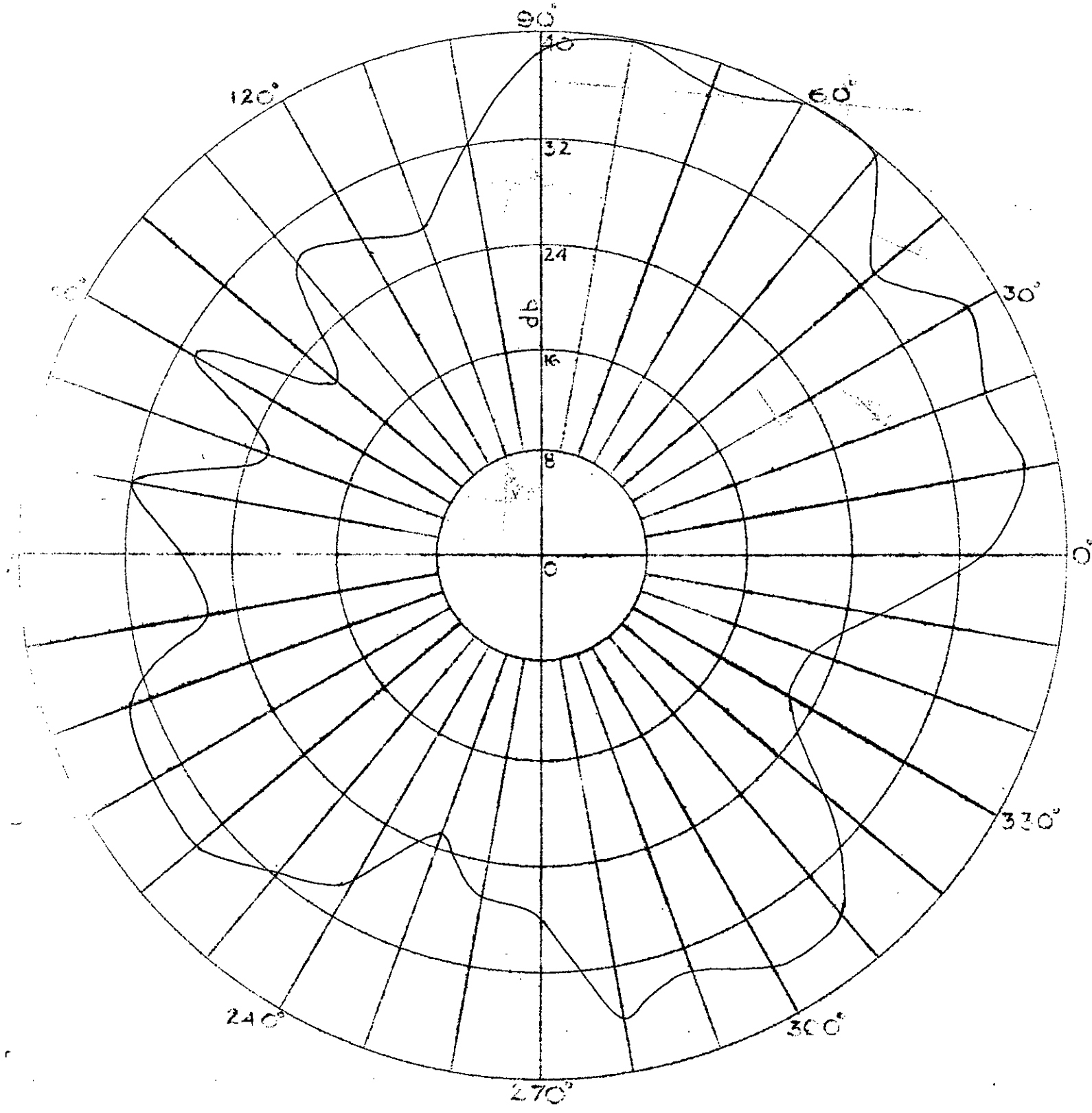

Fig. 31c Radiation Pattern at 500 Mega Cycles

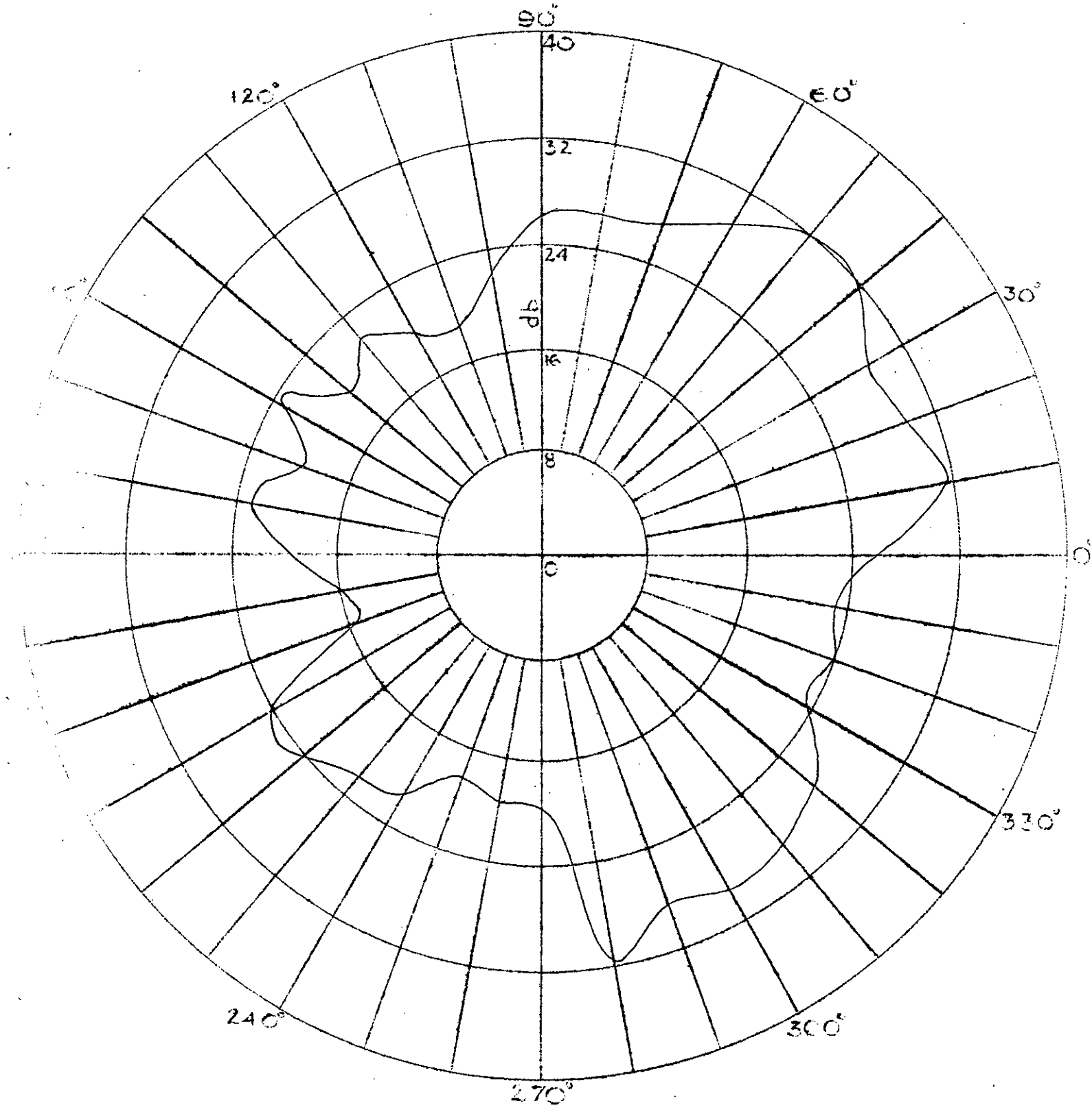

Fig. 31d Radiation Pattern at 600 Mega Cycles

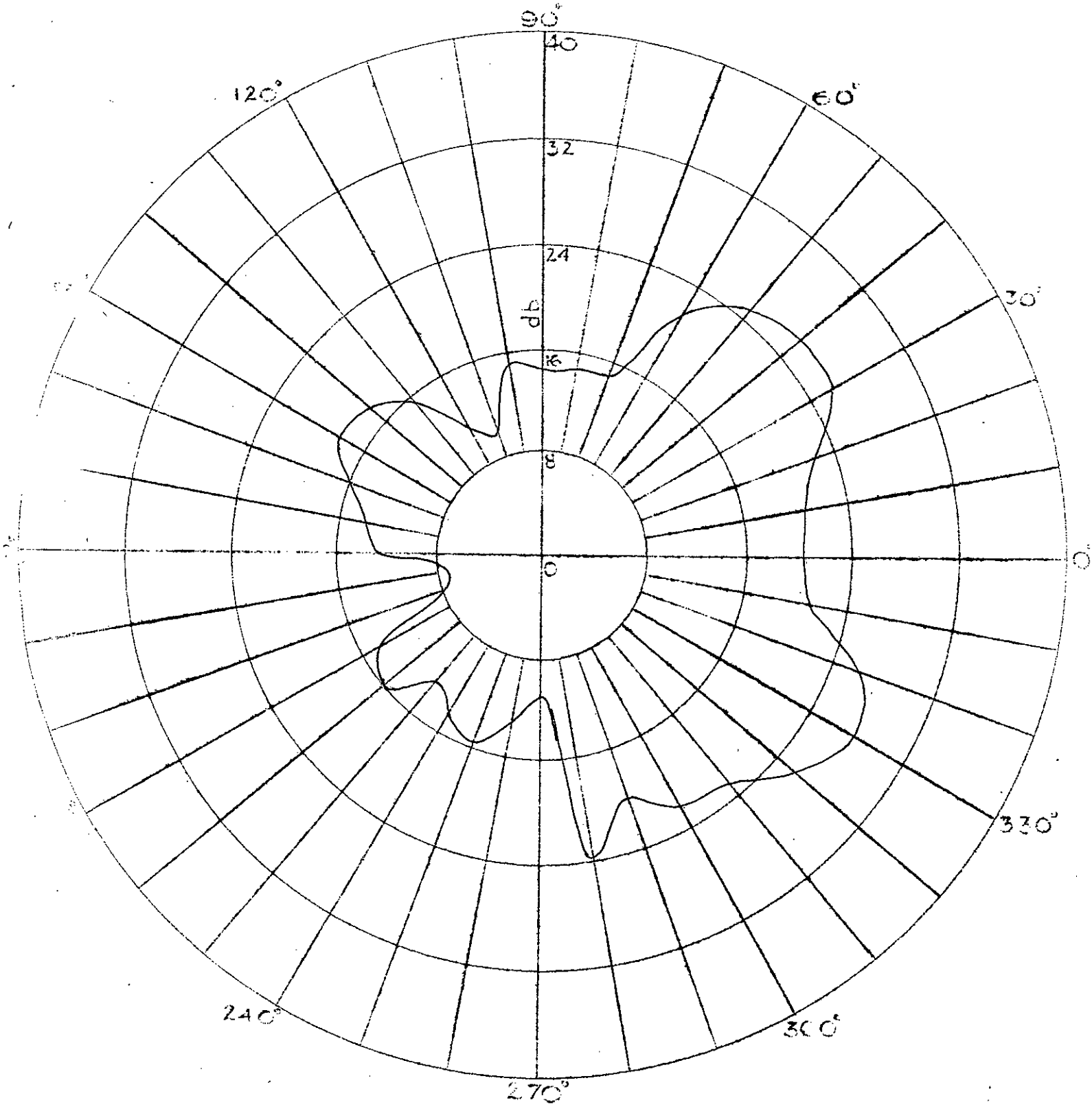

Fig. 31e Radiation Pattern at 700 Mega Cycles

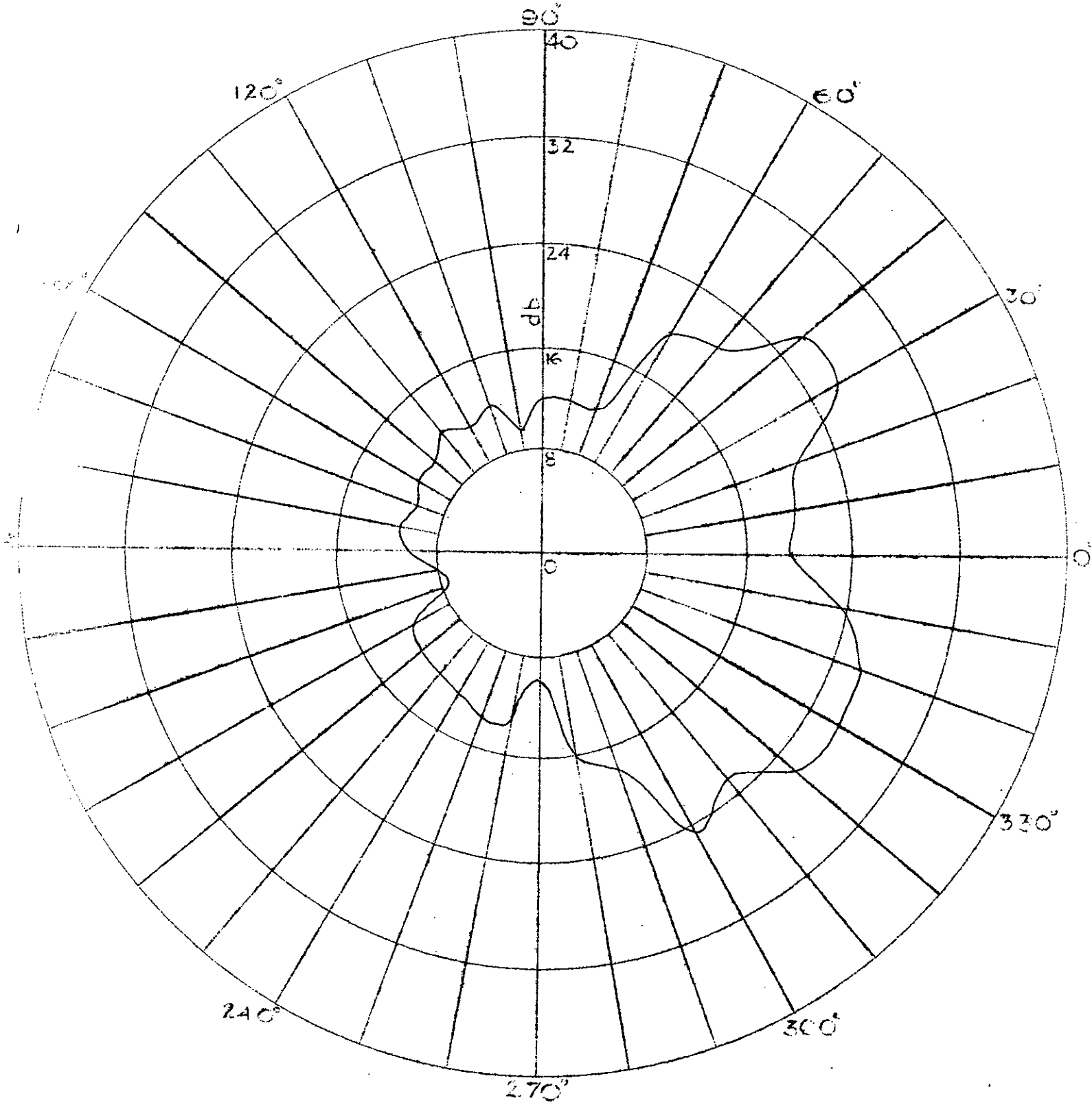

Fig. 31f Radiation Pattern at 800 Mega Cycles

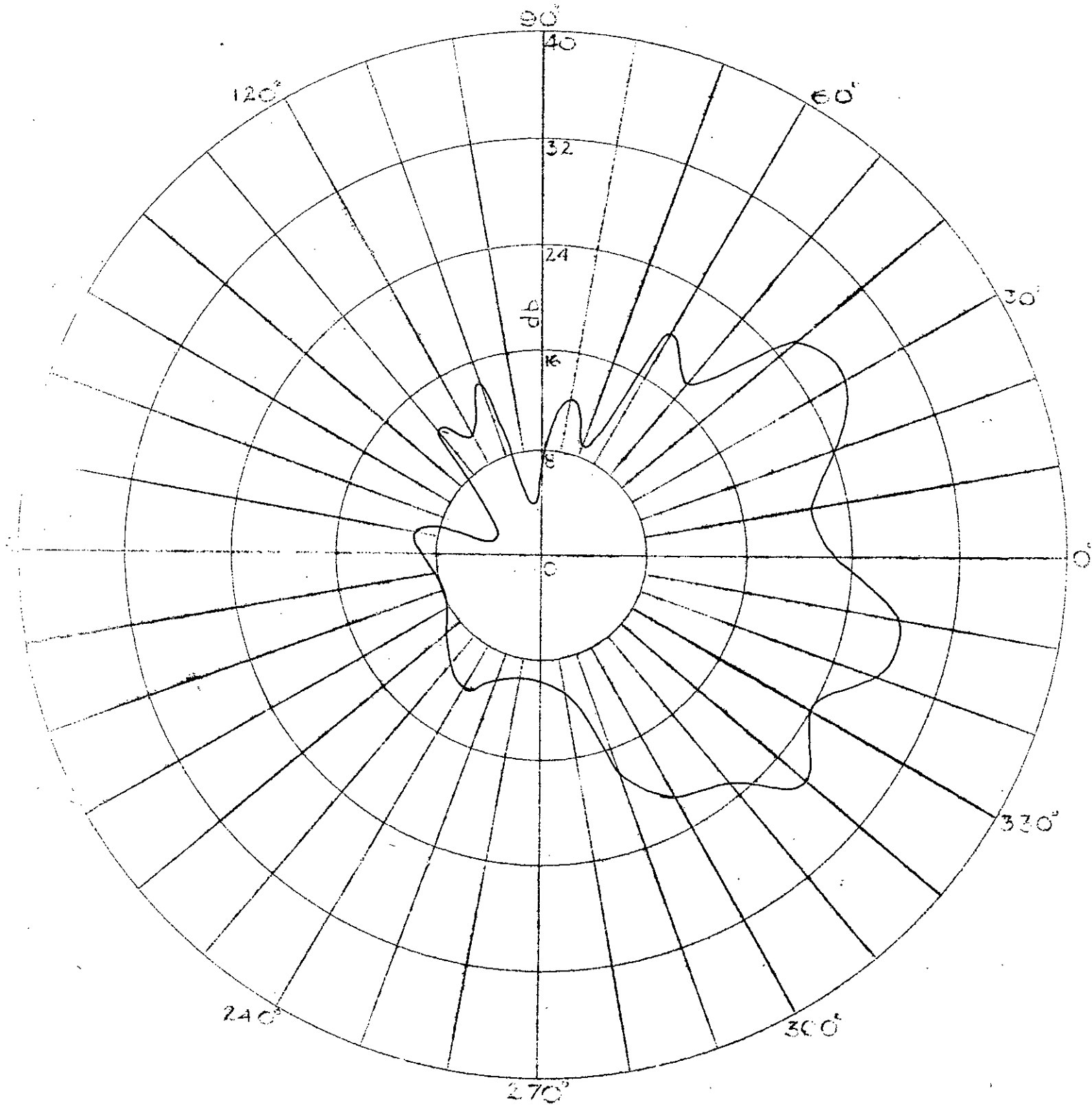

Fig. 31g Radiation Pattern at 900 Mega Cycles

TABLE - IX

MEASUREMENT OF RADIATION INTENSITIES

FOUR LOG-PERIODIC ANTENNAS COMBINED

AXIS VERTICAL

300 MEGA CYCLES

Pos.in deg.	Radiation in db.	Pos.in deg,	Radiation in db.	Pos.in deg.	Radiation in db.
0	31.5	120	27.0	240	28.0
10	32.0	130	28.0	250	29.0
20	28.0	140	27.0	260	32.0
30	27.0	150	28.0	270	32.0
40	29.0	160	27.0	280	31.5
50	30.0	170	27.0	290	32.0
60	27.0	180	27.0	300	29.0
70	28.0	190	28.0	310	32.0
80	29.5	200	29.0	320	28.0
90	27.0	210	29.0	330	30.0
100	27.0	220	29.0	340	32.0
110	27.5	230	28.0	350	30.0

400 MEGA CYCLES

0	30.0	120	27.0	240	27.0
10	34.0	130	26.0	250	25.0
20	32.0	140	26.0	260	33.0
30	29.0	150	26.0	270	26.0
40	29.0	160	24.0	280	28.0
50	30.0	170	26.0	290	26.0
60	26.0	180	27.0	300	24.0
70	26.0	190	27.0	310	23.0
80	27.0	200	28.0	320	21.0
90	27.0	210	27.0	330	23.0
100	28.0	220	25.0	340	30.0
110	26.0	230	24.0	350	28.0

500 MEGA CYCLES

Pos.in deg.	Radiation in db.	Pos.in deg.	Radiation in db.	Pos.in deg.	Radiation in db.
0	29.0	120	27.0	240	27.0
10	34.0	130	25.0	250	22.0
20	35.0	140	24.5	260	34.0
30	32.0	150	24.0	270	21.0
40	30.0	160	23.0	280	25.0
50	29.0	170	24.5	290	21.0
60	25.0	180	27.0	300	21.0
70	24.0	190	27.5	310	14.0
80	26.0	200	28.0	320	15.0
90	25.5	210	26.0	330	16.0
100	29.0	220	20.0	340	24.5
110	25.0	230	20.0	350	26.0

600 MEGA CYCLES

0	22.0	120	20.0	240	19.0
10	24.0	130	17.0	250	19.0
20	24.0	140	18.0	260	21.0
30	30.0	150	19.0	270	22.0
40	30.0	160	18.0	280	29.0
50	28.0	170	18.0	290	19.0
60	27.0	180	23.0	300	21.0
70	24.0	190	20.0	310	20.0
80	22.0	200	24.0	320	20.0
90	20.0	210	26.0	330	15.0
100	22.0	220	25.0	340	15.0
110	18.0	230	23.0	350	16.0

700 MEGA CYCLES

Pos.in deg.	Radiation in db.	Pos.in deg.	Radiation in db.	Pos.in deg.	Radiation in db.
0	16.0	120	11.0	240	21.5
10	22.0	130	12.0	250	18.0
20	22.0	140	8.0	260	19.0
30	18.0	150	10.0	270	19.0
40	26.0	160	14.0	280	23.0
50	26.0	170	13.0	290	24.0
60	25.0	180	13.0	300	19.0
70	24.0	190	13.0	310	17.0
80	18.0	200	17.0	320	20.0
90	19.5	210	21.0	330	20.0
100	17.0	220	16.0	340	18.0
110	18.5	230	21.0	350	15.0

800 MEGA CYCLES

0	17.0	120	9.0	240	20.0
10	17.0	130	10.0	250	19.0
20	24.0	140	14.0	260	21.0
30	23.0	150	14.0	270	22.0
40	21.0	160	14.0	280	17.0
50	20.0	170	13.0	290	15.0
60	15.0	180	15.0	300	15.0
70	13.0	190	15.0	310	14.0
80	15.0	200	14.0	320	13.0
90	14.0	210	17.0	330	13.0
100	8.0	220	19.0	340	17.0
110	9.0	230	18.0	350	19.0

9 00 MEGA CYCLES

Pos.in deg.	Radiation in db.	Pos.in deg.	Radiation in db.	Pos.in deg.	Radiation in db.
0	20.0	120	15.0	240	19.0
10	18.0	130	16.0	250	15.0
20	18.0	140	14.0	260	14.0
30	12.0	150	13.0	270	10.0
40	6.0	160	10.0	280	8.0
50	12.0	170	11.0	290	8.0
60	13.0	180	15.0	300	11.0
70	7.0	190	18.0	310	18.0
80	8.0	200	19.0	320	15.0
90	10.0	220	21.0	330	13.0
100	8.0	220	20.0	340	17.0
110	14.0	230	18.0	350	22.0

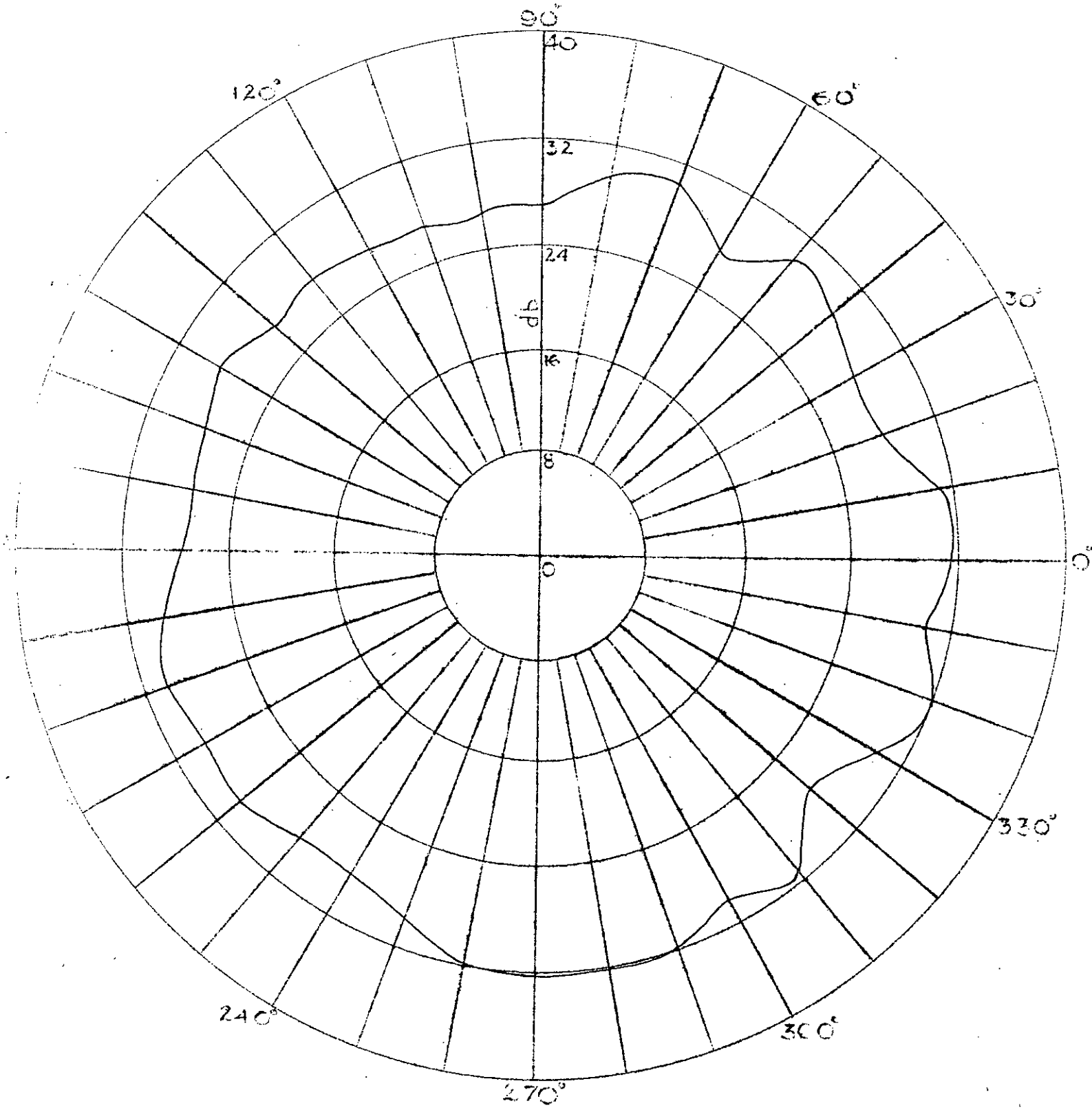

Fig. 32a Radiation Pattern at 300 Mega Cycles

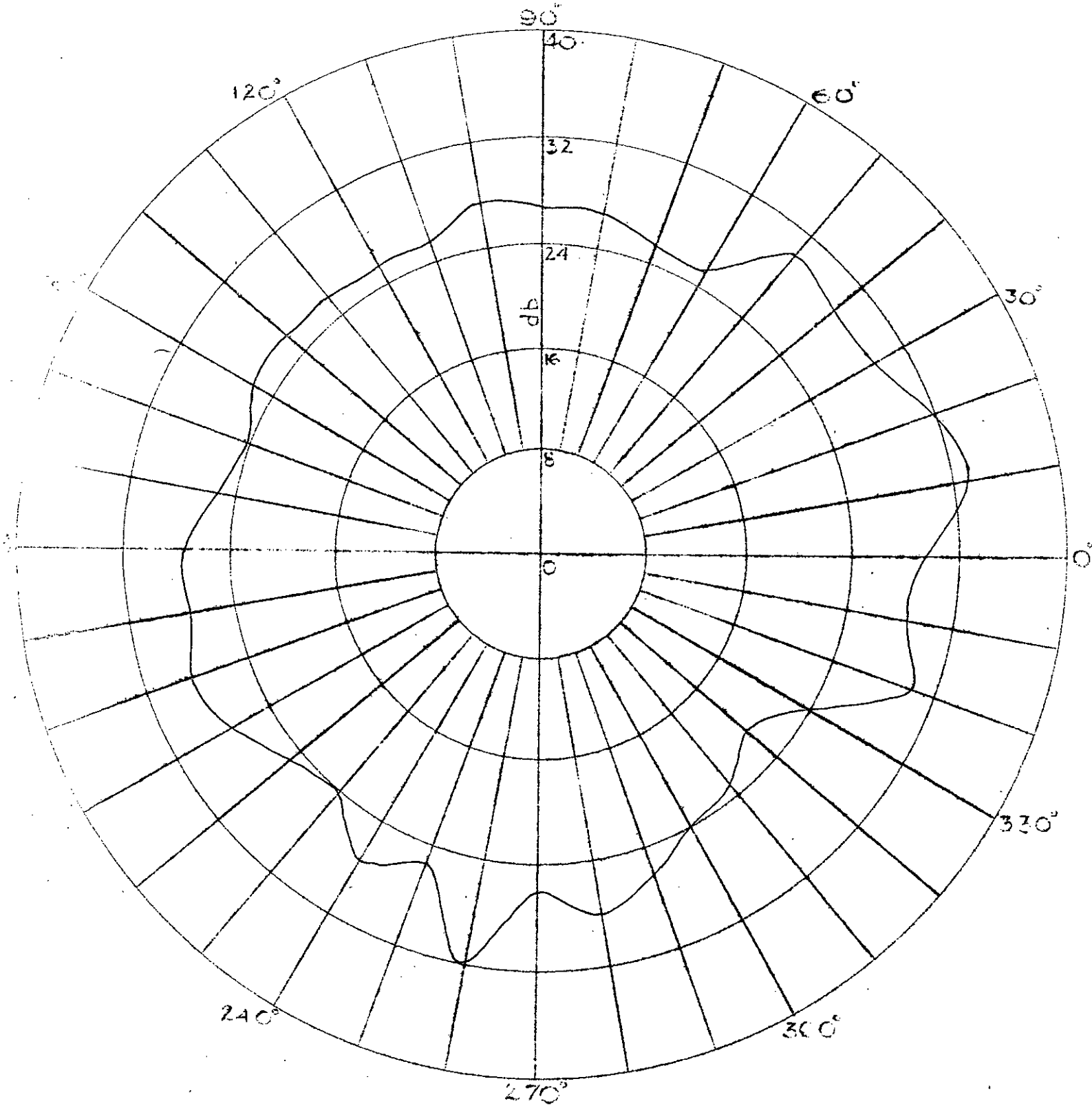

Fig. 32b Radiation Pattern at 400 Mega Cycles

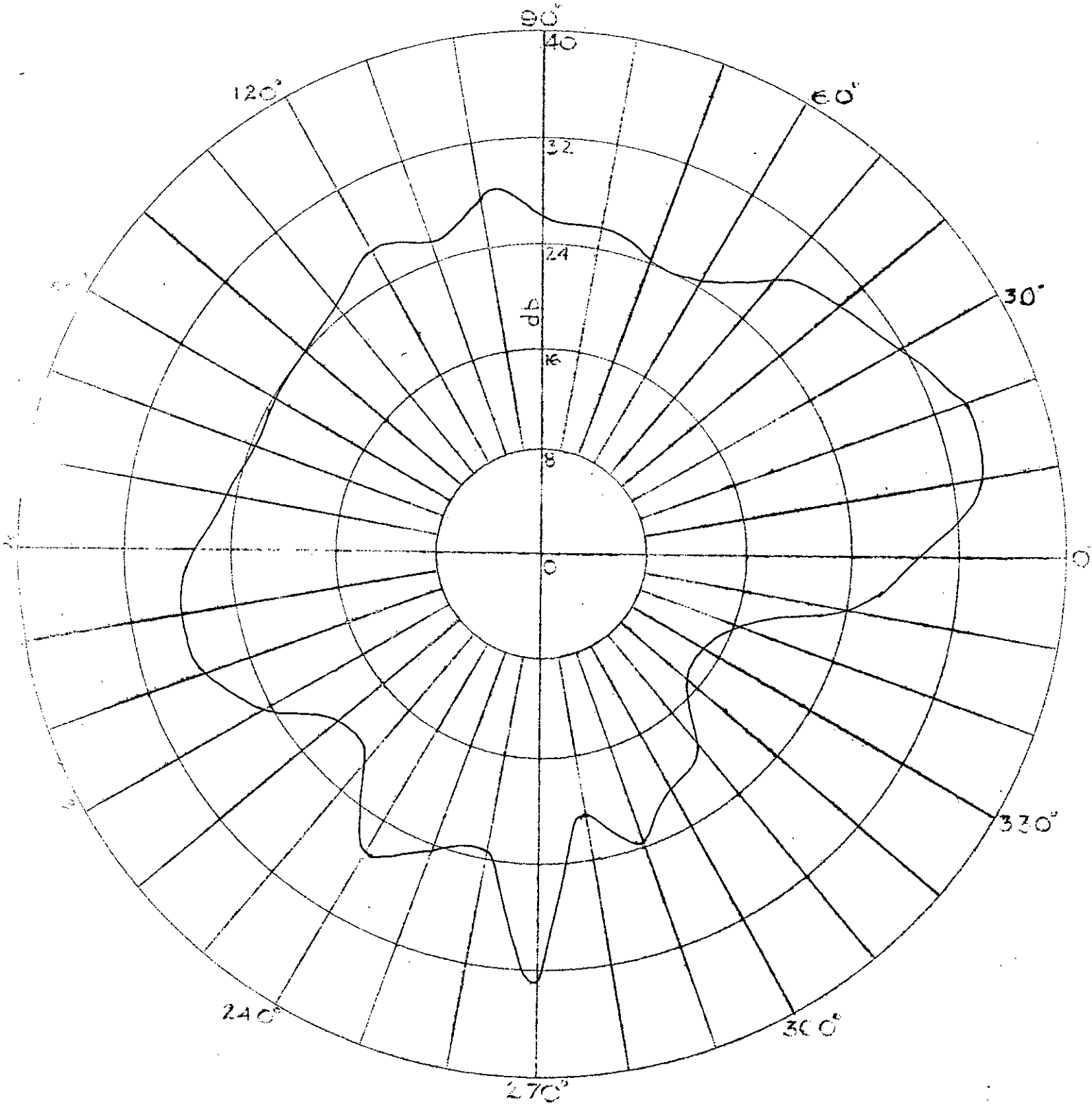

Fig. 32c Radiation Pattern at 500 Mega Cycles

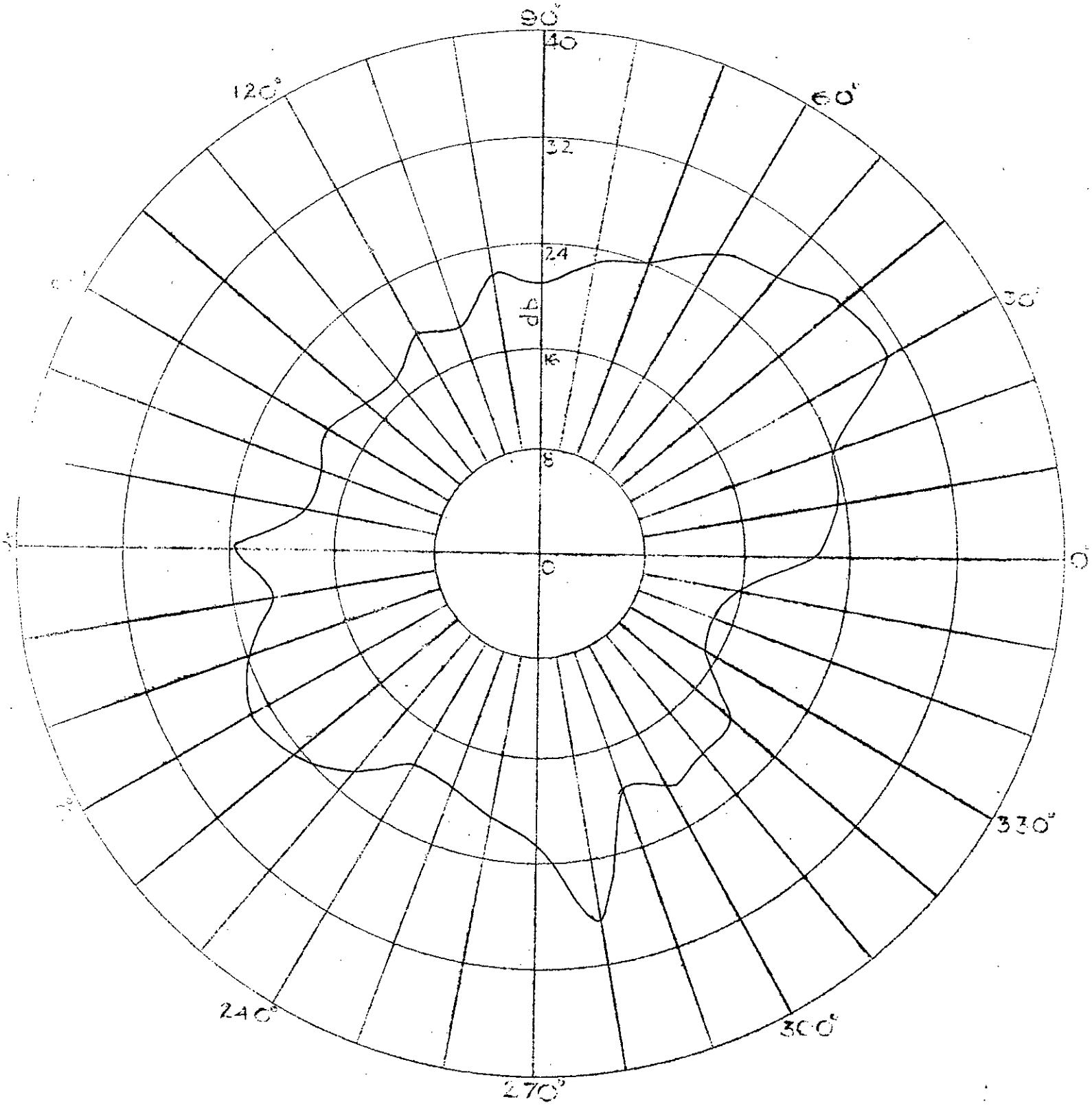

Fig. 32d Radiation Pattern at 600 Mega Cycles

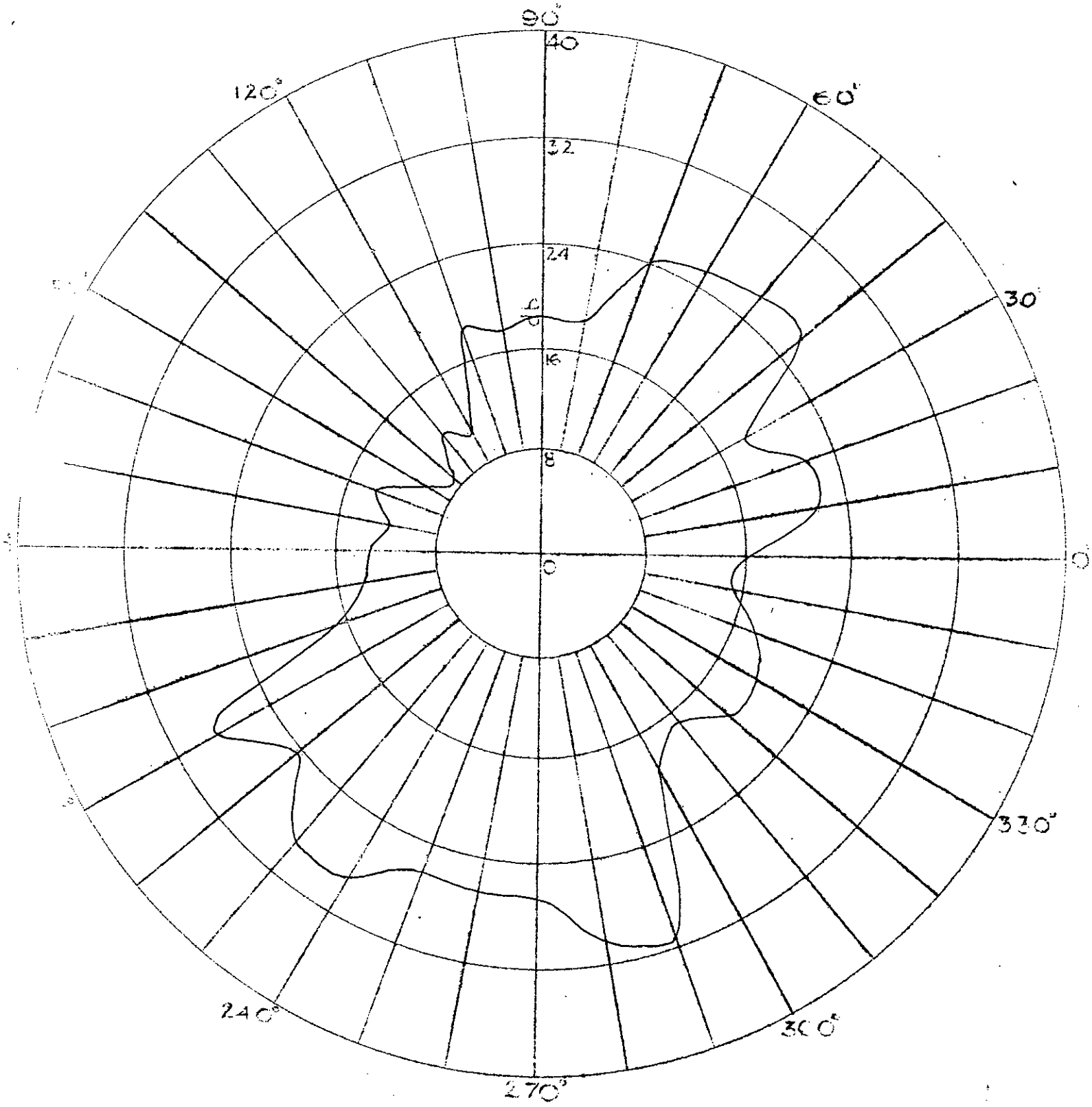

Fig.32e Radiation Pattern at 700 Mega Cycles

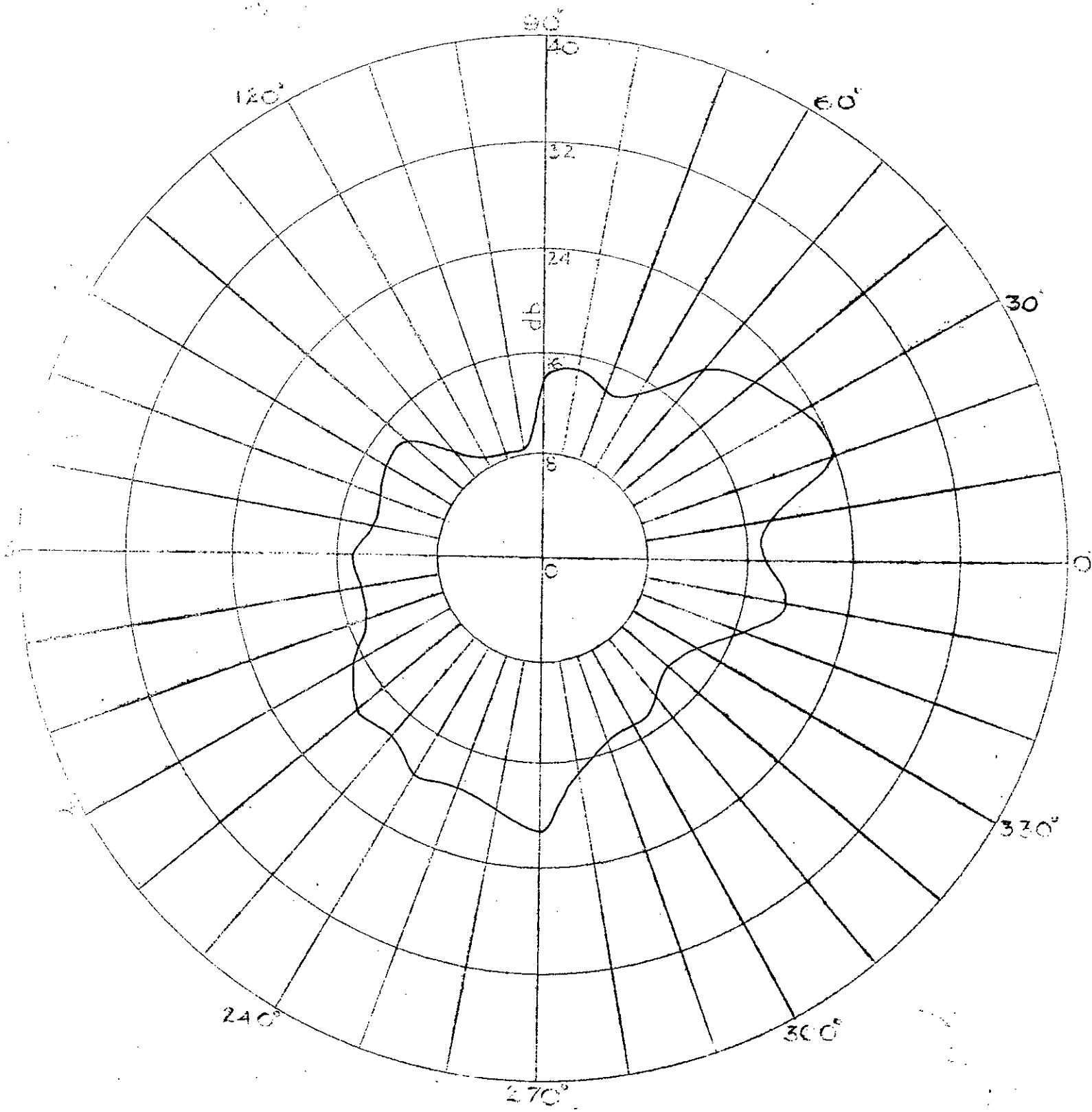

Fig. 32f Radiation Pattern at 800 Mega Cycles

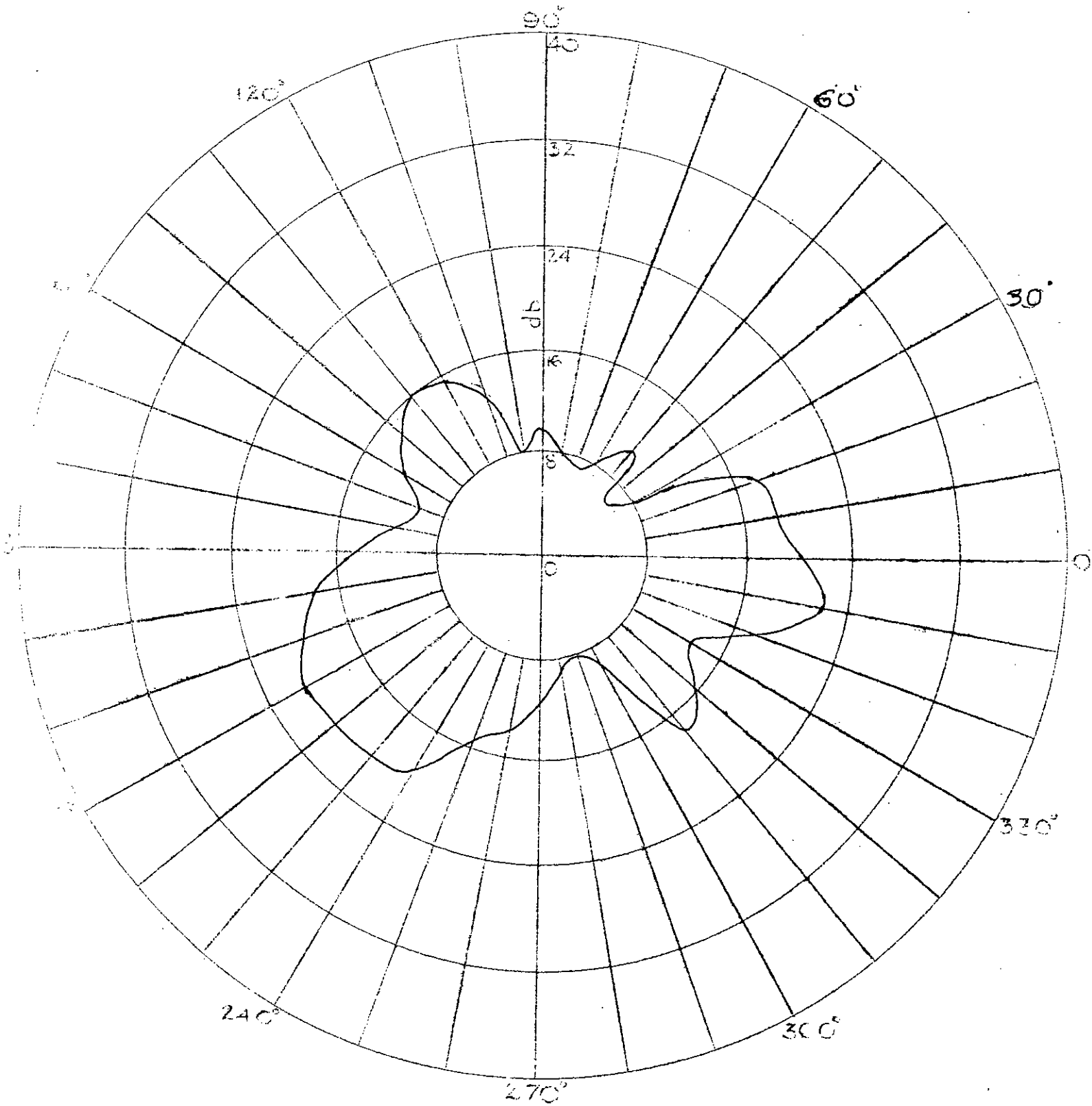

Fig. 32g Radiation Pattern at 900 Mega Cycles

TABLE - XI

CALCULATION OF INPUT IMPEDANCE OF FOUR LOG PERIODIC ANTENNAS COMBINED

Freq. in Mc/s	Shift in Pos.of min.current in λ		$I_{max.}$ μ amp	$I_{min.}$ μ amp	V_{max} mV	V_{min} mV	VSWR S	Z_{min}	Length of coaxl. cable in	Calculated impedance in Ohm.
	Gen.end	Load end.								
250		0.010	2.0	0.5	0.51	0.15	3.40	14.7	2.36	29+j45
300	0.025		5.0	2.0	1.30	0.51	2.55	19.6	2.83	77+j55
350		0.076	6.0	1.0	1.51	0.27	5.59	8.95	3.30	18+j47
400		0.087	7.5	2.0	1.90	0.51	3.72	13.4	3.77	32+j54
450	0.038		7.5	1.5	1.90	0.41	4.75	10.5	4.25	105-j110
500		0.166	8.0	6.0	2.00	1.50	1.33	37.6	4.72	46+j15
550	0.110		14.5	1.4	3.50	0.39	8.90	5.6	5.20	8-j31
600		0.040	15.5	1.3	3.75	0.38	9.86	5.1	5.67	70-j170
650		0.173	2.5	2.5	0.70	0.70	1.00	50.0	6.12	50+j0
700		0.338	14.0	2.5	3.40	0.70	4.86	10.3	6.62	11+j16
750		0.125	8.6	0.6	2.05	0.20	1.03	49.9	7.07	52-j2
800		0.294	12.5	0.7	3.05	0.21	14.50	3.5	7.55	11+j73
850		0.028	18.0	1.5	4.31	0.40	10.80	4.6	8.01	5.5-j12
900		0.180	13.5	1.2	3.25	0.30	10.80	4.6	8.50	25-j100

IMPEDANCE COORDINATES—50-OHM CHARACTERISTIC IMPEDANCE

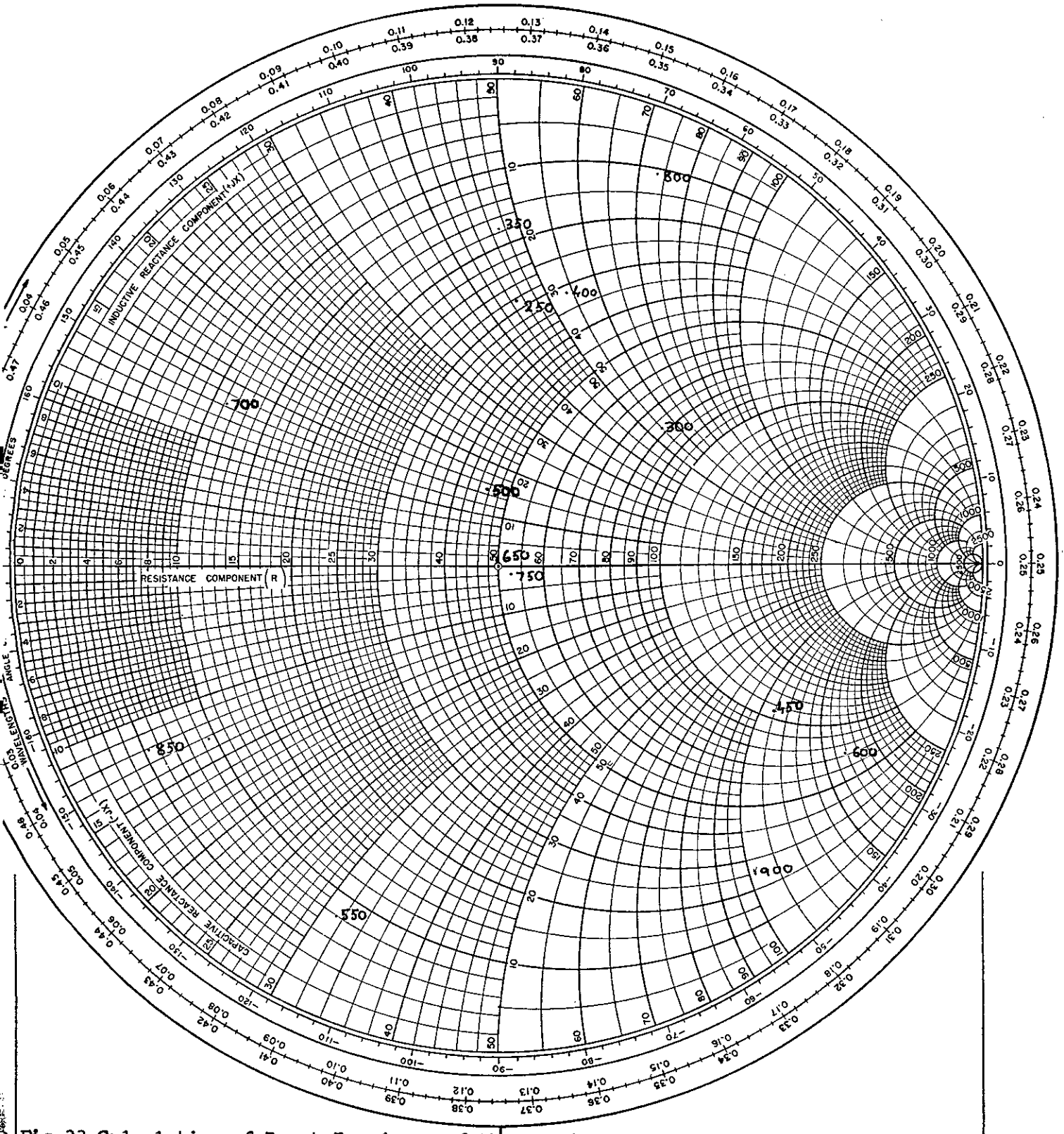

Fig.33.Calculation of Input Impedance of the combination of Four Log-period Antennas

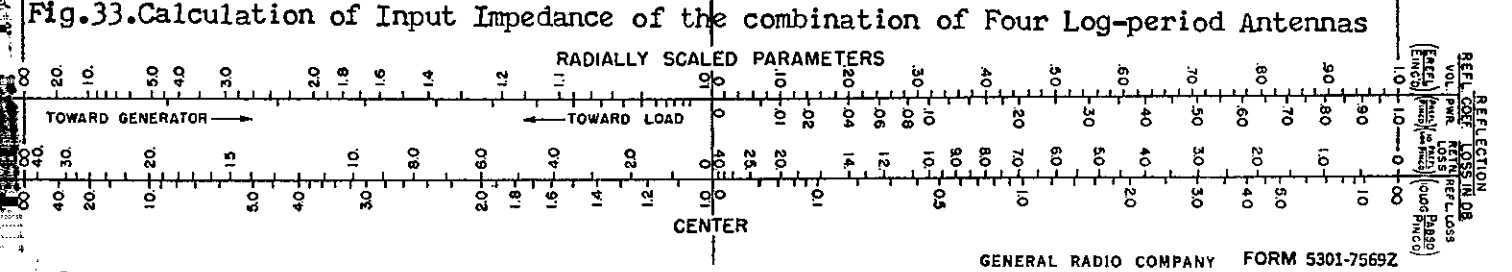

Fig. 34. Variation of the Resistive and Reactive components of the Input Impedance of the combination of four log-periodic antennas with frequency.

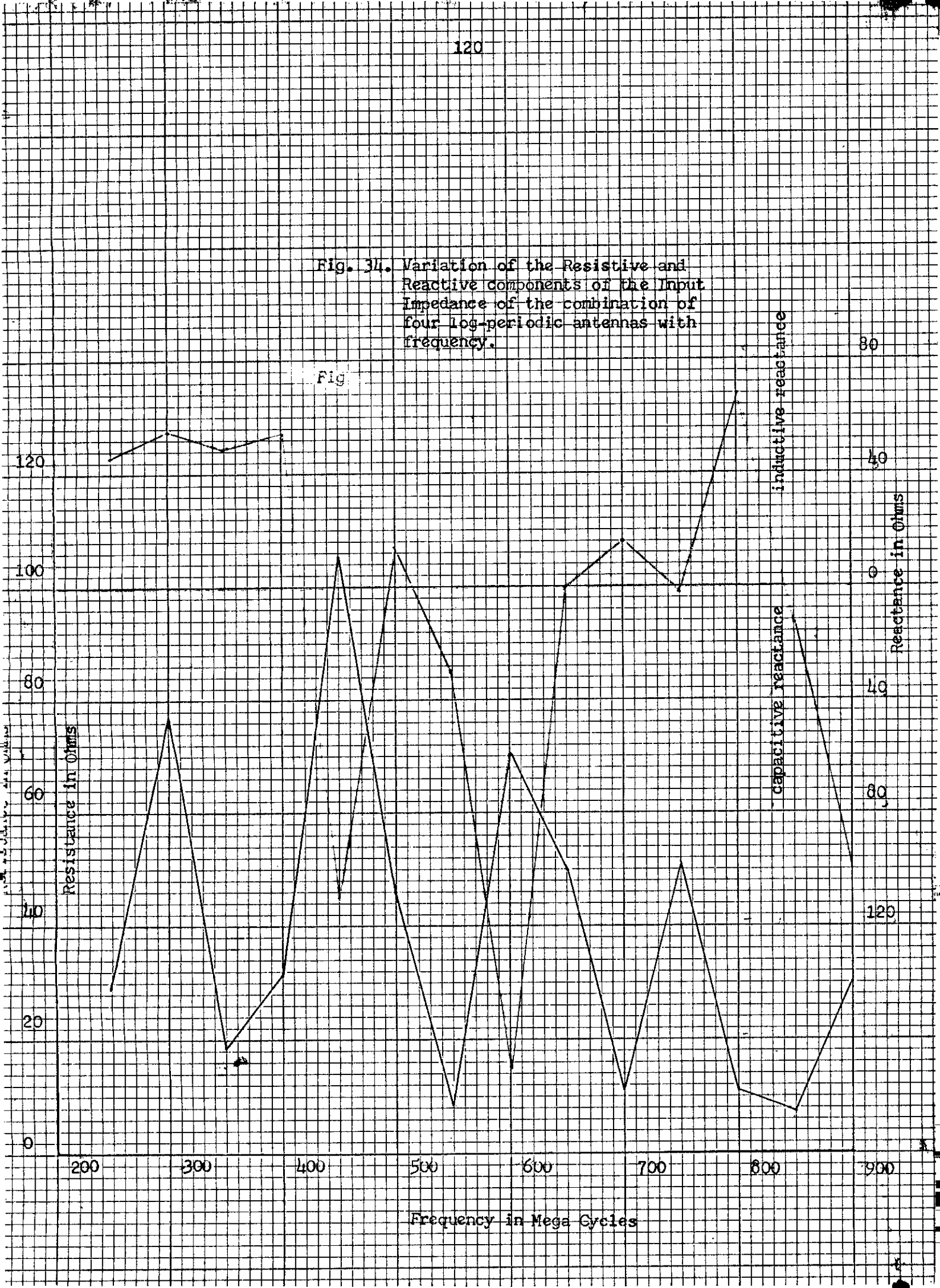

C H A P T E R - VI

D I S C U S S I O N

D I S C U S S I O N

This particular problem has never been studied before. Because of the limited range of the various apparatus used in the experiment the present problem was investigated between the frequency range of 250ϕ Mega cycles to 900 Mega cycles. In order to minimise errors the experiment was performed on the top of the roof in open air so that the electrical characteristics could become equal to the free space values. Because of space limitation the radiation intensities were measured in a circle of 4 m radius at intervals of 10 degrees.

Since no antenna pattern recorder was available, the radiation intensities were measured by using heterodyne principle(Fig.16). The instruments were very delicate and the balancing of the instruments was very much time consuming. Due to the fluctuation in the line voltage the output of the oscillators sometimes did not remain constant. These undesirable oscillations of the oscillators used in the heterodyne principle for the determination of radiation patterns greatly affected the experimental results.

Another important factor that affected the experimental results is the proximity effect. The antennas under investigation were sensitive to the conductive objects located in the near field. Because of the practical difficulties most of the instruments having metallic surfaces had to place in the near field. The person performing the experiment had to move also in the near field. These difficulties could have been avoided if longer co-axial cables were available.

A study of the shape of the radiation patterns with the change of the operating frequency reveals that the shapes become function of frequency.

For the case of the single antenna it is observed that the shape of the patterns changes markedly for lower values of the frequency. At higher values of the frequency (700 Mc/s to 900 Mc/s), the patterns exhibit some tendency of constancy except rotation (Figs. 17f,17g,17h).

When two antennas are combined, the radiation patterns show better tendency of constancy. For the frequency range of 700 Mc/s to 900 Mc/s, the patterns for the case when the axis is horizental, remain roughly constant except rotation (Figs. 21f,21g,21h). The front to back ratios have also higher values. That means directivity is also better.

For the case of the combination of four antennas the constancy of the radiation patterns is not observed.

But the case is somewhat different for the combination of four log-periodic antennas. When the axis of the antenna is horizontal, the patterns show the tendency of constancy for the frequency range of 700 Mc/s to 900 Mc/s (Figs. 31e,31f,31g). When the axis of the antenna is vertical, the patterns rotate at a faster rate.

From the above study it is found that of the four types of antennas under investigation, the combination of two antennas shows the best tendency of constancy in radiation patterns in the frequency range of 700 Mc/s to 900 Mc/s.

The input impedance was calculated by using a slotted transmission line. Because of some of the foregoing difficulties admittance meter was not used. The ultimate results were dependent upon so many intermediate steps, that included (i) determination of the shift in the position of minimum current when the transmission line was shorted and when the transmission line was loaded (ii) Determination of the magnitude of the voltage standing wave ratio. The process included the conversion of currents into the corresponding voltages by using a calibration curve. (iii) Determination of the length of the coaxial cable in term of the operating wavelength between the end of the transmission line and the feed point of the antenna. (iv) Finally the value of the input impedance was read from a Smith Chart. It is clear that any slight error in any of the intermediate steps will greately affect the final result.

It was observed that as the operating frequency was changed, the reactive components of the impedance sometimes became inductive and sometimes capacitive. This was because the physical lengths of the elements were fixed, the electrical lengths were changed as the operating frequency was changed. The reactance will be capacitive when the element length was less than the resonant length and the reactance will be inductive when the element length is greater than resonant length. But reactance zero will not occur for element lenghts that are integral multiple of quarter wavelength. This is due to ' endeffect' which results from a decrease in L and in crease in C near the end of the line. Hence reactance zero will occur for the physical length of the elements that are somewhat less than the multiples of quarter wavelengths.

It is interesting to note the behaviour of the input impedances of the four antennas under investigation , with the change of frequency. For

the case of the single antenna when the resistive component of the input impedance increases, the reactive component of the impedance changes its value from capacitive to inductive and when the resistive component decreases the reactive component starts its value changing from inductive to capacitive. The positions of reactance zero are nearly equally spaced in frequency (Fig. 20). On a Smith Chart the impedance moves on a bigger circle(Fig.19).

For the case of the combination of two antennas the behaviour of the input impedance with the change of frequency is more or less opposite to that of a single antenna. Here also reactance zero occurs approximately at regular interval measured in terms of frequency (Fig.24). The impedances move on a bigger circle on a Smith Chart (Fig. 23)

For the case of the combination of four antennas, the nature of the variation of resistive and reactive components with the change of frequency is not easily predictable (Fig. 29). The impedances lie inside a bigger circle on a Smith Chart (Fig. 28).

For the case of the combination of four log-periodic antennas also, the nature of the variation of the components of input impedance is not easily predictable (Fig. 34). The impedances lie inside a bigger circle on a Smith Chart (Fig. 33).

CONCLUSION

The above study reveals that the input impedances of the antennas under investigation did not fall inside a small circle on a Smith Chart,as is generally the case for frequency independent antennas. However, in practice no antenna is truly frequency independent. Only the band of the antenna is made broad to a satisfactory limit. If the structure of the present antenna could have been made infinitely long it would have exhibited frequency

independent characteristics. Or if the structure were made very long it would have showed some frequency independent properties. Since the present structure was made very small it did not exhibit frequency independent characteristics but it showed some of the properties of the pseudo frequency independent antenna as discussed in refs. 1 and 2.

It is expected that in future more work will be done upon this type of antenna and better theoretical explanation of some of the observed results will be given. Although, considerable work has been done upon broadband antennas in the past decade yet there are some important design problems upon which much work can be done. Among these are the design of broadband antennas having very high gain and the design of frequency independent antennas to produce specified rediation pattern.

BIBLIOGRAPHY

1. V.H.Rumsey, " Frequency Independent Antennas".
IRE National Convention Record. Antennas and Propagation, pt.1, pp 114-117, 1957.

2. R.H. DuHamel and D.E.Isbell, " Broadband Logarithmically Periodic Antenna Structure ."
IRE National Convention Record, Antenna and Propagation, pt. 1, pp 119-128, 1957.

3. [illegible]hn D.Dyson," The Equiangular Spiral Antenna."
[illegible] Transaction on Antennas and Propagation, [illegible]81-187, April,1959.

4. E.C. Jordan, G.A. Deschamps, J.D.Dyson, R.E. Mayes.
" Developments in broadband antennas".
IEEE Spectrum, pp 59-71, April, 1964.

5. Simon Ramo, John R. Whinnery, " Fields and Waves in Modern Radio." Second Edition.
John Wiely & Sons, Inc. New York, London.

6. David B. Langmuir, W.D. Hershberger,
" Foundations of Future Electronics." pp 482-487
Mc Graw-Hill Book Company, Inc.
New York Toronto London.

7. Louis A. Pipes,
" Applied Mathematics for Engineers and Physicists" pp 546-548
Mc Graw-Hill Book Company, Inc.
New York Toronto London.